DOI: 10.1070/RCR4739

Heterogeneous semiconductor photocatalysts for hydrogen production from aqueous solutions of electron donors

Ekaterina A. Kozlova,[a, b] Valentin N. Parmon [a, b]

[a] *Boreskov Institute of Catalysis, Siberian Branch of the Russian Academy of Sciences prosp. Akademika Lavrentieva 5, 630090 Novosibirsk, Russian Federation*
[b] *Novosibirsk State University ul. Pirogova 2, 630090 Novosibirsk, Russian Federation*

Current views on heterogeneous photocatalysts for visible- and near-UV-light-driven production of molecular hydrogen from water and aqueous solutions of inorganic and organic electron donors are analyzed and summarized. Main types of such photocatalysts and methods for their preparation are considered. Particular attention is paid to semiconductor photocatalysts based on sulfides that are known to be sensitive to visible light. The known methods for increasing the quantum efficiency of the target process are discussed, including design of the structure, composition and texture of semiconductor photocatalysts and variation of the medium pH and the substrate and photocatalyst concentrations. Some important aspects of the activation and deactivation of sulfide photocatalysts and the evolution of their properties in the course of hydrogen production processes in the presence of various types of electron donors are analyzed.
The bibliography includes 276 references.

Contents

I. Introduction 870
II. Semiconductor photocatalysts for hydrogen production: the action principle 872
III. Main types of heterogeneous semiconductor photocatalysts for visible light-driven production of hydrogen 877
IV. Key factors influencing the activity of semiconductor photocatalysts for hydrogen production from aqueous solutions 890
V. Activation and deactivation of semiconductor photocatalysts of hydrogen production reactions 899
VI. Conclusion 901

I. Introduction

There has been an inevitable trend towards decline in readily accessible high-quality fossil fuel resources, which are basic to the functioning of the fuel and energy complex in the developed countries. Hence there is a great demand for the development of alternative and first of all renewable energy sources. In the USSR, the strategy of research into renewable energy sources was substantiated in the 1970s by Academician N.N.Semenov awarded the 1956 Nobel Prize in Chemistry, who showed that only thermonuclear power engineering provides an actually inexhaustible energy source.[1] However, realization of controlled thermonuclear fusion is still a long way in the future; therefore, it is critical to learn how to use the available, almost perpetual natural thermonuclear reactor, *viz*., the Sun. At present, main R&D avenues in the field of solar energy engineering are as follows:

— design of solar cells for direct conversion of solar energy to electricity and

— development of methods for direct conversion of solar energy to energy of chemical carriers using thermochemical and quantum systems.

The most interesting way of utilizing quantum converters of solar energy to chemical energy is to produce hydrogen *via* photocatalytic processes mimicking natural bacterial photosynthesis and, which is more preferable, photosynthesis of green plants or cyanobacteria.[2–4]

Recently, there has been rapid progress in helioenergetics based on semiconductor solar cells owing to radical reduction of their cost. As a result, a record

E.A.Kozlova. Candidate of Chemical Sciences, Senior Researcher at the BIC SB RAS, Associate Professor of the Division of Physical Chemistry at the Department of Natural Sciences, NSU.
Telephone: +7 (383) 333 – 1617, e-mail: kozlova@catalysis.ru
Current research interests: semiconductor photocatalysis of hydrogen production and degradation of hazardous organic compounds.
V.N.Parmon. Academician of the RAS, Doctor of Chemical Sciences, Professor, Scientific Director at the BIC SB RAS, Head of the Division of Physical Chemistry at the Department of Natural Sciences, NSU.
Telephone: +7 (383) 330 – 8269, e-mail: parmon@catalysis.ru
Current research interests: development and studies of catalysts and catalytic processes, including those of conversion and accumulation of various kinds of energy, catalysis and photocatalysis in Nature; utilization of renewable and unconventional energy resources.

Received 27 March 2017
Translation: A.M.Raevskiy

© 2017 Russian Academy of Sciences and Turpion Ltd.

147 GW of renewable generating capacity was installed worldwide in 2015, which is higher than conventional generating capacity installed worldwide that year.[5] The development of novel technologies for direct conversion of solar energy to electricity faces severe problems related to electron-storage capacity and electron transport rate.[6] Therefore, the most promising line of development of helioenergetics is direct conversion of solar energy to energy of chemical compounds, as was done by Nature, which began with invention of bacterial photosynthesis and then modified it to photosynthesis of cyanobacteria and, finally, to that of green plants. One of the most efficient methods for conversion of solar energy to energy of chemical bonds is to design photocatalytic systems reproducing functions of all types of natural photosynthesis. The ultimate, hard-to-reach goal of this approach is the splitting of water into hydrogen and oxygen.[7]

Unique properties of hydrogen make it a versatile, green chemical energy carrier suitable for all types of heat engines and other generating facilities. Taking into account this fact, the development of novel efficient hydrogen production technologies based on systems mimicking natural photosynthesis seems to be topical in order to solve at least local problems in hydrogen energy engineering.[6, 8]

Indeed, there are various industrial technologies for hydrogen production;[9] usually they are energy-consuming and become cost-efficient only at high hydrogen production volumes as in, *e.g.*, nitrogen industry and petroleum refining. Local generating facilities require cost-efficient, moderate-performance hydrogen generators operating at low temperatures. Such systems represent an alternative to systems used for high-temperature reforming (conversion) of organic compounds (main method for commercial production of hydrogen).[2] From the standpoint of energy production based on renewable energy sources, the most attractive method is visible light-driven photocatalytic production of hydrogen.

The possibility for photocatalytic water splitting into hydrogen and oxygen to occur was for the first time reported by researchers from Japan.[10] This gave a powerful impetus to the worldwide development of studies on photocatalytic production of hydrogen. A number of relevant reviews and monographs were reported in the USSR before 1990.[11–14] Then, after long time of inactivity, a trend emerged towards restoration of interest of domestic researchers in the photocatalytic production of hydrogen. Namely, a review devoted to water splitting into hydrogen and oxygen in aqueous suspensions of complex-oxide photocatalysts was reported.[15]

As early as the first publications on photocatalytic splitting of water, mention was made that recombination of hydrogen and oxygen atoms produced in the same volume can significantly reduce the quantum efficiency of the process. In this connection, here we pay particular attention to photocatalytic production of hydrogen by reduction of water using aqueous solutions of organic and inorganic electron donors rather than splitting of water.[2, 16–23] The trend towards the use of inorganic sulfides and organic compounds (*e.g.*, glycerol available in large amounts[24]) as electron donors is quite attractive practically because this approach allows one to combine the production of H_2 with solution of severe environmental problems related to purification of water from various pollutants.[25] Thus, photocatalysis provides both purification of water and production of hydrogen.

There is considerable literature on photocatalytic hydrogen production combined with the oxidation of carboxylic acids,[21–26] organochlorine and organophosphorus compounds,[25, 27] as well as azo dyes.[28, 29] The

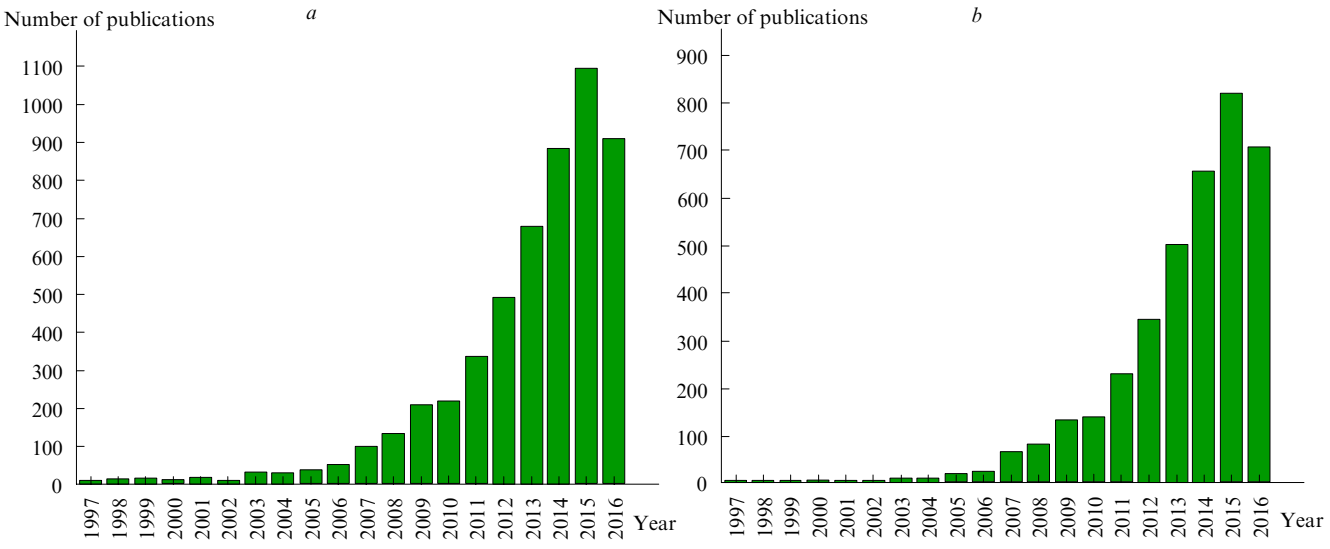


Figure 1. Annual number of scientific publications devoted to photocatalytic hydrogen production and reported between 1997 and 2016. Data analysis was performed using the Web of Science database with the terms 'photocatalytic hydrogen production' (*a*) and 'photocatalytic hydrogen production AND visible light' (*b*).

use of biomass-derived oxygen-containing compounds (ethanol,[30] methanol,[31] glycerol,[30–33] isopropyl alcohol[34] and saccharides[30]) as electron donors seems to be very promising because in this case hydrogen can be produced using three renewable (or inexhaustible) sources of raw materials, namely, biomass, solar light and water.

The development of highly efficient systems for hydrogen production *via* photocatalytic reduction of water has been carried out intensively since the early 1980s.[2] Since then, a number of systems (mainly semiconductor ones) suitable for implementation of the process in question were prepared; however, none of them was put into practice.[35] There has been steady interest in the synthesis and studies of visible-light-sensitive photocatalysts for production of hydrogen; this is of particular importance from the standpoint of utilization of solar energy in the future.[36,37] Recently, a number of new heterogeneous photocatalysts for visible light-driven hydrogen production were discovered,[38] including $BiVO_4$,[39] Ta_3N_5,[40] TaON,[41] GaN–ZnO solid solution,[42] CoO,[43] Ag_3PO_4 (Ref. 44) and polymeric graphitic carbon nitride g-C_3N_4.[45] Publications concerning various types of photocatalysts include original articles and reviews.[6,15,46–51] The diagrams in Fig. 1 illustrate the dynamics of the number of publications on various aspects of photocatalytic hydrogen production, especially, the visible light-driven process.

A distinctive feature of this review consists in analysis of interrelations between the photocatalytic activity of various materials and not only their structure and optical properties, but also the nature of the substrate (irreversible electron donor). Thus is due to the fact that the mechanisms and thermodynamics of photocatalytic hydrogen production from aqueous solutions of organic compounds and, *e.g.*, the best studied inorganic electron donor (S^{2-}–SO_3^{2-} mixture) are significantly different and moreover differ from the mechanism and thermodynamics of complete photoinduced splitting of water into oxygen and hydrogen.

This review summarizes information on the main groups of semiconductor photocatalysts for visible light-driven production of hydrogen, including aqueous suspensions of solid solutions of transition metal sulfides, metal- and nonmetal-doped titanium dioxide, as well as materials based on polymeric g-C_3N_4, nitrides, oxynitrides and oxysilfides. We will also consider methods for increasing the quantum efficiency of the processes in question *via* the design of systems with semiconductor/semiconductor and metal/semiconductor heterojunctions, establishment of optimal porous structure and dimensions of photocatalyst particles. The review begins with a brief outline of the mechanisms of photocatalytic splitting of water and hydrogen production *via* the oxidation of various types of electron donors. A particular Section is devoted to *in situ* activation of photocatalysts for hydrogen production under illumination of systems under study. The final Section summarizes the advances in the synthesis of photocatalysts for hydrogen production reactions and prospects for improvement of these systems.

II. Semiconductor photocatalysts for hydrogen production: the action principle

In accordance with the laws of quantum mechanics, electrons in isolated atoms and molecules can have only particular, discrete energies. The electron energy spectrum in a solid consists of bands, namely, the conduction band (CB) and the valence band (VB) separated by the band gap (BG).[52] The bands correspond to the allowed electron energy states. The band gap equals the energy difference between the bottom of the conduction band and the top of the valence band. There is a particular class of solids, *viz.*, semiconductors representing crystalline substances with a band gap of the order of 1 eV.

Absorption of a photon by a semiconductor is associated with electronic transitions between different states in the energy band structure. Since in an ideal semiconductor all states in the valence band are full while all states in the conduction band are empty, transition can only occur by electron transfer from the valence band to the conduction band. For a transition to occur, the energy absorbed by an electron should exceed the band gap value. Photons with lower energies cause no transitions between the electronic states of the semiconductor; therefore, such semiconductors are transparent at $\nu < E_{BG}/h$, where h is the Planck constant.[52] Actual semiconductor structures contain defects, dopant atoms and other features that can cause the formation of so-called impurity (usually, discrete) energy levels in the band gap.[53]

A photo-excited electron that arrived at the conduction band becomes mobile and has a high reduction potential. If this electron reaches the semiconductor surface, it can be treated as strong one-electron chemical reducing agent. The 'hole' formed in the valence band upon electron transfer is also mobile and can act as one-electron oxidizing agent on the semiconductor surface.

The action principle of a typical semiconductor photocatalyst (disperse particle) is illustrated in Fig. 2. Photo-excitation of an electron is followed by its transfer from the valence band to the conduction band of the semiconductor. The process is accompanied by the

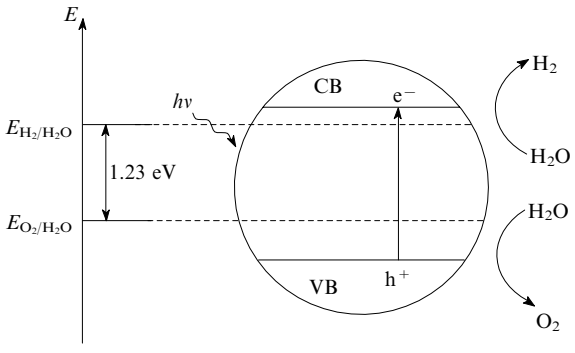


Figure 2. Energy diagram of the overall reaction for splitting of water into hydrogen and oxygen over disperse semiconductor photocatalysts.

formation of a mobile hole h^+ in the valence band. Mobile electrons and holes generated in the primary photophysical process can then recombine in the bulk of the semiconductor or migrate towards the surface of the catalyst and participate in complex dark redox reactions with external substrates, in particular, water.[54]

II.1. The mechanism of photocatalytic water splitting over semiconductor photocatalysts

A liquid-phase reaction of complete photocatalytic water splitting into hydrogen and oxygen over semiconductor photocatalysts

$$H_2O(liq) \longrightarrow H_2(gas) + \frac{1}{2}O_2(gas) \quad (1)$$

is usually described using two overall redox reactions, namely, hydrogen production *via* two-electron reduction of protons

$$2H^+ + 2e^- \longrightarrow H_2(gas) \quad (2)$$

and oxygen production *via* four-electron oxidation of water

$$2H_2O(liq) - 4e^- \longrightarrow O_2(gas) + 4H^+ \quad (3)$$

Thermodynamically, the reaction of complete water splitting under normal conditions is a highly endothermic process because the change in the standard Gibbs energy in reaction (1) is very large (237.2 kJ, see Ref. 6).

It should be noted that the primary photophysical event involves transfer of a single electron only. If the electron energy is sufficiently high, next events can also occur with no photo-excitation of subsequent electrons. At the same time, the lowest necessary photon energy assumes that the reduction of protons to molecular hydrogen [reaction (2)] is a two-electron process, while water oxidation to oxygen [reaction (3)] is a four-electron process without formation of energetic intermediates, such as free radicals, radical ions, *etc*. (see, *e.g*., Ref. 11). Taking into account this fact and based on the general principles of thermodynamics of the process in hand and on the maximum efficiency of solar energy conversion, the band gap of an efficient catalyst for photocatalytic water splitting into hydrogen and oxygen should lie between 1.23 and 3.0 eV, which corresponds to near-IR radiation (λ = 1000 nm) and a blue photon (λ = 420 nm), respectively. The energy levels of the bottom of the conduction band and the top of the valence band should satisfy the energy requirements specified by the electrochemical potentials for two-electron reduction and four-electron oxidation of water, respectively.[47] In particular, reduction of protons to produce hydrogen requires that the electrode potential of the bottom of the conduction band be more negative than the reduction potential of H^+ to H_2 [E_{H^+/H_2} = 0 V *vs*. normal hydrogen electrode (NHE) at pH 0]. At the same time, the formation of oxygen requires that the electrode potential of the top of the valence band be higher than the potential of water oxidation to oxygen (E_{O_2/H_2O} = 1.23 V *vs*. NHE) at pH 0.

It should be noted that unavoidable energy loss during electron transfer in the reactions of hydrogen and oxygen production on the surface of a heterogeneous photocatalyst causes a noticeable kinetic overpotential. As a consequence, efficient photocatalytic splitting of water can occur if the band gaps of the semiconductor materials in hand are close to or greater than ~2 eV.[22, 55, 56]

The electrode potential of the bottom of the conduction band in semiconductors (E_{CB}/V *vs*. NHE) depends strongly on the pH of the reaction solution[6]

$$E_{CB} = E^\circ_{CB} - 0.059\ pH \quad (4)$$

where E°_{CB} is the standard electrode potential at pH 0 and the slope (0.059) is expressed in V per pH.

The reduction potential of water is also a linear function of pH with the same slope equal to 0.059. This provides an explanation for the fact that the overpotential on the functioning semiconductor varies insignificantly as the medium pH changes.[6]

II.2. Improving spatial charge separation to increase the quantum efficiency of hydrogen production over semiconductor materials

A key problem in photocatalytic water splitting over disperse semiconductor photocatalysts is useless recombination of electron–hole pairs in the bulk or on the surface of semiconductors. Nevertheless, improved spatial separation of photogenerated charges allows one to significantly increase the quantum efficiency of hydrogen production.

To this end, specific composite semiconductor materials are engineered,[6, 57] *e.g*., semiconductor-1/semiconductor-2 and semiconductor/cocatalyst heterojunctions where charge carriers are transferred across the interface.[58] These types of heterojunctions provide energy band bending and, therefore, significantly enhance the activity of photocatalysts.[59] There are phase junctions between different structure modifications of same-type semiconductors (Fig. 3 *a*), type-1 semiconductor/type-2 semiconductor heterojunctions (Fig. 3 *b*,*c*), and the Schottky junction between the metal and semiconductor (Fig. 3 *d*).

II.2.a. Phase junctions

Phase junctions imply separation of electron–hole pairs between two different structure modifications (phases) of the same semiconductor compound. A typical example is provided by commercially available Degussa P25 titanium dioxide containing an anatase phase (80%) and a rutile phase (20%). Photocatalysts based on this material demonstrate enhanced activity in the photocatalytic production of hydrogen as compared to the activity of 100% anatase.[60]

A method was proposed for the synthesis of titanium dioxide, which allows one to obtain different bulk and surface TiO_2 phases by varying the calcination temperature.[61] The photocatalytic activity was shown to be directly related to the phase composition of the surface. A tentative activity enhancement mechanism is shown in Fig. 3 *a*: photogenerated electrons in the conduction band of rutile are transferred to anatase particles, which leads to charge separation and, corre-

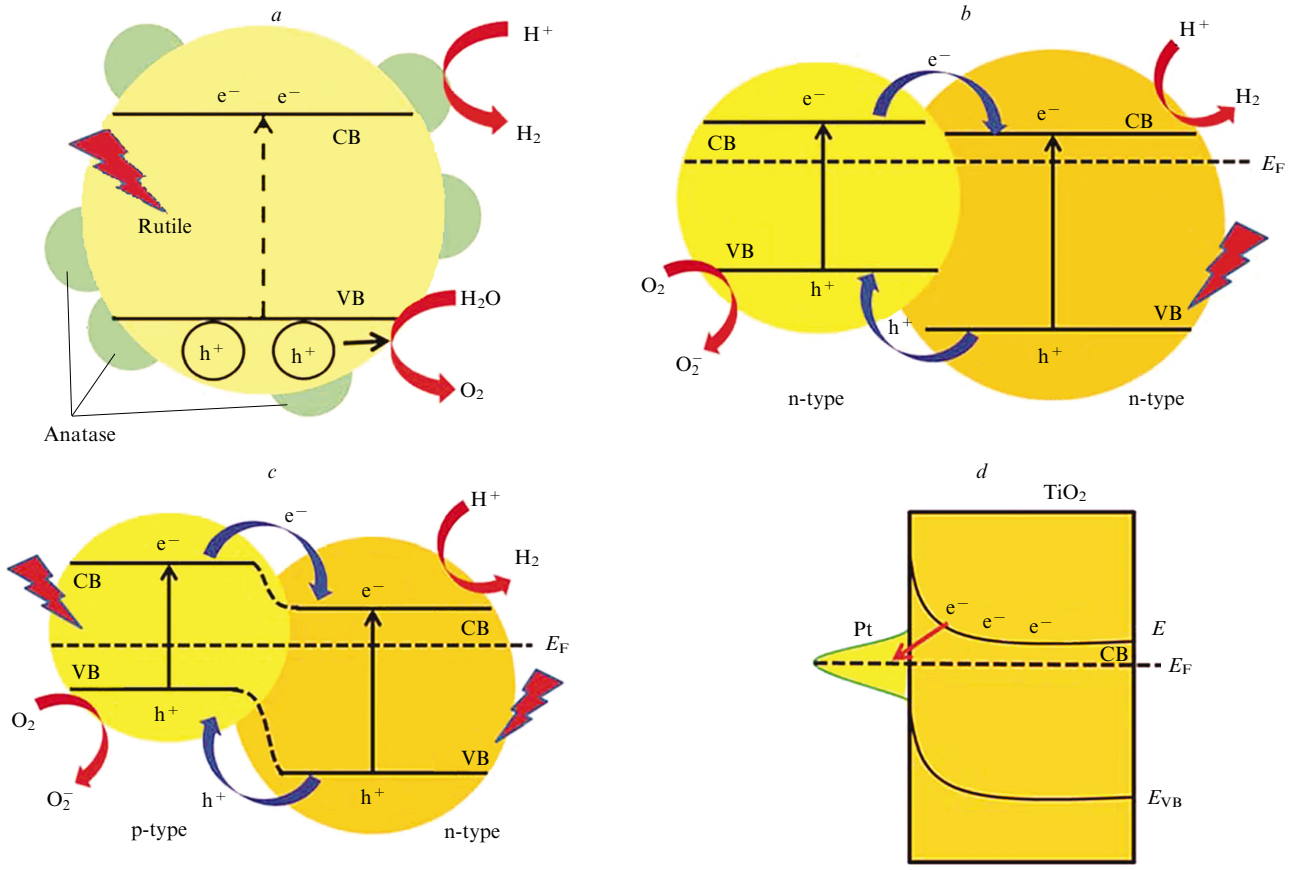


Figure 3. Schematic diagram of photogenerated charge transfer in composite semiconductor materials with different types of heterojunctions.[6]
Phase junction (*a*); n-type photocatalyst/n-type photocatalyst (n–n-heterojunction, *b*); p-type photocatalyst/n-type photocatalyst (p–n-heterojunction, *c*); and Schottky junction (*d*).

spondingly, to an increase in the quantum efficiency and activity of the photocatalyst.[61] The existence of heterojunctions between α-Ga_2O_3 and β-Ga_2O_3 was proved. Gallium oxide samples containing both phases also exhibit higher photocatalytic activity in hydrogen production compared to single-phase samples of Ga_2O_3.[62]

II.2.b. Semiconductor/semiconductor heterojunctions

The main route to preparation of active semiconductor photocatalysts for hydrogen production is to design materials with p–n or n–n heterojunctions (see Fig. 3 *b*,*c*). This gives rise to local electric fields responsible for Fermi level bending in both semiconductors. Internal electric field favours separation of photogenerated charges and thus an increase in the quantum efficiency of subsequent chemical processes including production of hydrogen.

Systems based on CdS/TiO_2 heterojunction belong to the best studied systems with n–n heterojunctions.[6] Visible light-driven photocatalytic water splitting into oxygen and hydrogen was also studied using other representatives of this family, namely, Sr_2TiO_4/$SrTiO_3$(La,Cr),[63] CdS/C_3N_4 (Ref. 64) and CdS/CeO_x.[65]

Systems with p–n-heterojunctions can also be used for photocatalytic splitting of water. For instance, efficient photocatalytic water splitting was achieved using $CaFe_2O/PbBi_2Nb_{1.9}W_{0.1}O_9$ (Ref. 66) and $CaFe_2O_4/TaON$.[67]

II.3. Evaluation of photocatalytic activity of different materials: specific features

Like conventional catalysts, photocatalysts for hydrogen production are usually compared using the specific activity expressed in [(mmol H_2) h^{-1} g^{-1}] as the critical parameter. The formation of hydrogen is detected by monitoring the composition of the gas phase over the suspension of the photocatalyst using, *e.g.*, a gas chromatograph. However, since the production rate of products in photochemical processes is related to the incident luminous flux and spectral characteristics of incident light, the use of the specific activity of photocatalysts is incorrect. The problem of correct quantitative description of the action of a photocatalytic system was considered in detail in the IUPAC recommendations 2011.[68]

Unfortunately, such a universal parameter as the quantum efficiency of heterogeneous photocatalytic processes is used much more rarely because of non-monochromatic light emitted by most light sources utilized in the photocatalytic studies. Following the IUPAC recommendations 2011 (Ref. 68; see also a review[46]), a correct quantitative description of the photocatalytic activity of materials used for photocata-

lytic production of hydrogen requires that particular attention be paid to such parameters as the turnover number (TON) of the catalyst, the quantum yield of the process and the action spectrum of the photocatalyst.

II.3.a. The turnover number of catalyst

The number of moles of hydrogen produced should exceed that of the photocatalyst. Otherwise, hydrogen production can be associated with irreversible changes in the state of the catalyst. The TON value is calculated as

$$\mathrm{TON} = \frac{\text{number of reacted molecules}}{\text{number of active sites}} \quad (5)$$

However, it is usually unknown what are active sites in the photocatalyst. Therefore, the denominator of expression (5) usually represents the total number of atoms in the photocatalyst or the number of atoms on the photocatalyst surface rather than the number of active sites. Specific activity values calculated with respect to the mass of the photocatalyst, *e.g.*, in (μmol H_2) h^{-1} (g of catalyst)$^{-1}$, are sometimes incorrect because the hydrogen production rate (W) is not always proportional to the mass of photocatalyst. It should be noted that a criterion for the occurrence of a photocatalytic process has the form $\mathrm{TON} \gg 1$.

II.3.b. The quantum yield of photocatalytic process

The rate of photocatalytic production of hydrogen is usually measured in (μmol H_2) h^{-1}. However, the photocatalytic activity depends on experimental conditions, in particular, on the power and type of light source, on the geometry of the experimental system, *etc*. Thus, the photocatalyst activities measured under different conditions can hardly be compared correctly. Indeed, a correct comparison of activities requires knowledge of the quantum yields of the reaction calculated with respect to the number of photons absorbed by the active sites of the photocatalyst. The number of incident photons can be determined with ease, but the number of photons absorbed by the photocatalyst is difficult to determine because of light reflection and scattering, absorption by inactive components of the system, *etc*. It should be noted that in most cases photocatalytic production of hydrogen over disperse semiconductor photocatalysts is studied in suspensions. Therefore, the quantum yield determined using the number of incident photons is actually an apparent quantum yield or the quantum efficiency (Φ; see IUPAC recommendations 2011).[68] The quantum efficiency (in %) is calculated using the expression

$$\Phi = \frac{\text{number of reacted (or evolved) molecules}}{\text{number of incident photons}} \times 100 \quad (6)$$

Clearly, the apparent quantum efficiency is always lower than the actual quantum yield of an elementary photocatalytic reaction. For monochromatic light, Φ equals the apparent quantum yield; for non-monochromatic light, Φ is the apparent quantum efficiency.[68]

II.3.c. The action spectrum of a photocatalyst

The action spectrum of a photocatalyst is the dependence of biological or chemical photoresponse (quantum yield) on the emission wavelength or energy or on the emission frequency (or wavenumber).[68] An analysis of the action spectrum is critical to evaluation of the photosensitivity of samples to different-wavelength radiation, especially, to visible light. The action spectrum is measured using monochromators or light filters. Hydrogen production over some oxide materials can also occur in the dark under vigorous stirring of suspensions.[46, 69, 70] Taking account of this fact, blank experiments carried out with no photocatalyst and illumination are necessary in order to distinguish between the dark and light stages of the processes under study.

II.4. Hydrogen production in aqueous solutions of organic compounds

Often, researchers study not only water splitting into oxygen and hydrogen *per se*, but also photocatalytic hydrogen production from aqueous solutions of organic compounds.[48] Utilization of certain organic compounds as electron donors is substantiated from a practical point of view because water is most often polluted by just organic compounds. The approach in question makes it possible to purify water and produce hydrogen simultaneously.[25] Besides, this is a possible route to hydrogen production from biomass of different nature.[30] Photocatalytic hydrogen production from aqueous solutions of organic compounds can be considered as combination of processes (2) and oxidation of organics.[48] Like in the case of water splitting into oxygen and hydrogen, the primary photophysical event usually involves transfer of a single electron (see Fig. 2), while subsequent chemical transformations can proceed in the dark.

It is important that the change in the standard Gibbs energy of water splitting following Eqn. (1) is 237.2 kJ mol^{-1} *vs.* −1325.4 kJ mol^{-1} for ethanol oxidation by oxygen following the equation

$$C_2H_5OH(liq) + \frac{7}{2}O_2(gas) \longrightarrow 2\,CO_2(gas) + 3\,H_2O(liq) \quad (7)$$

The change in the standard Gibbs energy of anaerobic decomposition of ethanol into hydrogen and carbon dioxide treated as 12-electron redox reaction

$$C_2H_5OH(liq) + 3\,H_2O(liq) \longrightarrow 2\,CO_2(gas) + 6\,H_2(gas) \quad (8)$$

is 97.4 kJ mol^{-1} or merely 8.1 kJ mol^{-1} per electron. Therefore, the process is thermodynamically much less hindered compared to water splitting into oxygen and hydrogen [see reaction (1)], and photocatalytic reaction (8) can proceed using photons with much lower energies and(or) require a much smaller number of photons.[48]

The general expression for complete anaerobic photocatalytic reforming of organic compounds has the form

$$C_xH_yO_z + (2x - z)\,H_2O \longrightarrow (2\,x + y/2 - z)\,H_2 + x\,CO_2 \quad (9)$$

For instance, the changes in the standard Gibbs energy of anaerobic reforming of glycerol, a biomass-derived substrate of biofuel production from vegetable oils

$$C_3H_8O_3 + 3H_2O \longrightarrow 7H_2 + 3CO_2 \quad (10)$$

decarboxylation

$$C_6H_{12}O_6 + 6H_2O \longrightarrow 12H_2 + 6CO_2 \quad (11)$$

and methanol reforming

$$CH_3OH + H_2O \longrightarrow 3H_2 + CO_2 \quad (12)$$

are respectively 5.3, −84.7 and −9.3 kJ mol^{-1}.[48] According to thermodynamic calculations, the equilibrium constants of reactions (8)–(12) are higher than that of reaction (1). Emphasize that negative changes in the Gibbs energy of reactions (11) and (12) suggest the possibility for dark processes to occur. However, this is not the case for room-temperature reactions in the presence of conventional catalysts. The role of photocatalysts in these processes is to drive thermodynamically allowed transformations at low temperatures. As is typically the case in chemical kinetics and conventional catalysis, the rate and quantum efficiency of photocatalytic hydrogen production from aqueous solutions of organic substances is often much higher than those of thermodynamically forbidden water splitting.

In addition to hydrogen and carbon dioxide, anaerobic photocatalytic decomposition of organics can result in alkanes[48,71] and other compounds.[48] In particular, photocatalytic hydrogen production from aqueous alcoholic solutions over Pd/TiO_2 photocatalyst can be described[48,71] by the following hypothetical scheme:

— adsorption of alcohol on palladium

$$RCH_2CH_2OH(liq) \longrightarrow RCH_2CH_2OH(ads) \quad (13)$$

— dehydrogenation of alcohol with the formation of adsorbed H atom

$$RCH_2CH_2OH(ads) \longrightarrow RCH_2\dot{C}HO(ads) + H^{\bullet}(ads) \quad (14)$$

— desorption of H atoms with the formation of H_2

$$2H^{\bullet}(ads) \longrightarrow H_2(gas) \quad (15)$$

— dissociation of adsorbed alkoxide into adsorbed carbon monoxide and hydrogen atoms

$$RCH_2\dot{C}HO(ads) \longrightarrow R\dot{C}H_2(ads) + CO(ads) + 2H^{\bullet}(ads) \quad (16)$$

— formation of alkane

$$R\dot{C}H_2(ads) + H^{\bullet}(ads) \longrightarrow RCH_3(gas) \quad (17)$$

— photo-activation of photocatalyst

$$Ti^{4+} + O^{2-} + h\nu \longrightarrow Ti^{3+} + O^{-} \quad (18)$$

— oxidation of CO(ads) and formation of oxygen vacancy ($V_O^{\cdot}$)

$$O^{-} + CO(ads) \longrightarrow CO_2(gas) + V_O^{\cdot} \quad (19)$$

— charge transfer

$$Ti^{3+} + V_O^{\cdot} \longrightarrow Ti^{4+} + V_O^{2-} \quad (20)$$

— and reduction of water

$$V_O^{2-} + H_2O \longrightarrow O^{2-} + H_2(gas) \quad (21)$$

It should be noted that reactions (13)–(17) proceed on metallic palladium and do not require illumination. Again, this is a hypothetical scheme because it assumes kinetic irreversibility of all elementary stages, which is of course impossible.

Interrelations between the rate of hydrogen production and the chemical composition of products of anaerobic decomposition of organic substrates of different nature are considered below.

II.5. Photocatalytic hydrogen production in aqueous solutions of inorganic sulfides

Hydrogen sulfide and water-soluble sulfides belong to the most widely used electron donors utilized in photocatalytic hydrogen production.[72,73] In nature, H_2S is a component of natural gas, as well as oil-dissolved and volcanic gases;[74] dissolved hydrogen sulfide is present in natural water (*e.g.*, in the Black sea). Hydrogen sulfide is a weak dibacid characterized by pK_a values of 7.0 and 12.0.[72,75] In alkali solutions at pH ⩾ 12, hydrogen sulfide dissociates to S^{2-} and HS^{-}. At pH 7–12, HS^{-} dominates. At pH ⩽ 7, almost no hydrogen sulfide dissociation occurs.

The change in the standard Gibbs energy of anaerobic decomposition of hydrogen sulfide following the equation

$$H_2S(gas) \longrightarrow S + H_2(gas) \quad (22)$$

is 33.44 kJ mol^{-1}, being much smaller than that of water splitting into hydrogen and oxygen (237.2 kJ mol^{-1}).[73] If the process is conducted in water, not only hydrophobic elemental sulfur, but also water-soluble polysulfides can form as products of oxidation of the sulfide anion; this makes hydrogen production even less energy-consuming. Therefore, in some cases production of molecular hydrogen as a result of hydrogen sulfide decomposition can occur without illumination. Nevertheless, the rate of photoassisted hydrogen production from dissolved hydrogen sulfide is always much higher.

The following mechanism of hydrogen production in alkali hydrogen sulfide solutions in the presence of semiconductor photocatalysts is considered substantiated. Irradiation of a semiconductor produces charge carriers (electron and hole) on the semiconductor surface. Photogenerated holes oxidize S^{2-} and HS^{-} ions to the water-soluble disulfide ion[72]

$$2S^{2-} + 2h^{+} \longrightarrow S_2^{2-} \quad (23)$$

$$2HS^{-} + 2h^{+} \longrightarrow S_2^{2-} + 2H^{+} \quad (24)$$

Photogenerated electrons from the conduction band reduce water with the formation of molecular hydrogen

$$2\,H_2O + 2\,e^- \longrightarrow H_2 + 2\,HO^- \quad (25)$$

Unfortunately, the disulfide ions S_2^{2-} produced in the reaction are highly coloured; therefore, they absorb visible light, which decreases the quantum efficiency of photocatalytic hydrogen production.[6] To prevent the undesired action of disulfide ions, water-soluble salts, *e.g.*, sodium sulfide are often added to the reaction mixture. If the solution contains sulfite anions, the reaction

$$S_2^{2-} + SO_3^{2-} \longrightarrow S_2O_3^{2-} + S^{2-} \quad (26)$$

resulting in the water-soluble, colourless anion S^{2-} proceeds. That is why the water-soluble mixture S^{2-}–SO_3^{2-} is most often used for photocatalytic production of hydrogen.[75]

The overall reaction can be described by the equation[76]

$$S^{2-} + SO_3^{2-} + 2\,H_2O \xrightarrow{\text{Phc, } h\nu} H_2 + S_2O_3^{2-} + 2\,OH^- \quad (27)$$

where Phc is photocatalyst.

Photocatalytic hydrogen production from aqueous solutions of organic and inorganic substrates is much more thermodynamically favourable than complete water splitting into hydrogen and oxygen (see above). This underlies higher quantum efficiency of hydrogen production using electron donors that act as 'sacrificial agents'.

III. Main types of heterogeneous semiconductor photocatalysts for visible light-driven production of hydrogen

To date, more than 130 semiconductor materials (*e.g.*, TiO_2, $SrTiO_3$, Nb_2O_5, SiC, CdS, GaP, *etc.*) were tested in UV- and visible light-driven photocatalytic production of hydrogen.[47,77] These include metal oxides, sulfides, oxysilfides and oxynitrides, as well as composites thereof.[22] In most these materials, metals are in the highest oxidation state and have the electronic configuration d^0 or d^{10}, while nonmetals (O, S and N) are in the lowest oxidation state. The conduction band of semiconductors is composed of d- and sp-orbitals of metal cations. The valence band of metal oxides is composed of O2p-orbitals. This feature is responsible for an oxidation electrode potential of photogenerated holes of about +3 V *vs.* NHE or even higher (in the normal state); this is sufficient for the oxidation of water to O_2 (Refs 46 and 78). The valence bands of metal oxysilfides and oxynitrides are composed of S3p-orbitals (and O2p-orbitals), N2p-orbitals (and O2p-orbitals). A typical energy level diagram of the best studied semiconductor photocatalysts is shown in Fig. 4.

In addition to the materials mentioned above, recently considerable attention has been paid to systems based on polymeric graphitic carbon nitride g-C_3N_4 as photocatalysts for water splitting and hydrogen production.[45,79] This material has a band gap of 2.7 eV, while positions of the top of the valence band and the bottom of the conduction band at pH 0 correspond to the electrode potentials of 1.6 and −1.1 V *vs.* NHE.[80]

The activity of semiconductor photocatalysts is enhanced by doping them with metals,[81] by sensitization with organic dyes,[82] by the design of composite structures, *etc.*

III.1. Solid solutions of transition-metal sulfides

The valence band of metal sulfides is usually composed of S3p-orbitals. Therefore, metal sulfides have a narrower band gap compared to metal oxides and a more 'negative position' of the top of the valence band on the electrode potential scale. Platinized cadmium sulfide is the first semiconductor photocatalyst used for visible light-driven production of hydrogen from aqueous solutions of the S^{2-}–SO_3^{2-} system used as electron donor.[18–20,83] Cadmium sulfide is characterized by low solubility in water (solubility product $> 1.6 \times 10^{-28}$ at 25 °C)[84] and has a band gap of 2.4 eV, which corresponds to the energy of green photons ($\lambda \approx 520$ nm). In principle, positions of the valence and conduction

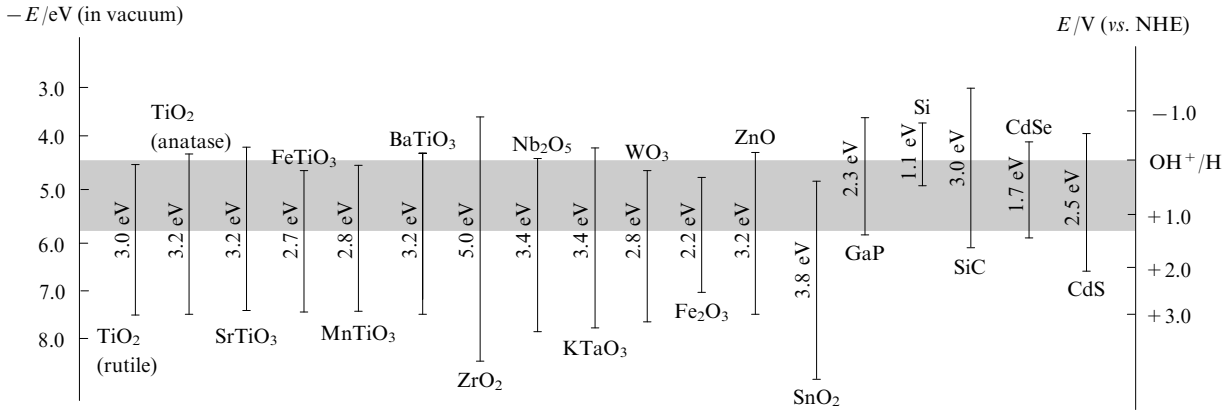


Figure 4. The band gap positions for typical semiconductor catalysts on the absolute scale (on the left) and *vs.* NHE at pH 0 (on the right).[47]

bands of CdS are suitable for visible light-driven photocatalytic production of hydrogen even under water splitting conditions.[22] However, the sulfide ion in solid CdS is readily oxidized by photogenerated holes, which leads to photocorrosion of the material since Cd^{2+} ions go to solution. Note that photocorrosion is a drawback of most solid metal sulfides.

Cadmium sulfide is highly active in visible light-driven photocatalytic production of hydrogen in aqueous solutions of the $S^{2-}-SO_3^{2-}$ system because this system is not only an electron donor, but also protects the catalyst from photocorrosion.

Zinc sulfide is also a highly active photocatalyst for hydrogen production. However, since it has a band gap of 3.6 eV, which corresponds to UV photons ($\lambda \approx 340$ nm), the material is photo-active only under UV irradiation.[22] There are four lines of research aimed at improving the catalytic properties of cadmium sulfide and zinc sulfide:

— synthesis of porous cadmium sulfide with 3D(2D) structure;

— production of mixed solid solutions of cadmium sulfide, zinc sulfide and other transition metal sulfides;

— loading of cocatalysts onto the surface of cadmium sulfide;

— synthesis of catalysts containing cadmium sulfide supported on a porous substrate with 3D structure.

III.1.a. Synthesis of porous cadmium sulfide with 3D(2D) structure

At present, studies on the synthesis of nanostructured hierarchical 3D structures based on cadmium sulfide are developed.[6] Such structures exhibit high activity in hydrogen production owing to the presence of large pores, which improves transport of reactants in suspensions. Besides, if the average linear pore size in the 3D structure is of the order of the visible light wavelength, one deals with multiple reflection of light inside pores, which favours better absorption of light and, as a consequence, increases the quantum efficiency of the target process.

Hierarchical cadmium sulfide with a 3D structure built of beads ~ 5 μm in diameter is three times more active than non-structured CdS nanoparticles in the photocatalytic hydrogen production from aqueous lactic acid solutions under illumination at $\lambda \geqslant 420$ nm.[85]

Mesoporous CdS particles with narrow pore size distribution with a maximum near 5 nm and an average particle size in the range of 4–6 nm were synthesized by template-free deposition of cadmium nitrate with sodium sulfide under sonication.[86] The activity of these particles in photocatalytic hydrogen production from aqueous $Na_2S-Na_2SO_3$ solutions was five times higher than that of the cadmium sulfide particles having no mesoporous structure.

Recently, studies of 2D structures (cadmium sulfide nanotubes) have begun. It was found the CdS nanotubes with high photocatalytic activity in visible light-driven production of hydrogen can be produced under hydrothermal synthesis conditions.[87, 88]

III.1.b. Preparation of mixed solid solutions of cadmium sulfide, zinc sulfide and other transition metal sulfides

Sructural similarity between zinc sulfide and cadmium sulfide leads to ready formation of $Cd_{1-x}Zn_xS$ solid solutions. Besides, the use of ZnS/CdS solid solutions is of interest from a practical point of view because precursors of the photocatalyst, *i.e.*, compounds of cadmium and zinc, are cheap and the band gap can be varied with ease by varying the mole fractions of the components.[47] In particular, a series of $Cd_{1-x}Zn_xS$ samples ($x = 0-0.92$) were prepared by codeposition of zinc and cadmium salts followed by annealing in nitrogen atmosphere.[47] The band gap was varied by varying the mole fractions of the components. Positions of the top of the valence bands and the bottom of the conduction bands of the mixed solid solutions of cadmium sulfide and zinc sulfide are shown in Fig. 5.[47]

As mentioned above, sulfide zinc has a wide band gap, which excludes the possibility of its operation under visible light. By doping and combining ZnS with narrow band-gap semiconductors one can produce materials that are sensitive to visible light. For instance, narrow-band-gap solid solutions $(AgIn)_xZn_{2(1-x)}S_2$ exhibit high photocatalytic activity in visible light-driven ($\lambda > 420$ nm) production of hydrogen from aqueous solutions of the $S^{2-}-SO_3^{2-}$ system used as electron donor.[89] As the Ag^+/Zn^{2+} and In^{3+}/Zn^{2+} mole ratios increase, the absorption edge of the solid solution is monotonically shifted towards the visible region. The dependences of the

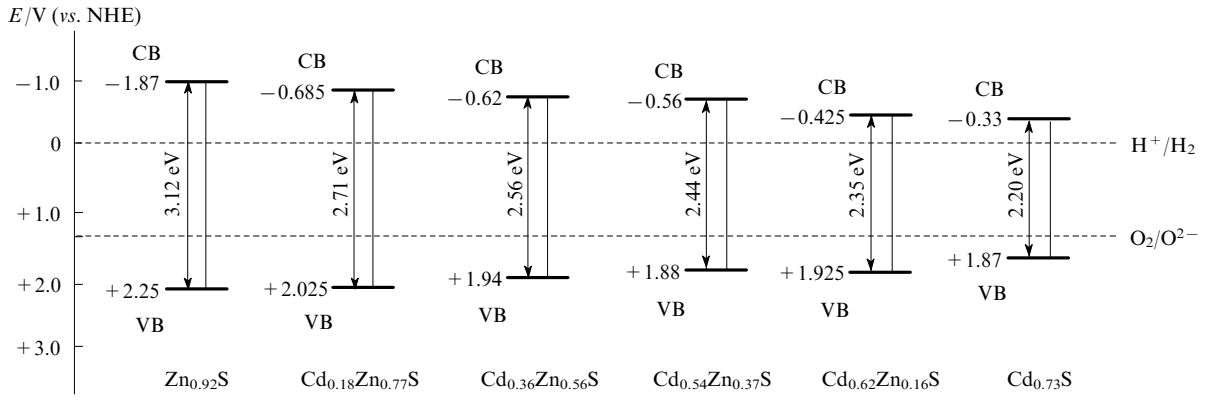


Figure 5. The band gap positions for mixed solid solutions of cadmium sulfide and zinc sulfide.[47]

photophysical and photocatalytic properties on the composition of the semiconductor material are related to changes in positions of the band gap and the conduction band of the ternary solid solution, namely, Ag4d- and S3p-orbitals influence the position of the valence band, while Zn4s- and Zn4p-orbitals as well as In5s- and In5p-orbitals influence the position of the top of the conduction band.

Among promising sulfide photocatalysts, there are mixed zinc and indium sulfides $ZnIn_2S_4$ belonging to the AB_2X_4 family of layered semiconductors. The structure and morphology of the mixed sulfides AB_2X_4 can be varied by varying the conditions of hydrothermal synthesis using different solvents and surfactants.[90] Systematic studies on the influence of the nature of the solvent, surfactant and duration of hydrothermal treatment on the activity of $ZnIn_2S_4$ catalysts in the course of visible light-driven photocatalytic production of hydrogen showed[91–93] that the synthesis of $ZnIn_2S_4$ using cetyltrimethylammonium bromide as surfactant not only leads to enhancement of the photocatalytic activity of the semiconductor, but also causes an increase in the crystallinity of the mixed sulfide as compared to that of the samples prepared using other surfactants. The activity of the Cu-doped $ZnIn_2S_4$ photocatalyst is also enhanced.[94]

III.1.c. Loading of cocatalysts onto the surface of cadmium sulfide

In the early stage of studies on CdS it was found that loading of a cocatalyst (platinum) onto the surface of solid sulfides leads to significant intensification of hydrogen production.[95] Also, titanium dioxide was platinized in order to intensify photocatalytic water splitting.[96] It is believed that noble metals loaded onto the cadmium sulfide surface favour spatial photoseparation of charges *via* the appearance of Schottky barriers and thus preclude recombination of photogenerated electron–hole pairs.[97] Besides, such metals are known to be good catalysts of many electrode processes. All these features cause an increase in the quantum efficiency of various photocatalytic processes.

Loading of metals has a strong effect on the electrochemical properties of semiconductors. If the work function of the metal exceeds that of the semiconductor, an electron is transferred to the metal particle. As a result, a Schottky barrier appears in each metal/semiconductor contact region (platinum is characterized by the highest Schottky barrier because the work function of Pt is higher than that of other metals).[98] The formation of Schottky barriers suppresses recombination of electron–hole pair and increases the efficiency of spatial separation of photogenerated charges.[99] There has been active search for cocatalysts for hydrogen production based on non-noble transition metals, *e.g.*, copper,[100] molybdenum,[101] nickel[102–104] and cobalt.[103] The work function of metals like copper, nickel and molybdenum is lower than that of noble metals; however, in some cases decoration of the surface of CdS samples with NiS nanocrystals is more efficient than loading of platinum or ruthenium.[104]

Molybdenum disulfide belongs to the most active cocatalysts for photocatalytic production of H_2 over cadmium sulfide.[48,105–108] It was found that the rate of visible light-driven photocatalytic hydrogen production

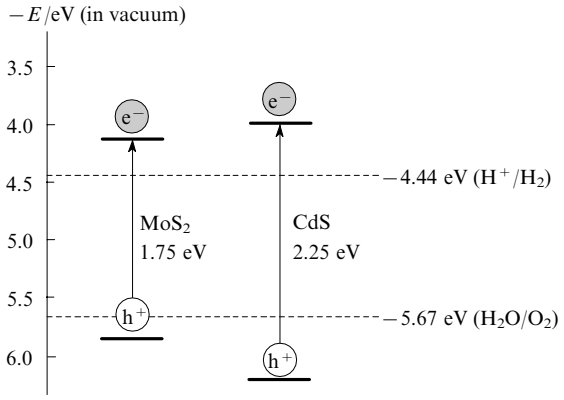


Figure 6. Formation of heterojunctions in MoS_2/CdS system.[109]

over cadmium sulfide increases by a factor of 36 upon loading of MoS_2 (0.2 mass %) compared to the rate of the process proceeding over unloaded CdS. The activity of the MoS_2/CdS composite material appeared to be higher than that of cadmium sulfide loaded with metals including platinum, ruthenium, rhodium, palladium and gold.[107] Loading of molybdenum sulfide onto the surface of cadmium sulfide or $Cd_{1-x}Zn_xS$ solid solution leads to formation of MoS_2/CdS heterojunctions. Under illumination, an electron goes from the valence band to the conduction band of CdS and, since the bottom of the conduction band of molybdenum sulfide is lower than that of cadmium sulfide, a photogenerated electron in CdS can migrate towards MoS_2 particles (Fig. 6) where hydrogen production occurs.[109] The process favours spatial separation of photogenerated electron–hole pairs and thus increases the quantum efficiency of the photocatalytic process. Production of hydrogen on molybdenum disulfide particles *via* reduction of protons is described by the following equations:[109]

$$MoS_2 + e^- + H^+ \longrightarrow HMoS_2 \quad (28)$$

$$HMoS_2 + e^- + H^+ \longrightarrow MoS_2 + H_2 \quad (29)$$

Multiple enhancement of photocatalytic activity upon loading of Cu_xS particles onto the surface of cadmium sulfide particles or $Cd_{1-x}Zn_xS$ solid solution was for the first time reported by Savinov and coworkers.[110,111] They proved that high activity of the composite photocatalysts based on $Cd_{1-y}Zn_yS$ and Cu_xS is due to the formation of p–n-microheterojunctions (Fig. 7). In some cases, this feature causes the photocatalytic activity of copper sulfide-loaded cadmium sulfide to enhance to a greater extent compared to the effect of platinization of CdS.[112,113] High quantum efficiency in photocatalytic hydrogen production was also reported for PbS/CdS systems.[114,115] Enhancement of photocatalytic activity upon loading of lead sulfide onto the cadmium sulfide surface can also be explained by the formation of microheterojunctions.

The activity of WC/CdS photocatalysts in the visible light-driven production of hydrogen from aqueous solutions using the S^{2-}–SO_3^{2-} system as electron donor

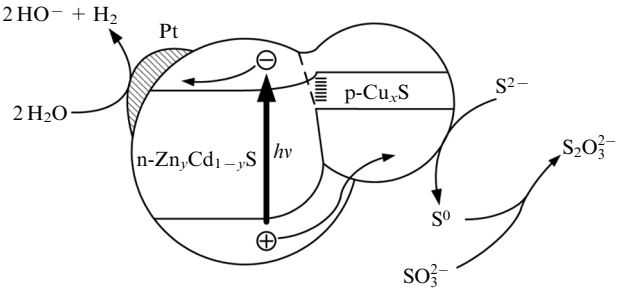


Figure 7. Idealized scheme of photocatalytic hydrogen production in $PtZn_yCd_{1-y}S/Cu_xS$ system.[110]

was comparable with that of Pt/CdS.[116] Similarly to platinum loaded onto the cadmium sulfide surface, tungsten carbide creates active sites on the semiconductor surface and provides fast diffusion of photogenerated electrons from the CdS surface to WC and favours spatial separation of photogenerated charges and, therefore, high photocatalytic activity in the hydrogen production reaction.

A number of recent studies are devoted to correlations between the activity of sulfide photocatalysts and the chemical state of the loaded cocatalysts.[106, 117] For instance, Ran *et al.*[95] studied the effect of the nature of the surface-loaded nickel compounds [Ni, NiO, NiS, $Ni(OH)_2$] on the photocatalytic activity of $Cd_{0.2}Zn_{0.8}S$ in hydrogen production from aqueous triethanolamine solutions. The maximum rate of hydrogen production was achieved using nickel hydroxide as cocatalyst. It is believed that high activity of $Ni(OH)_2/Cd_{0.2}Zn_{0.8}S$ photocatalysts is due to the formation of metallic nickel nanoparticles in the course of photocatalytic hydrogen production. The composite cocatalyst $Ni/Ni(OH)_2$ forming *in situ* has two functions, namely, the loaded metallic phase favours spatial separation of photogenerated charges while the hydroxide catalyzes the dissociation of water.[95]

A comparison of two methods for activation of the solid solution $Cd_{0.5}Zn_{0.5}S$, *viz.*, loading of copper sulfide and incorporation of Cu^{2+} ions into the crystal lattice of $Cd_{0.5}Zn_{0.5}S$, showed[112] that the rate of hydrogen production in the presence of the composite photocatalyst CuS (2 at.%)/$Cd_{0.5}Zn_{0.5}S$ was twice as high as in the presence of the photocatalyst $Cu_{0.02}Cd_{0.49}Zn_{0.49}S$. Also, the rate of hydrogen production over the copper-loaded photocatalysts was higher than in the presence of a reference sample Pt(1 mass %)/$Cd_{0.5}Zn_{0.5}S$. A study[118] of transformations of two copper-based cocatalysts, metallic Cu and $Cu(OH)_2$, loaded on $Cd_{0.3}Zn_{0.7}S$ revealed that both of them are transformed to copper sulfide in the course of photocatalytic hydrogen production. The rate of hydrogen production over $Cu(OH)_2/Cd_{0.5}Zn_{0.5}S$ was higher owing to higher dispersion of *in situ*-forming Cu_xS.

The maximum quantum efficiency and rate of hydrogen production in aqueous solutions of the $S^{2-}-SO_3^{2-}$ system were achieved[114, 115] using sulfide photocatalysts. The quantum efficiency of hydrogen production in the presence of the Pt/PdS/CdS photocatalyst under illumination at $\lambda = 450$ nm is 47% (per H_2 molecule).†

III.1.d. Preparation of catalysts containing cadmium sulfide supported on porous substrate with 3D structure

The quantum efficiency of photocatalytic production of hydrogen over cadmium sulfide nanoparticles can be increased by immobilizing CdS particles on various substrates including Al-HMS molecular sieves,[120] microporous and mesoporous silica gels and zeolite ETS-4.[121, 122] Cadmium sulfide nanoparticles were also incorporated into mesoporous titanium dioxide Ti-MCM-41 in the course of two-step synthesis including treatment of Ti-MCM-41 with a cadmium acetate solution followed by sulfidizing with hydrogen sulfide at 70 °C. The activity of the CdS/Ti-MCM-41 photocatalyst considerably increased due to formation of microheterojunctions between cadmium sulfide and titanium dioxide.[123] Besides, ordered porous structure of Ti-MCM-41 favours better diffusion of reacting substrates towards active sites, *i.e.*, cadmium sulfide nanoparticles.

A great body of information on the photocatalytic activity of CdS-based materials was reported in the last three decades.[48, 76, 95, 105–109, 112–115, 117, 118, 124–142] These data are summarized in Tables 1 and 2. The Φ values were calculated using expression (6). The number of photons emitted by a light source per unit time (N_{ph}) was determined from

$$NS = N_{ph}\phi_i \sum_i h\frac{c}{\lambda_i} \qquad (30)$$

where N is the emission power, S is the surface area of the light spot, ϕ_i is the relative intensity of the ith peak, hc/λ_i is the photon energy, and λ_i is the wavelength corresponding to the ith peak in the emission spectrum of the light source.

Unfortunately, the authors of most publications report only the wavelength at maximum emission. In this case, the i value was set to unity and λ_i was treated as the wavelength at maximum emission. In many studies the quantum efficiency is calculated taking account of the fact that production of molecular hydrogen requires two electrons; therefore, the expression for Φ is augmented with a factor of 2. However, IUPAC recommendations 2011[68] do not relate the parameter 'quantum efficiency' to a particular mechanism of a photoprocess and consider it as simply the ratio of two numbers characterizing the initial action (incident light) and the result (formation of molecular hydrogen). Therefore, a correction factor of 2 associated with the mechanism of formation of molecular hydrogen is redundant.

The highest activity and quantum efficiency in the course of visible light-driven photocatalytic production of hydrogen was achieved using systems based on

† Mention should be made that similar systems, namely, $Pt/Cu_xS/Cd_{1-x}Zn_xS$ were for the first time synthesized and described much earlier at Boreskov Institute of Catalysis, Siberian Branch of the Russian Academy of Sciences (see Refs 110 and 119). These systems also exhibited a record high quantum efficiency of 50% (calculated per H_2 molecule) under illumination at $\lambda = 450$ nm.

Table 1. Summary of data on hydrogen production from aqueous solutions of $S^{2-} - SO_3^{2-}$ mixture in the presence of sulfide photocatalysts.

Photocatalyst [a]	Concentration /mol litre^{-1}		Filter bandpass /nm	W /(μmol H_2) h^{-1} g^{-1}	Φ (%) (see [b])	Ref.
	S^{2-}	SO_3^{2-}				
Light source — 300 W xenon lamp						
$Cu_{1.94}S/Zn_{0.23}Cd_{0.77}S$	0.1	0.1	> 420	7740	2.6	124
5% $Pt/Cu_{1.94}S/Zn_{0.23}Cd_{0.77}S$	0.1	0.1	> 420	13 500	3.2	124
$Cd_{0.2}Zn_{0.8}S$	0.4	0.4	> 420, < 780	3430	8.1	126
0.15% Bi_2S_3/CdS	0.7	1.2	> 400	5500	–	129
0.1% NiS/CdS	0.1	0.1	> 420	1200	–	117
0.2% CoS/CdS	0.1	0.1	> 420	1100	–	117
0.1% CuS/CdS	0.1	0.1	> 420	1000	–	117
1% Pt/CdS	0.1	0.1	> 420	760	–	117
0.1% $NiS/Cd_{0.4}Zn_{0.6}S$	0.1	0.1	> 420	600	–	117
0.1% $CoS/Cd_{0.4}Zn_{0.6}S$	0.1	0.1	> 420	500	–	117
0.1% $CuS/Cd_{0.4}Zn_{0.6}S$	0.1	0.1	> 420	750	–	117
1% $Pt/Cd_{0.4}Zn_{0.6}S$	0.1	0.1	> 420	1210	–	117
1.5% $Ru/(CuIn)_{0.2}Zn_{1.6}S_2$	0.35	0.25	> 430	1000	7.7	131
3% $Pt/AgInZn_{10}S_{18}$	0.35	0.25	> 420	680	–	133
Pt/PdS/CdS	0.5	0.5	> 420	29 200	47	114, 115
PdS/CdS	0.5	0.5	> 420	20 000	32	114, 115
Pt/CdS	0.5	0.5	> 420	16 500	27	114, 115
$Zn_{0.65}Cd_{0.35}S$	0.1	0.1	> 420	97	0.2	113
1% $Pt/Zn_{0.7}Cd_{0.3}S$	0.1	0.1	> 420	387	0.9	113
5.9% $CuS/Zn_{0.65}Cd_{0.35}S$	0.1	0.1	> 420	1830	4.0	113
1% $Pt/5.9\%CuS/Zn_{0.65}Cd_{0.35}S$	0.1	0.1	> 420	2460	5.5	113
$Zn_{0.3}Cd_{0.7}S$	0.05	0.02	> 420	3300	–	134
2% Pt/CdS	0.35	0.25	> 430	1020	12.0	135
1% $Pt/(CuIn)_{0.09}Zn_{1.82}S_2$	0.35	0.25	> 420	2280	6.3	136
Light source — 36 W fluorescent lamp (UV light < 3% with respect to energy)						
0.2% Pt/0.2% $RuS_2/Cd_{0.5}Zn_{0.5}S$	0.3	0.4	–	724	~ 2	125
1% $RuS_2/Cd_{0.5}Zn_{0.5}S$	0.3	0.4	–	616	~ 1.5	125
Light source — 30 mW light-emitting diode (450 nm)						
0.1% $Cu_xS/Cd_{0.3}Zn_{0.7}S$	0.1	0.1	–	8100	14.6	118
0.3% $Cu/Cd_{0.3}Zn_{0.7}S$	0.1	0.1	–	3700	7.2	118
1% $CuS/Cd_{0.3}Zn_{0.7}S$	0.1	0.1	–	3500	6.5 [å]	127
Light source — 350 W xenon lamp						
2% $CuS/Cd_{0.5}Zn_{0.5}S$	0.35	0.25	> 420	4640	10.5	112
$Cu_{0.02}Cd_{0.49}Zn_{0.49}S$	0.35	0.25	> 420	2500	5.9	112
Light source — 150 W xenon lamp						
0.81% CuS/14.7% CdS/ZnS	0.4	0	> 420	838	–	128

Table 1 (contunued).

Photocatalyst [a]	Concentration /mol litre^{-1}		Filter bandpass /nm	W /(μmol H_2) h^{-1} g^{-1}	Φ (%) (see [b])	Ref.
	S^{2-}	SO_3^{2-}				
Light source — 1000 W mercury lamp						
$Cd_{0.3}Zn_{0.7}S$	0.1	0.05	> 420	600	6.5	76
Light source — 500 W xenon lamp						
$Cd_{0.44}Zn_{0.56}S$	0.35	0.25	> 420	2640	–	130
Light source — 300 W tungsten halogen lamp						
2% Pt/$(CuIn)_{0.05}Cd_{1.9}S_2$	0.35	0.25	> 420	2460	13.1	132

[a] Here and in other Tables the photocatalyst compositions are given in mass %. [b] Calculated per H_2 molecule. [c] Estimated by the authors of this review.

Table 2. Summary of data on hydrogen production from aqueous solutions of organic compounds in the presence of sulfide photocatalysts.

Photocatalyst	Solute		Filter bandpass /nm	W /(μmol H_2) h^{-1} g^{-1}	Φ (%) (see [a])	Ref.
	name	concentration (vol.%)				
Light source — 250 W mercury lamp						
0.5% Pt/$Cd_{0.5}Zn_{0.5}S$	Glycerol	10 [b]	> 420	630	–	48, 137
Light source — 400 W metal halide lamp						
0.5% Pt/17% ZnS/$ZnIn_2S_4$	Glucose	1.1	> 420	147	–	48, 138
Light source — 150 W mercury lamp						
0.5% Pt/$Cd_{0.5}Zn_{0.5}S$	Glucose	0.6	> 420	301	–	48, 139
Light source — 750 W xenon lamp						
0.5% Pt/CdS	Methanol	50	> 450	170	–	140
0.5% Pt/CdS	"	1 [b]	> 450	38	–	48, 141
Light source — 500 W mercury lamp						
3.8% Pt/CdS	Methanol	12 [b]	> 400	152	–	48, 142
Light source — 300 W xenon lamp						
0.2% MoS_2/CdS	Methanol	10	> 420	60	0.04 [c]	48, 105
0.2% Pt/CdS	"	10	> 420	25	0.02 [c]	48, 105
0.2% MoS_2/CdS	Ethanol	10	> 420	230	0.2 [c]	48, 105
0.2% Pt/CdS	"	10	> 420	150	0.1 [c]	48, 105
0.2% MoS_2/CdS	Glycerol	10	> 420	370	0.3 [c]	48, 105
0.2% Pt/CdS	"	10	> 420	170	0.1 [c]	48, 105
0.2% MoS_2/CdS	Lactic acid	10	> 420	5300	3.7	48, 105
0.2% Pt/CdS	"	10	> 420	4200	2.9 [c]	48, 105
CdS	"	10	> 420	150	–	48, 106
0.2% MoS_2/CdS	"	10	> 420	5440	–	48, 106
0.2% Pt/CdS	"	10	> 420	4400	–	48, 106
0.2% Ru/CdS	"	10	> 420	3650	–	48, 106
0.2% Rh/CdS	"	10	> 420	2500	–	48, 106
0.2% Pd/CdS	"	10	> 420	1800	–	48, 106

Table 2 (continued).

Photocatalyst	Solute		Filter bandpass /nm	W /(μmol H_2) h^{-1} g^{-1}	Φ (%) (see [a])	Ref.
	name	concentration (vol.%)				
Light source — 300 W xenon lamp						
0.2% Au/CdS	Lactic acid	10	> 420	400	–	48, 106
1% Pt/CdS	"	10	> 420	8170	–	48, 107
1% Pt_3Co/CdS	"	10	> 420	15 900	–	48, 107
1% Co/CdS	"	10	> 420	1070	–	48, 107
1% Pt_3Au/CdS	"	10	> 420	14 900	–	48, 107
1% Pt_3Ni/CdS	"	10	> 420	12 800	–	48, 107
1% Pt_3Cu/CdS	"	10	> 420	3890	–	48, 107
CdS	"	10	> 400	239	–	109
0.2% MoS_2/CdS	"	10	> 400	4060	–	109
0.6% Ni/$Cd_{0.2}Zn_{0.8}S$	Triethanolamine	25	> 420	3240	7.2	95
0.6% NiO/$Cd_{0.2}Zn_{0.8}S$	"	25	> 420	117	0.3	95
0.6% NiS/$Cd_{0.2}Zn_{0.8}S$	"	25	> 420	2510	5.1	95
0.6% $Ni(OH)_2$/$Cd_{0.2}Zn_{0.8}S$	"	25	> 420	7160	14.8	95
1% Pt/$Cd_{0.2}Zn_{0.8}S$	"	25	> 420	6080	12.6	95

[a] Calculated per H_2 molecule. [b] In mol $litre^{-1}$. [c] Estimated by the authors of this review.

mixed transition metal sulfides. To date, quantum efficiencies of the order of 50% (calculated per H_2 molecule) and specific activities of the order of tens mmol H_2 h^{-1} g^{-1} have been reported. Most publications are devoted to studies on the activity of sulfide photocatalysts in hydrogen production in aqueous solutions of the $S^{2-} - SO_3^{2-}$ system used as electron donor. Recently, other organic substances such as ethanol,[105] glycerol[105, 137] and glucose[138, 139] have been utilized. Also, there has been a trend towards replacement of noble metals as cocatalysts. Indeed, high-platinum-loaded Pt/CdS photocatalysts widely used[140 – 142] for visible light-driven production of hydrogen in the 1980s and 1990s are now replaced by copper, molybdenum or nickel sulfide-loaded $Cd_{1-x}Zn_xS$ and CdS solid solutions, which reduces the cost of the photocatalysts.[95, 102, 105, 106, 117] It should be noted that the data presented in Tables 1 and 2 make it possible to compare the rates of hydrogen production. Usually, the rate of this process is proportional to the light intensity; therefore, it seems to be most appropriate to compare the quantum efficiencies of photocatalytic systems. Unfortunately, quantum efficiency calculations for hydrogen production in many systems reported in the literature are difficult because no data on the intensity of incident light were presented.[46]

III.2. Photocatalysts based on nanostructured titanium dioxide

Among various materials used as photocatalysts of hydrogen production, titanium dioxide attracts particular attention because it is light resistant, relatively cheap and available, and nontoxic.[22, 143] At present, limited use of pure TiO_2 in photocatalytic production of hydrogen is mainly due to the lack of sensitivity to visible light owing to a wide band gap of 3.2 eV corresponding to UV photons ($\lambda \approx 390$ nm, see Fig. 4). In particular, this makes titanium dioxide inefficient for helioenergetics applications.

At present, considerable efforts have been devoted to sensitization of titanium dioxide in the visible region. Main lines of research in this field are as follows:

— doping TiO_2 with metal atoms and ions;[144, 145]
— doping TiO_2 with nonmetal atoms; and
— partial reduction of TiO_2.[48, 146, 147]

In all these cases, one should preferably use methods suitable for uniform modification of titanium dioxide particles and leading to the appearance of new electron energy levels (mainly local ones) that will be uniformly distributed in the bulk of the material. Doping titanium dioxide usually leads to production of rather highly coloured materials that absorb visible light. Unfortunately, colouration does not guarantee efficient operation of photocatalysts under irradiation with visible light because additional absorption is often due to the presence of isolated absorption sites.[48, 148]

Below we consider main methods used to shift the absorption edge of titanium dioxide to the visible region.

III.2.a. Doping with metal atoms and ions

Most often, metal cations are incorporated into the titanium dioxide structure during the growth of the primary TiO_2 particles by adding appropriate dopants to the precursor reaction mass.[146] Besides, post-syn-

thesis methods of doping with metal cations have been reported.[48, 149]

Metal cations in a 4+ oxidation state can replace Ti^{4+} cations with no changes in the overall electroneutrality of the system. Doping with metal cations in lower oxidation states causes formation of oxygen vacancies and segregation of cations on the surface of TiO_2 particles. If the oxidation state of the dopant metal cations is higher than 5+, additional oxygen anions are required to maintain the charge balance.[48] Unfortunately, the shift of the TiO_2 absorption edge upon doping with metal cations with the formation of point defects (*e.g.*, oxygen vacancies) can be accompanied by abrupt acceleration of recombination of photogenerated charges and, therefore, a decrease in the quantum efficiency of photocatalytic processes.

There are a few publications on photocatalytic hydrogen production over metal-doped titanium dioxide. For instance, hydrothermal synthesis of titanium dioxide doped with iron and(or) nickel atoms in a zero oxidation state, Fe–Ni@TiO_2, was reported.[150] The highest efficiency was achieved in the case of simultaneous doping with iron and nickel atoms resulting in the formation of two impurity levels. This favours spatial separation of photogenerated charges and an increase in the quantum efficiency.

Silver deposition onto titanium dioxide doped with iron and nickel was studied.[151] An Ag/Fe–Ni@TiO_2 photocatalyst was synthesized by adding aqueous solutions of silver, iron and nickel salts in the course of hydrolysis of titanium tetrabutoxide.[151] It was found that iron and nickel atoms are incorporated into the titanium dioxide lattice, while most silver atoms are located on the surface of TiO_2 and 'collect' electrons necessary to produce molecular hydrogen. The activity of the Fe–Ni@TiO_2 photocatalyst can be doubled using silver-deposited samples.[150, 151]

A study[152] of co-doping titanium dioxide with nitrogen atoms and metal cations (Cr^{5+}, Co^{2+}, Ni^{2+} or Cu^{2+}) showed that the activity of M–N@TiO_2 photocatalysts in hydrogen production from aqueous glycerol solutions enhances from chromium to copper, namely, Cr < Co < Ni < Cu. It was found that nitrogen atoms and metal cations incorporated into the TiO_2 lattice cause a shift of TiO_2 absorption edge to the visible region and modulation of TiO_2 photoluminescence.

III.2.b. Doping with nonmetal atoms

Doping with nonmetals of different nature (nitrogen, sulfur, fluorine) is a widely used method for sensitization of titanium dioxide.[153–158] The most pronounced effect was achieved upon replacement of oxygen by nitrogen, *viz.*, the interaction of N2p-orbitals with O2p-orbitals causes the energy level of the top of the valence band of titanium dioxide to increase *via* the appearance of new energy levels and, correspondingly, narrow the band gap of the catalyst. Usually, nitrogen-containing photocatalysts are synthesized by sintering titanium dioxide and a nitrogen-containing compound, *e.g.*, urea.[153, 158] Unfortunately, usually the amount of nitrogen incorporated into the crystal lattice of TiO_2 is small.[153, 159] The nitrogen content in the structure of titanium dioxide can be increased using the sol–gel technique and surfactants as structure-forming agents.[160] Nitrogen-containing photocatalysts thus synthesized showed much higher activity than Degussa P25 catalyst in photocatalytic hydrogen production from aqueous methanol solutions under illumination at $\lambda > 400$ nm.

Doping TiO_2 with sulfur also enhances the activity of catalysts in visible light-driven hydrogen production.[157] In this case, the TiO_2 absorption edge is shifted from 290 to 540–570 nm (to the visible region).[158] Sulfur-containing titanium dioxide was synthesized by the sol–gel method and by mixing titanium dioxide with thiourea followed by calcination.[158] The TiO_2 absorption edge was shifted to 570 nm in the former and to 540 nm in the latter case. The photocatalysts prepared by mixing were more active in the photocatalytic oxidation of trichloroethylene and dimethy sulfide in the gas phase. Unfortunately, these photocatalysts were not tested in the hydrogen production reactions.[158]

Another method to shift the absorption edge of titanium dioxide is to sensitize the system by coating the TiO_2 surface with various organic dyes and metal complexes.[158–167] For instance, Eosin-sensitized nitrogen-doped TiO_2 was more efficient than nitrogen-doped TiO_2 (Table 3).[161]

III.2.c. Partial reduction of titanium dioxide

Partial reduction of TiO_2 with the formation of Ti^{3+} cations and oxygen vacancies, *i.e.*, 'self-doping' of titanium dioxide resulting in 'black' titanium dioxide also makes TiO_2 sensitive to visible light.[162] 'Self-doping' usually takes a period of 5 days in severe reduction conditions (H_2 atmosphere; a pressure of 20 bar, 200 °C). Platinum-loaded 'black' titanium dioxide exhibited very high photocatalytic activity, *viz.*, to 10 (mmol H_2) h^{-1} g^{-1} at $\Phi \approx 6\%$ (calculated per H_2 molecule) in hydrogen production from aqueous methanol solutions under solar-simulated radiation. Long-term cyclic experiments on photocatalytic production of hydrogen were carried out over a period of 20 days.[163] The TON value calculated using expression (5) was 160. This proves that 'black' titanium dioxide is a photocatalyst rather than an electron donor used for hydrogen production.

A method for the synthesis of 'black' titanium dioxide in milder conditions (reduction in H_2 atmosphere at 250 or 500°C and normal pressure) was proposed.[164, 165] Reduced gold- and(or) platinum-loaded anatase thus prepared was also highly active in hydrogen production in aqueous ethanol and glycerol solutions under solar-simulated radiation. Nevertheless, the activity of platinum-loaded reduced titanium dioxide in photocatalytic hydrogen production from aqueous ethanol solutions under irradiation at $\lambda > 420$ nm was relatively low, being at most 0.05 (mmol H_2) h^{-1} g^{-1}; this is 24 times lower than the activity of the 1% Pt/TiO_{2-x} photocatalysts and solar-simulated radiation at the same initial concentration of ethanol.[164]

An analysis of data on hydrogen production in the presence of TiO_2-based photocatalysts (see Table 3) showed that even using high-precision methods of synthesis of, *e.g.*, 'black' titanium dioxide, the photocatalytic activity of such materials under irradiation with

Table 3. Summary of data on hydrogen production from aqueous solutions of organic compounds using photocatalysts based on titanium dioxide.

Photocatalyst	Solute		Filter bandpass /nm	W /(μmol H_2) h^{-1} g^{-1}	Φ (%) (see [a])	Ref.
	name	concentration (vol.%)				
Light source — 500 W xenon lamp						
Fe/TiO_2	Ethanol	10	> 400	248	0.1 [b]	151
Ni/TiO_2	"	10	> 400	205	0.1 [b]	151
Ag/TiO_2	"	10	> 400	265	0.1 [b]	151
$Fe–Ni/TiO_2$	"	10	> 400	348	0.1 [b]	151
$Fe/Ag/TiO_2$	"	10	> 400	512	0.1 [b]	151
$Ni/Ag/TiO_2$	"	10	> 400	336	0.1 [b]	151
$Fe–Ni/Ag/TiO_2$	"	10	> 400	793	0.2	151
Light source — medium pressure 450 W mercury lamp						
$Cr–N@TiO_2$	Glycerol	10	–	126	–	152
$Co–N@TiO_2$	"	10	–	313	–	152
$Ni–N@TiO_2$	"	10	–	506	–	152
$Cu–N@TiO_2$	"	10	–	1615	–	152
Light source — xenon lamp (visible light intensity 100 mW cm^{-2})						
1.5% $Au@TiO_2$ (nanotubes)	Methanol	25	> 400	482	0.1 [b]	48, 166
1.5% Au/TiO_2 (nanotubes)	"	25	> 400	223	0.1 [b]	48, 166
Light source — medium pressure 400 W mercury lamp						
0.5% $Pt–N–TiO_2$	Triethanolamine	11	> 420	80	–	161
0.5% $Pt–N–TiO_2$ with adsorbed Eosin Y dye	"	11	> 420	575	–	161
0.5% $Au–0.5\%$ Pt/TiO_{2-x}	Ethanol	50	> 420	20	2.0	164
1% Au/TiO_{2-x}	"	50	> 420	17	1.7	164
1% Pt/TiO_{2-x}	"	50	> 420	46	4.6	164
Light source — 150 W xenon lamp						
1% $Au–1\%$ Pt/TiO_{2-x}	Ethanol	50	> 300	1100	–	164
0.5% $Au–0.5\%$ Pt/TiO_{2-x}	"	50	> 300	1700	–	164
1% Pt/TiO_{2-x}	"	50	> 300	1100	–	164
1%Au/TiO_{2-x}	"	50	> 300	800	–	164
1% $Au–1\%$ Pt/TiO_{2-x}	Glycerol	7.3	> 300	1300	–	164
0.5% $Au–0.5\%$ Pt/TiO_{2-x}	"	7.3	> 300	700	–	164
1% Pt/TiO_{2-x}	"	7.3	> 300	700	–	164
1%Au/TiO_{2-x}	"	7.3	> 300	500	–	164
Light source — 300 W xenon lamp						
0.1% Pt/TiO_{2-x}	Methanol	25	> 400	50	0.4	48, 167

[a] Calculated per H_2 molecule. [b] Estimated by the authors of this review.

visible light is much lower than that of the photocatalysts based on cadmium sulfide. This can be explained by the fact that doping titanium dioxide with metals and nonmetals causes the formation of impurity centres where recombination of photogenerated electron – hole pairs can occur.[48] Besides, the reduction potential of titanium dioxide (position of the bottom of the conduction band) is about −0.1 V

vs. NHE (see Fig. 4), which is insufficient for efficient production of hydrogen.

III.3. Materials based on polymeric g-C_3N_4 and carbon-based photocatalysts

III.3.a. Polymeric g-C_3N_4

Polymeric graphitic carbon nitride is one of the most widely used non-oxide and(or) non-sulfide photocatalysts, which was thoroughly considered in numerous recent reviews.[79,168–171] The structure of g-C_3N_4 is shown in Fig. 8. It exhibits the properties of a semiconductor with a band gap of 2.7 eV ($\lambda \approx 460$ nm) and the energy levels of the top of the valence band and the bottom of the conduction band lie at +1.6 and −1.1 V *vs*. NHE, respectively. The latter value is one of the most negative for the known semiconductor photocatalysts (see Fig. 4). Besides, g-C_3N_4 is stable in acidic and alkaline media below 700 °C and can be synthesized from readily available nitrogen-containing organic substances, namely, cyanamides, melamine and carbamide.

Traditionally, g-C_3N_4 is synthesized by thermal condensation of nitrogen-rich organic precursors. Nevertheless, the photocatalytic activity of g-C_3N_4 thus obtained is usually low due to fast recombination of photogenerated electron–hole pairs. Main approaches developed to enhance the activity of photocatalysts based on g-C_3N_4 are as follows:[79]

— synthesis of nanosized layers of 2D-structured g-C_3N_4;

— design of heterostructures based on g-C_3N_4;

— doping with metals and nonmetals; and

— choice of active cocatalyst.

III.3.b. Synthesis of nanosized layers of 2D-structured g-C_3N_4

Intensive research into 2D-structured materials of graphene and layered MoS_2 type generated considerable interest in ultrathin (a few atomic layers thick) g-C_3N_4. The electronic, surface and optical properties of g-C_3N_4 differ considerably from those of its bulk analogues. Great attention was paid to the use of ultrathin samples of g-C_3N_4 for visible light-driven photocatalytic production of hydrogen. A relatively simple method for the synthesis of ultrathin (2 nm thick) samples of g-C_3N_4 is to carry out thermal oxidative etching of bulk g-C_3N_4 in air.[173] The specific surface area of a sample of 2D g-C_3N_4 synthesized in this manner exceeded a value of 300 m^2 g^{-1} and the band gap appeared to be 0.2 eV larger than that of bulk g-C_3N_4 due to the quantum size effect. It was established that the lifetime of photogenerated charges in ultrathin g-C_3N_4 increases. A threefold increase in activity in the photocatalytic hydrogen production from aqueous triethanolamine solutions on going from 3D samples of g-C_3N_4 to ultrathin (0.4 nm) 2D samples was reported.[119]

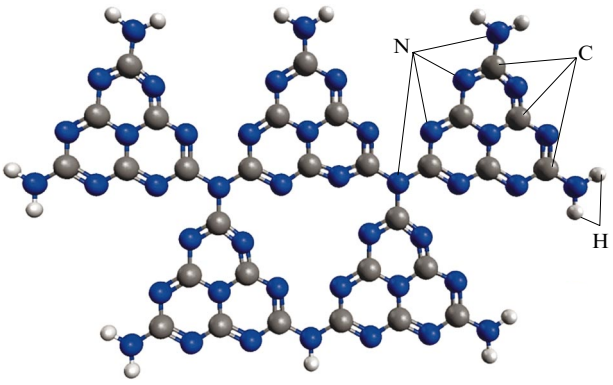


Figure 8. Structure of polymeric graphitic carbon nitride.[172]

III.3.c. Design of heterostructures based on g-C_3N_4

The synthesis of composite photocatalysts with semiconductor/semiconductor heterojunctions has become a routine method for enhancement of the photocatalytic activity of materials.[174] As applied to g-C_3N_4, systems with Cu_2O/g-C_3N_4,[175] graphene/g-C_3N_4,[176] CdS/g-C_3N_4,[177] and TiO_2/g-C_3N_4 (Ref. 178) heterojunctions can be synthesized. Besides, one can prepare two-phase g-C_3N_4/g-C_3N_4 photocatalysts composed of polymeric graphitic carbon nitride obtained using two different precursors.[179,180] The formation of heterojunctions between untreated and sulfidized g-C_3N_4 was reported.[181] This also favours spatial separation of photogenerated charges and thus an increase in the quantum efficiency of photocatalysts.

Although visible light-driven photocatalytic hydrogen production using graphitic carbon nitride as photocatalyst is characterized by high activity and quantum efficiency, in most cases the attainment of high photocatalytic activity requires samples with high platinum content (Table 4).

III.4. Nitrides and oxynitrides

Among photocatalysts of light-assisted splitting of water, there are also d^{10}-metal nitrides.[46,191] For instance, GaN (Ref. 192) and Ge_3N_4 (Ref. 193) are active in water splitting into oxygen and hydrogen under UV irradiation.

Most individual metal nitrides are active under UV irradiation. However, solid solutions GaN–ZnO or gallium-zinc oxynitride $(Ga_{1-x}Zn_x)(N_{1-x}O_x)$ are also active under irradiation with visible light. The absorption edges of individual components are in the UV region;[194] however, owing to p–d electron repulsion ($N_{2p}-Zn_{3d}$ electrons) the top of the valence band in the solid solution GaN–ZnO, which is composed of N2p-orbitals, is shifted upward, thus causing the band gap to decrease.[22] Solid solutions of gallium nitride and zinc oxide are prepared by high-temperature treatment of a mixture of zinc oxide and gallium oxide with ammonia at 850–950 °C. Loading of $Rh_{2-x}Cr_xO_3$ cocatalysts on the surface of GaN–ZnO allows one to achieve a a quantum efficiency of 3.0% (calculated per H_2 molecule) and a hydrogen production rate of 800 [(μmol H_2) h^{-1} g^{-1}] upon illumination at $\lambda = 420$–440 nm.[195]

It should be noted that oxynitrides considered in this Section are mainly used for complete splitting of water into hydrogen and oxygen. As far as we know there are no publications devoted to application of oxynitrides for hydrogen production from aqueous solutions of organic and inorganic electron donors.

Table 4. Summary of data on hydrogen production in aqueous solutions of organic compounds using photocatalysts based on g-C_3N_4.

Photocatalyst	Solute		Filter bandpass /nm	W /(μmol H_2) h^{-1} g^{-1}	Φ (%) (see [a])	Ref.
	name	concentration (vol.%)				
Light source — 350 W xenon lamp						
0.5% $Ni(OH)_2$/g-C_3N_4	Triethanolamine	10	> 400	152	0.6	79, 181
1.0% Pt/g-C_3N_4	"	10		164	0.6 [b]	79, 181
Light source — 300 W xenon lamp						
6% Pt/g-C_3N_4	Triethanolamine	10	> 440	13	–	182
6% Pt/C_3N_4 (amorph.)	"	10	> 440	158	–	182
3% Pt/2D-g-C_3N_4 (nanolayers)	"	10	> 400	3790	–	183
3% Pt/g-C_3N_4	"	10	> 420	1010	1.3	184
3% Pt/15% graphene/g-C_3N_4	"	10	> 420	2180	2.7	184
$Co(OH)_2$/EY-RB/g-C_3N_4 (see [c])	"	10	> 420	7170	17	187
$Co(OH)_2$/EY/g-C_3N_4	"	10	> 420	4330	10 [b]	187
$Co(OH)_2$/RB/g-C_3N_4	"	10	> 420	2830	6.5 [b]	187
0.2% MoS_2/g-C_3N_4	Lactic acid	10	> 420	1350	1.1	79, 189
2% Pt/g-C_3N_4	"	10	> 420	1050	0.8 [b]	79, 189
0.5% MoS_2/g-C_3N_4	"	10	> 420	1030	0.8 [b]	79, 189
0.5% Pt/g-C_3N_4	"	10	> 420	240	0.2 [b]	79, 189
0.5% WS_2/g-C_3N_4	"	10	> 420	340	0.3 [b]	79, 189
g-C_3N_4	Triethanolamine	15	> 420	2	~0 [b]	79, 190
1.25% NiS/g-C_3N_4		15	> 420	482	1.0	79, 190
Light source — 150 W xenon lamp						
1% Pt/g-C_3N_4	Triethanolamine	10	–	502	–	185
1% Pt/1.5% β-$Ni(OH)_2$/g-C_3N_4	"	10	–	954	–	185
Light source — 3 W light-emitting diode (420 nm), 4 items						
g-C_3N_4	Lactic acid	10	–	3	–	186
3% MoS_2 (crystalline)/g-C_3N_4	"	10	–	50	–	186
3% MoS_x (amorph.)/g-C_3N_4	"	10	–	273	–	186
Light source — 500 W xenon lamp						
g-C_3N_4	Methanol	25	> 420	9	–	79, 188
1% Ag/g-C_3N_4	"	10	> 420	101	–	79, 188

[a] Calculated per H_2 molecule. [b] EY is Eosin yellow dye and RB is Bengal rose dye. [c] Estimated by the authors of this review.

III.5. Composite materials

As mentioned above, photocatalysts based on titanium dioxide have attracted considerable attention because the material is stable, nontoxic and highly active when exposed to UV light. Titanium dioxide is mainly used for photocatalytic purification of water from hazardous organics (*via* complete oxidative mineralization of the organics) rather than photocatalytic hydrogen production.[196–199] In addition to doping TiO_2 with nonmetal atoms[153–158] (see Section III.2), a promising way to shift the absorption band of TiO_2-based systems to the visible region is to compose heterostructures using titanium dioxide and a narrower-band-gap semiconductor. A promising narrow band-gap semiconductor is CdS; however, this material is of limited use as photocatalyst because it is prone to photocorrosion.[23] To improve the stability of cadmium sulfide and to simultaneously make titanium dioxide more sensitive to visible light, it was proposed to fabricate a structure with a heterojunction between the two semiconductors. Indeed, the formation of heterojunctions at contacts between them may retard recombination of photogenerated electrons and holes and thus increase the effective quantum yield of photocatalytic processes.[51,200–202] Systems containing CdS-loaded titanium dioxide were used for photocatalytic hydrogen produc-

tion[203–205] and for aerobic oxidation of various organic dyes.[200]

Specific features of the synthesis and heat treatment of multiphase composite sulfide photocatalysts $Cd_{1-x}Zn_xS$ and $Cd_{1-x}Zn_xS/\beta$-$Zn(OH)_2/\varepsilon$-$Zn(OH)_2$/ZnO were studied and the method for their preparation was optimized.[206,207] The activity of these photocatalysts was studied taking visible light-driven hydrogen production from aqueous ethanol solutions using a high-pressure mercury lamp with a cutoff filter ($\lambda > 420$ nm) and a LED emitting monochromatic light at 450 nm. The highest photocatalytic activity was achieved with the multiphase catalysts $Cd_{1-x}Zn_xS/Zn(OH)_2/ZnO$ and $Cd_{1-x}Zn_xS/Zn(OH)_2$. For instance, $Cd_{0.6}Zn_{0.4}S/\varepsilon$-$Zn(OH)_2$ [2260 (μmol H_2) h^{-1} quantum efficiency of 5.2% per H_2 molecule] appeared to be four times more active than corresponding single-phase solid solution of cadmium sulfide and zinc sulfide under identical conditions.[207]

According to quantum chemical calculations, position of the bottom of the conduction band of zinc hydroxide is more appropriate for hydrogen production than that of zinc oxide; correspondingly, ε-$Zn(OH)_2$ as component of composite photocatalyst is more efficient than ZnO (Fig. 9).

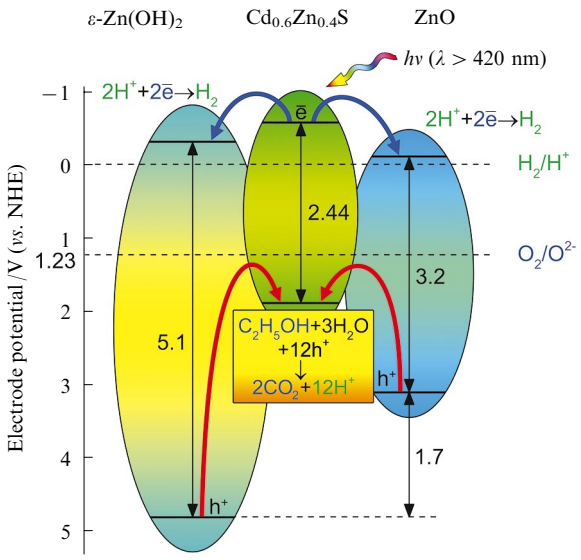


Figure 9. Schematic diagram of heterojunctions in the composite photocatalyst $Cd_{0.6}Zn_{0.4}S/ZnO/Zn(OH)_2$.[207]

There is a considerable body of data on visible light-driven photocatalytic hydrogen production from aqueous solutions of organic and inorganic electron donors over composite semiconductor photocatalysts;[208–223] they are summarized in Tables 5 and 6. The photocatalytic activity reaches a value of 14 (mmol H_2) h^{-1} g^{-1} for systems with organic electron donors and 33 (mmol H_2) h^{-1} g^{-1} for the sulfide–sulfite system, being higher than the activity achieved using single-phase solid solutions of metal sulfides in identical conditions.

It should be noted that multiphase composite semiconductor photocatalysts with heterojunctions used to drive hydrogen production from aqueous solutions of organic compounds are combined with rather simple cocatalysts containing noble metals (usually, metal content is less than 3 mass %). Photocatalysts based on CdS and $Cd_{1-x}Zn_xS$ containing zinc oxides and hydroxides[206,207,210] or cadmium tungstate[212] as admixtures exhibit higher activity than difficult-to-prepare photocatalysts based on graphitic carbon nitride (see Table 4). Interestingly, composite materials prepared from g-C_3N_4 and transition metal sulfides exhibit very high activity [up to 33400 (μmol H_2) h^{-1} g^{-1}] and quantum efficiency (up to 23.4%, see Table 6).[221]

Table 5. Summary of data on hydrogen production in aqueous solutions of organic substrates using composite semiconductor photocatalysts.

Photocatalyst	Solute		Filter bandpass /nm	W /(μmol H_2) h^{-1} g^{-1}	Φ (%) (see [a])	Ref.
	name	concentration (vol.%)				
Light source — 300 W xenon lamp						
CdS/g-C_3N_4	Triethanolamine	10	> 420	77	–	208
6% NiS/ CdS/g-C_3N_4	"	10	> 420	2560	–	208
9% NiS/g-C_3N_4	"	10	> 420	128	–	208
5% Ru/ZnS/CdS	Ethanol	10	> 420	2800	5.5 [b]	48, 209
	Methanol	10	> 420	4900	8.5 [b]	48, 209
	Formic acid	10	> 420	5800	10 [b]	48, 209
CdS/$CdWO_4$	Lactic acid	10	> 420	9170	3.2 [b]	212
0.5% Pt/CdS/$CdWO_4$	"	10	> 420	14000	4.9 [b]	212
0.2% Au/g-C_3N_4–TiO_2 P25	Methanol	30	> 420	219	–	213
g-C_3N_4/0.2% Au/TiO_2 P25	"	30	> 420	253	–	213
3% Pt/FeO_x/g-C_3N_4	Triethanolamine	30	> 420	1080	2.7	214

Table 5 (continued).

Photocatalyst	Solute		Filter bandpass /nm	*W* /(μmol H_2) h^{-1} g^{-1}	*Φ* (%) (see [a])	Ref.
	name	concentration (vol.%)				
Light source — 300 W xenon lamp						
TiO_2 P25/5.0% g-C_3N_4	Methanol	25	> 400	103	–	215
B@TiO_2/5.0% g-C_3N_4	"	25	> 400	473	–	215
3% Pt/30% $W_{18}O_{49}$/g-C_3N_4	Triethanolamine	10	> 420	74	0.9	216
Light source — 30 W light-emitting diode (450 nm)						
10% $Zn(OH)_2$(amorph.)/ $Cd_{0.3}Zn_{0.7}S$	Ethanol	10	–	72	0.2	210
1% Pt/10% $Zn(OH)_2$(amorph.)/ $Cd_{0.3}Zn_{0.7}S$	"	10	–	1240	3.1	210
1% Pt/$Cd_{0.4}Zn_{0.65}$/ε-$Zn(OH)_2$	"	10	–	2260	5.2	207
Light source — high pressure 1000 W mercury lamp						
1% Pt/$Cd_{0.2}Zn_{0.8}S$/ZnO/ ε-$Zn(OH)_2$	Glycerol	1 [c]	> 420	252	3.5	206
Light source — 500 W mercury-xenon lamp						
Pt/$Cd_{0.6}Zn_{0.4}S$/γ-$Zn(OH)_2$	Glycerol	50	> 418	239	–	211

[a] Calculated per H_2 molecule. [b] Estimated by the authors of this review. [c] In mol $litre^{-1}$.

Table 6. Summary of data on hydrogen production in aqueous solutions of S^{2-} – SO_3^{2-} system in the presence of composite semiconductor photocatalysts.

Photocatalyst	Concentration /mol $litre^{-1}$		Filter bandpass /nm	*W* /(μmol H_2) h^{-1} g^{-1}	*Φ* (%) (see [a])	Ref.
	S^{2-}	SO_3^{2-}				
Light source — 400 W xenon lamp						
ZnO/Pt/20% CdS	0.1	0.1	–	6880	3.4	217
ZnO/20% CdS	0.1	0.1	–	1320	0.7	217
$(TiO_2)_{0.17}(NiO)_{0.83}/Cd_{0.8}Zn_{0.2}S$	0.1	0.1	> 395	1600	1.5	220
NiO/$Cd_{0.8}Zn_{0.2}S$	0.1	0.1	> 395	810	0.7	220
TiO_2/$Cd_{0.8}Zn_{0.2}S$	0.1	0.1	> 395	30	0.03	220
Light source — 300 W xenon lamp						
$CdLa_2S_4$/20% g-C_3N_4	0.1	0.5	> 420	5990	0.6	218
$CdLa_2S_4$	0.1	0.5	> 420	779	3.6	218
3% g-C_3N_4/10% CuS/CdS	0.35	0.25	> 420	1150	8.3	219
10% CuS/CdS	0.35	0.25	> 420	572	4.1 [b]	219
3% g-C_3N_4/CdS	0.35	0.25	> 420	492	36 [b]	219
3% Pt/32% $Cd_{0.5}Zn_{0.5}S$/g-C_3N_4	0.35	0.15	> 420	33 400	23.4	221
3% Pt/$Cd_{0.5}Zn_{0.5}S$	0.35	0.15	> 420	3640	2.6 [b]	221
3% Pt/g-C_3N_4	0.35	0.15	> 420	1220	0.9 [b]	221
$Mn_{0.8}Cd_{0.2}S$	0.1	0.5	> 420	1200	0.7	222
0.75%Pt/$Mn_{0.8}Cd_{0.2}S$	0.1	0.5	> 420	3800	2.0 [b]	222
$Mn_{0.8}Cd_{0.2}S$/10%g-C_3N_4	0.1	0.5	> 420	4000	2.1	222

Table 6 (continued).

Photocatalyst	Concentration /mol litre^{-1}		Filter bandpass /nm	W /(μmol H_2) h^{-1} g^{-1}	Φ (%) (see [a])	Ref.
	S^{2-}	SO_3^{2-}				
Light source — 300 W xenon lamp						
1.2% MoS_2-graphene/$ZnIn_2S_4$	0.25	0.25	> 420	3570	–	223
1% Pt/$ZnIn_2S_4$	0.25	0.25	> 420	1530	–	223
Light source — 30 W light-emitting diode (450 nm)						
20% $Zn(OH)_2$(amorph.)/$Cd_{0.3}Zn_{0.7}S$	0.1	0.1	–	7930	19.9	210
1% Pt/20% $Zn(OH)_2$(amorph.)/ $Cd_{0.3}Zn_{0.7}S$	0.1	0.1	–	7470	18.3	210

[a] Calculated per H_2 molecule. [b] Estimated by the authors of this review.

IV. Key factors influencing the activity of semiconductor photocatalysts for hydrogen production from aqueous solutions

IV.1. Structure, morphology and size of photocatalyst particles

The activity of semiconductor photocatalysts in hydrogen production from aqueous solutions depends strongly on their structure and morphology, which in turn depend on specific features of the method for the synthesis of the photocatalysts. For instance, by varying the temperature of different stages of the synthesis of nanosized photocatalysts one can produce materials with different structure, habit and crystallite size.[224] The morphology of photocatalysts is also strongly influenced by the pH of the mother solution,[225, 226] as well as by the nature of solvents and surfactants used in the synthesis.[191]

Consider how the synthesis conditions affect the morphology and photocatalytic activity of $CdIn_2S_4$ solid solution during visible light-driven hydrogen production.[227]

In the course of synthesis of $CdIn_2S_4$ the time of hydrothermal treatment at 150 °C was varied from 8 to 30 h; in some cases, metal sulfides were deposited in the presence of surfactants (polyvinylpyrrolidone or cetyltrimethylammonium bromide). Data on the synthesis of $CdIn_2S_4$, morphological features and activity of photocatalysts are collected in Table 7. Figure 10 presents a number of SEM images (SEM is scanning electron microscopy) of the $CdIn_2S_4$ photocatalysts synthesized in hydrothermal treatment conditions. As can be seen, the addition of surfactants during the synthesis causes modification of the morphology of the nanostructures. There is a threefold variation of the photocatalytic activity of the same crystalline polymorph of $CdIn_2S_4$, which substantiates the assumption that both the structure and morphology have strong effect on the activity of semiconductor catalysts.[223]

The particle size of disperse semiconductor photocatalysts is of importance.[228, 229] Due to the quantum size effect the band gap increases as the semiconductor particle size decreases to a critical value (Bohr radius).[6] In particular, the band gap in CdS changes from 2.33 to 2.53 eV with decreasing diameter of cadmium sulfide nanoparticles from 20 to 10 nm.[230] An increase in the band gap due to the quantum size effect reduces the photocatalytic activity because the amount of light absorbed decreases. For instance, a decrease in the size of strontium titanate crystallites from 30 ± 5 to 6.5 ± 1 nm reduces its activity in the photocatalytic hydrogen production under UV irradiation at

Table 7. Structure and photocatalytic properties of $CdIn_2S_4$ depending on the hydrothermal synthesis conditions (150 °C).[227]

Reaction time /h	Diameter of spheres /μm	Morphological features	W /(μmol H_2) h^{-1} g^{-1}
8	4–5	No nanopetals formed	–
16	7–8	Formation of nanopetal microclusters	–
24	4–6	Compact puffy flowers	2010
30	6–11	Open and puffy 'marigold flowers' with inter-petal distance of 500–700 nm	4640
(30 + CTAB) [a]	8–12	Nanopetals are curved, cavities 2 μm in diameter are formed in the flowers	6340
(30 + PVP) [b]	4–13	Bipyramids of length 0.7–1 μm and height 50–70 nm grow on the surface of flowers	6480

Note. Conditions: K_2S as electron donor and a 300 W xenon lamp with 420 nm cutoff filter as light source.
[a] Cetyltrimethylammonium bromide (CTAB) was added in the deposition step. [b] Polyvinylpyrrolidone (PVP) was added in the deposition step.

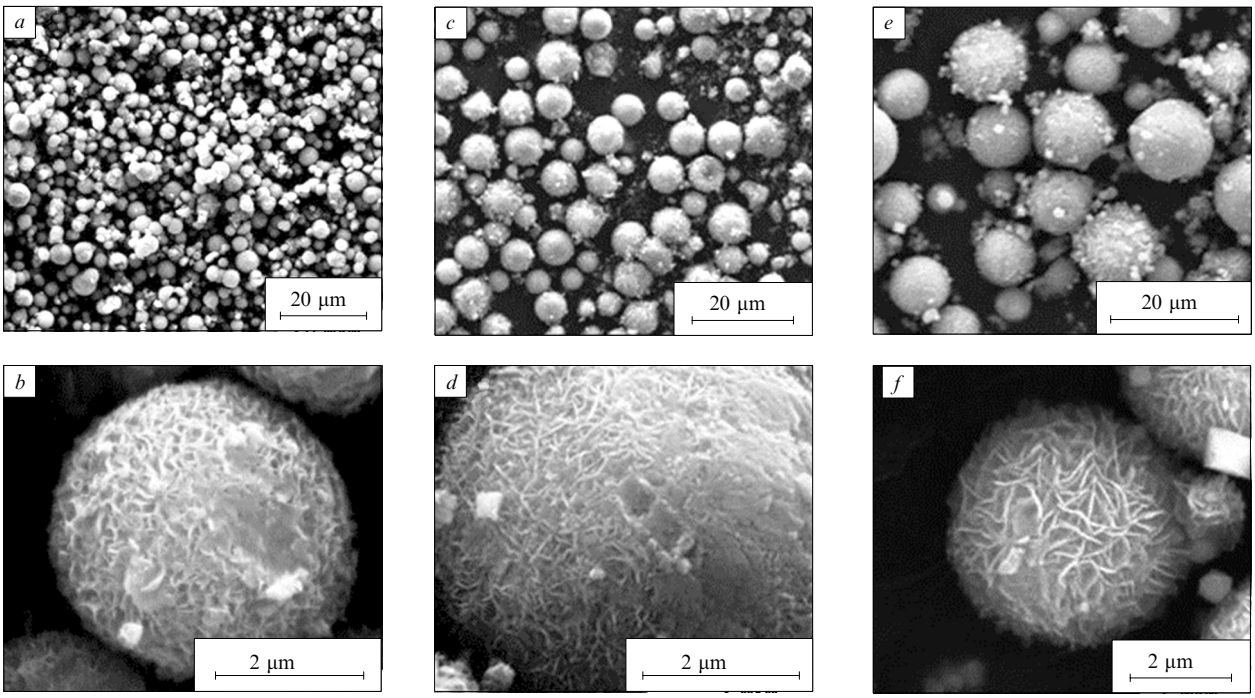


Figure 10. SEM images of $CdIn_2S_4$ photocatalysts depending on hydrothermal treatment conditions (150 °C): no surfactants over a period of 8 (*a*, *b*), 16 (*c*, *d*) and 24 h (*e*, *f*).[227]

$\lambda = 365$ nm from 19.4 to 3.0 (μmol H_2) h^{-1} g^{-1}, *i.e.*, by a factor of 6.5.[231]

The quantum size effect influences not only the band gap, but also positions of the valence and conduction bands of semiconductor materials.[6] Although the band gap of nanostructured CoO is close to that of bulk CoO (~2.6 eV), the electrode potential of the bottom of the conduction band of nanostructured CoO *vs.* NHE is 1.0 V more negative than that of bulk CoO. A decrease in the size of cobalt oxide particles from a few micrometres to 5–8 nm leads to noticeable enhancement of the CoO activity in the photocatalytic splitting of water to produce hydrogen gas.[232] Thus, by varying the semiconductor crystallite size one can 'tune' its optical properties, *viz.*, the band gap and positions of the valence and conduction bands.

IV.2. Photocatalyst textures. Hierarchical structures

The possibility of targeted control of not only the chemical composition of a photocatalyst, but also its macroscopic texture belongs to key factors that govern the synthesis of highly active photocatalysts.[6,233] In the early 2000s, it was established[234] that incorporation of CdS nanoparticles into a porous silica gel matrix can lead to a tenfold enhancement of the photocatalytic activity of cadmium sulfide in various redox processes. The formation of Si–O–Cd bonds causes the band gap to increase and the electrode potential of the bottom of the conduction band to shift towards more negative values. For instance, going from CdS to CdS/SiO_2 leads to enhancement of photocatalytic activity in the liquid-phase cyclopentene addition to Schiff bases under irradiation with light at $\lambda > 420$ nm. Besides, the activity of composite materials is enhanced owing to better adsorption of substrate because CdS/SiO_2 has a large specific surface area.[234]

There has been considerable interest in 3D-structured nanosized hierarchical materials with micro-mesoporous and ordered macroporous structure. For instance, colloidal particles of organic polymers can serve hard templates for production of TiO_2 with the morphology of monodisperse porous microbeads or 'inverse opals' with a 3D-ordered macroporous structure.[235] The template is usually removed by burnout in the final step of synthesis. The activity of platinized 3D-structured hierarchical TiO_2 in the photocatalytic hydrogen production is twice as high as that of platinized nanocrystalline TiO_2.[203] Among 3D-structured composite photocatalysts of visible light-driven photocatalytic hydrogen production, there are $Cd_{1-x}Zn_xS$/SBA-15,[16] CdS/ZrO_2,[17] MoS_2/TiO_2 (Ref. 18) and CdS/Au/WO_3.[19] Data on the activity of hierarchical nanostructured photocatalysts in the visible light-driven hydrogen production are presented in Table 8.

A novel method for the synthesis of composite photocatalysts $Cd_{0.4}Zn_{0.6}S$/3D-TiO_2 (meso-macroporous) includes template synthesis of titanium dioxide using polystyrene microbeads and deposition of a solid solution of cadmium sulfide and zinc sulfide on the surface of TiO_2 samples.[235] Heterostructures $Cd_{0.4}Zn_{0.6}S$/3D-TiO_2 thus prepared revealed high activity [1800 (μmol H_2) h^{-1} g^{-1}] in visible light-driven photocatalytic hydrogen production from aqueous Na_2S–Na_2SO_3 solutions under illumination at $\lambda = 450$ nm. Deposition of $Cd_{0.4}Zn_{0.6}S$ (40 mass %) on the surface of a titanium dioxide sample with regular meso-macroporous structure allowed one to enhance the catalyst activity by a factor of 2.5 compared to

Table 8. Summary of data on hydrogen production from aqueous solutions of organic and inorganic substrates using 3D structured semiconductor photocatalysts.

Photocatalyst	Concentration /mol litre^{-1}		Filter bandpass /nm	W /(μmol H_2) h^{-1} g^{-1}	Φ (%) (see [a])	Ref.
	Na_2S	Na_2SO_3				
Light source — 30 W light-emitting diode (450 nm)						
40% $Cd_{0.4}Zn_{0.6}S$/3D-TiO_2	0.1	0.02	–	1800	3.2	235
40% $Cd_{0.4}Zn_{0.6}S$/TiO_2 P25	0.1	0.02	–	630	1.1	235
$Cd_{0.4}Zn_{0.6}S$	0.1	0.02	–	750	1.3	235
Light source — 350 W xenon lamp						
$Cd_{0.8}Zn_{0.2}S$/3D-SiO_2 SBA-15	0.35	0.25	> 420	1000	–	236
CdS/3D-SiO_2 SBA-15	0.35	0.25	> 420	220	–	236
Light source — 300 W xenon lamp						
9.5% CdS/3D-ZrO_2	0.25	0.35	> 400	1080	–	237
9.5% CdS/ZrO_2	0.25	0.35	> 400	230	–	237
4% CdS – 3.3% Au/3D-WO_3	0.2	0.2	> 400	1700	–	238
3.3% Au/CdS	0.2	0.2	> 400	825	–	238
4% CdS – 3D-$WO_{30.2}$	0.2	> 400	> 400	315	–	238
Light source — light-emitting diode (365 nm)						
10% MoS_2/3D-TiO_2	See [b]		–	550	2.6	239
10% MoS_2/TiO_2 P25	The same		–	140	0.7 [c]	239

[a] Calculated per H_2 molecule. [b] Lactic acid (10 vol.%) as substrate. [c] Estimated by the authors of this review.

that of pure solid solution $Cd_{0.4}Zn_{0.6}S$. No marked activity enhancement was observed when $Cd_{0.4}Zn_{0.6}S$ was deposited onto TiO_2 samples synthesized by different methods, including commercially available Degussa P25 titanium dioxide. Samples of $Cd_{0.4}Zn_{0.6}S$/3D-TiO_2 catalyst were found to be more stable than pure solid solution $Cd_{0.4}Zn_{0.6}S$. Deactivation of deposited meso-macroporous catalysts $Cd_{0.4}Zn_{0.6}S$/3D-TiO_2 is within the limits of experimental error, whereas the rate of hydrogen production in the presence of pure $Cd_{0.4}Zn_{0.6}S$ decreases by 25% over a period of 12 h (Fig. 11).

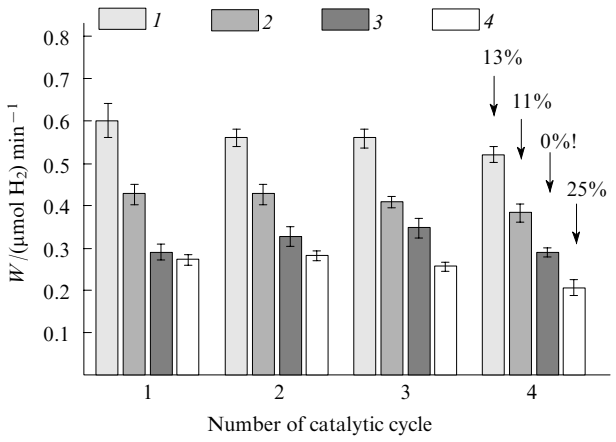


Figure 11. Rate of hydrogen production in 3-h photocatalytic cycles on the $Cd_{0.4}Zn_{0.6}S$/3D-TiO_2 composite catalysts.[235] $Cd_{0.4}Zn_{0.6}S$ content (%): 40 (*1*), 30 (*2*), 20 (*3*) and 0 (*4*). For catalytic cycle 4, shown are the changes in W with respect to the corresponding values for catalytic cycle 1.

Utilization of nanostructured titanium dioxide makes it possible to achieve higher dispersion of $Cd_{0.4}Zn_{0.6}S$ nanoparticles with a narrow size distribution. This favours good contact between cadmium sulfide and titanium dioxide particles and therefore the formation of phase heterojunctions.[235]

IV.3. How the substrate and photocatalyst concentrations and the solution pH influence the photocatalytic activity

In Section IV.2 we have shown that the structural properties and texture of photocatalysts significantly influence the rate of hydrogen production. Now we will consider the effect of the substrate and photocatalyst concentrations and the medium pH on the photocatalytic activity. It should be noted that most studies on the photocatalytic production of hydrogen were carried out at constant (room) temperature using suspensions of photocatalysts in aqueous solutions of 'sacrificial' substrates; therefore, the parameters mentioned above are critical to the rate of the process.

IV.3.a. Photocatalytic hydrogen production from aqueous solutions of organic compounds

Dependence of the rate of hydrogen production on the content of photocatalyst. The rate of a photocatalytic process is proportional to the number of photons absorbed by the photocatalyst and to the maximum apparent quantum efficiency. The photocatalyst concentration should ensure a maximum absorption of incident photons.[48]

A study[240] of the photocatalytic production of hydrogen from aqueous methanol solutions using a suspension of Pt/TiO_2 (photocatalyst) showed that the rate of hydrogen production linearly increases with the photocatalyst concentration and reaches a maximum corresponding to the maximum absorption of light by the semiconductor photocatalyst.[240] Similar results were reported by other researchers. In particular, studies[241–243] on the photocatalytic production of hydrogen from aqueous solutions of certain organic substances including mono- and polyols as well as sugars over platinized titanium dioxide revealed a dependence of the rate of hydrogen production passing through a maximum at a photocatalyst concentration of about 2 g litre^{-1}. As to hydrogen production from aqueous glycerol solutions over ZnO/ZnS photocatalyst, the maximum rate of hydrogen production was achieved at a photocatalyst concentration of 1 g litre^{-1}.[244]

Dependence of the rate of photocatalytic hydrogen production on solution pH. Changes in the acidity of the reaction medium are followed by changes in positions of the energy levels of the bottom of the conduction band and the top of the valence band, the band gap of the photocatalyst, the sign and density of the surface charge and the electrokinetic potential (ζ-potential, isoelectric point potential) of suspended photocatalyst particles, *etc*. Besides, the reaction medium pH influences adsorption processes, the redox potentials of reactants and products of photocatalytic transformations, stabilization of intermediates and particle aggregation of suspended photocatalyst.[48] Eventually, all these factors affect the rate of photocatalytic production of hydrogen.

A study[206] on the influence of medium pH on the rate of hydrogen production from aqueous glycerol solutions over the semiconductor photocatalyst 1% $Pt/Cd_{0.2}Zn_{0.8}S/ZnO/Zn(OH)_2$ showed that the rate of hydrogen production in a neutral medium is nearly zero; however, it increases as an alkali (*e.g.*, NaOH) solution is added to the reaction system and passes through a maximum at alkali concentrations in the range of 50–200 mmol litre^{-1} (Fig. 12 *a*).

This fact can be explained by the influence of the acidity on the surface state of the photocatalyst. One can assume that in aqueous suspensions, different forms of cadmium coexist in equilibrium on the surface of cadmium sulfide particles:

$$CdSH_2^+ \rightleftharpoons CdSH + H^+ \quad (31)$$

$$CdSH \rightleftharpoons CdS^- + H^+ \quad (32)$$

$$CdOH_2^+ \rightleftharpoons CdOH + H^+ \quad (33)$$

$$CdOH \rightleftharpoons CdO^- + H^+ \quad (34)$$

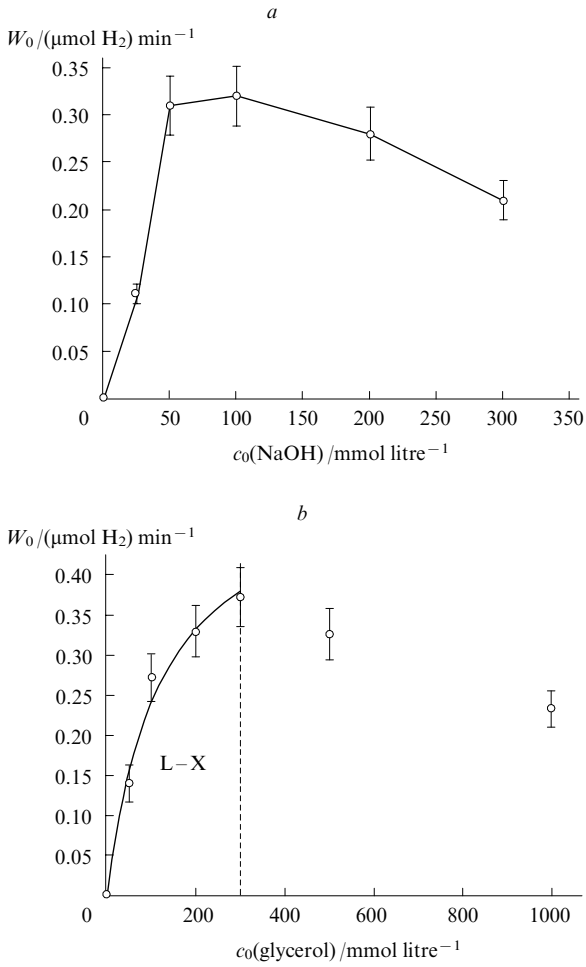


Figure 12. Initial rate of hydrogen production over the photocatalyst 1% $Pt/Cd_{0.2}Zn_{0.8}S/ZnO/Zn(OH)_2$ plotted *vs.* initial concentration of NaOH (*a*) and glycerol (*b*).[206]
Concentration of photocatalyst is 0.77 g litre^{-1}; c_0(glycerol) = 200 mmol litre^{-1} (*a*), c_0(NaOH) = 100 mol litre^{-1} (*b*); temperature 20 °C; a high-pressure mercury lamp (1000 W) as light source; filter bandpass: $\lambda > 420$ nm; L–H: the curve is the approximation of experimental data by the Langmuir–Hinshelwood equation.

The isoelectric point (pI) is the pH value at which a particular molecule or surface bears no net electric charge. For cadmium sulfide, one has pI ~6.5. Therefore, $CdSH_2^+$ and $CdOH_2^+$ predominate in acidic (pH 4.1–4.3) and neutral (pH 5.8–7.7) media, respectively, whereas negatively charged forms CdS^- (pH 7.3–7.7) and CdO^- (pH 8.9–9.9) prevail in alkaline media.[245] The isoelectric point of ZnS is in the range of 3.0–8.5 depending on the crystal structure of the material.[246] In other words, in alkaline media the surface of cadmium sulfide and zinc sulfide carries a negative charge and the surface anion S^{2-} is replaced by hydroxyl groups. Zinc and cadmium hydroxides are characterized by pI values in the range of 9.6–11.5 (Ref. 247). Therefore, under basic conditions the surface species on the photocatalyst $Cd_{0.2}Zn_{0.8}S/ZnO/Zn(OH)_2$ mainly represent ZnOH or ZnO^- and CdOH or CdO^- (Ref. 248). It is believed[206] that at pH ~13, glycerol forms $C_3H_7O_3^-$

anions, which can compete with hydroxyl groups for surface sites on the cadmium sulfide/zinc sulfide solid solution. The addition of NaOH causes the adsorption of organic substrates on the CdS/ZnS photocatalysts to enhance[248] and the rate of photocatalytic hydrogen production to increase. Alkalization of a reaction suspension to pH > 13.5 makes the photocatalytic production of hydrogen by reaction (2) less thermodynamically favourable.

The effect of medium pH on the activity of photocatalysts based on titanium dioxide and erbium-doped yttrium aluminate $Er^{3+}@YAlO_3/Pt-TiO_2$ in visible light-driven hydrogen production from aqueous glucose solutions was studied.[249] It was established that the rate of hydrogen production increases as suspension pH increases from 3.5 to 6.5, then slowly decreases at pH 8.0 and abruptly decreases at pH 11. Therefore, the optimum condition for hydrogen production is a pH interval of 6.5–8. One can assume that, like in the example with glycerol (see above), the medium acidity influences the rate of photocatalytic production of hydrogen in a complex manner *via* the change in the surface state of titanium dioxide, the degree of dissociation of glucose in solution and the redox potential of H^+/H_2. Indeed, at room temperature, the glucose pK_a is 12.3. Correspondingly, at lower suspension pH, glucose exists in the molecular form and can readily interact with the surface titanium atoms *via* oxygen atoms of hydroxyl groups. When the pH value of $Er^{3+}@YAlO_3/Pt-TiO_2$ suspension increases, glucose undergoes acidic dissociation with the formation of negatively charged $C_6H_{11}O_6^-$ anion. It is believed that the anion is more reactive towards photogenerated holes than glucose molecule and thus favours an increase in the rate of hydrogen production.[138] However, the photocatalytic hydrogen production by Eqn (2) becomes thermodynamically less favourable with increasing pH. Thus, it is neutral and weak alkaline media that are optimum for photocatalytic production of hydrogen from aqueous glucose solutions in the presence of $Er^{3+}@YAlO_3/Pt-TiO_2$.[249]

Dependence of the rate of photocatalytic hydrogen production on substrate concentration. The rate of photocatalytic hydrogen production from aqueous solutions of organic compounds depends on the substrate concentration. For instance, an increase in the initially low concentration of glycerol used as substrate is accompanied by a linear increase in the rate of hydrogen production which reaches a plateau at higher concentrations of the substrate. The dependence is well approximated by the Langmuir–Hinshelwood model, according to which the reaction rate is proportional to the number of adsorbed substrate particles; as the surface of the photocatalyst becomes saturated with substrate particles, the rate of hydrogen production reaches a maximum value.[48] The Langmuir–Hinshelwood equation has the form[206]

$$W_0 = k\frac{Kc_0}{1+Kc_0} \qquad (35)$$

where W_0 is the initial rate of hydrogen production /(μmol H_2) min^{-1}; k is the phenomenological apparent rate constant /μmol min^{-1}; K is the adsorption constant of the substrate /mmol^{-1} litre; and c_0 is the initial concentration of glycerol /mmol litre^{-1}.

The validity of the Langmuir–Hinshelwood model was substantiated for photocatalytic hydrogen production in aqueous solutions of various organic compounds.[48] An increase in the rate of hydrogen production at low substrate (electron donor) concentrations to nearly-zero order with respect to methanol at high substrate concentrations was proved taking photocatalytic hydrogen production using aqueous suspension of Pt/TiO_2 as an example.[250] Similar dependences were also observed in the photocatalytic hydrogen production from aqueous solutions of isopropyl alcohol,[251] oxalic acid,[21] acetic acid,[252] glucose[253] and saccharose[254] over platinized titanium dioxide. Visible light-driven hydrogen production over $Cd_{1-x}Zn_xS$ photocatalyst using glucose[139] and glycerol[137] as substrates also proceeds by the Langmuir–Hinshelwood mechanism. The phenomenological constants of Eqn (35) calculated for aqueous glucose solutions are as follows: k = 0.26 μmol min^{-1} and K = 0.024 mmol^{-1} litre for the $ZnS/ZnIn_2S_4$ photocatalyst[138] and k = 4.75 μmol min^{-1} and K = 2.03 mmol^{-1} litre for Pt/TiO_2 photocatalyst.[23]

The influence of the initial concentration of glycerol on the initial rate of hydrogen production over the photocatalyst 1% $Pt/Cd_{0.2}Zn_{0.8}S/ZnO/Zn(OH)_2$ under irradiation with visible light at $\lambda > 420$ nm was studied.[206] It was found that the rate linearly increased with increasing initial concentration of glycerol in the range of 0–100 mmol litre^{-1}, then slowly increased to a maximum value at 300 mmol litre^{-1} (2.8 vol.% of glycerol), and then decreased (Fig. 12 *b*). For the photocatalytic hydrogen production in aqueous glycerol solutions the first portion of the dependence obeyed Eqn (35) up to a glycerol concentration of 0.3 mmol litre^{-1}.[206] However, at higher glycerol concentrations, the rate of hydrogen production began to decrease, which contradicts the Langmuir–Hinshelwood model. One can assume this is due to the effect of diffusion processes that abruptly slow down as the medium viscosity increases at high glycerol concentrations.

It should be noted that the Langmuir–Hinshelwood model was initially used to describe one-step catalytic transformations of adsorbed particles, whereas photocatalytic hydrogen production from aqueous solutions of organic compounds is a multistep process [see, *e.g.*, Eqns (13)–(21)]. This model correctly describes photocatalytic production of hydrogen at low substrate concentrations where the rate of the process is not limited by diffusion and adsorption of reactants on the photocatalyst surface and the surface oxidation of the substrate proceeds very rapidly.[48,255,256] Here, a photogenerated hole directly or *via* the formation of an $^{\bullet}OH$ radical oxidizes the molecule of the organic compound, while an electron reduces water with the formation of hydrogen molecule, recombination of photogenerated electrons and holes being the major side process. An actual mechanism of photocatalytic hydrogen production can be even more complicated. For instance, an *in situ* IR study[257] of hydrogen production in aqueous methanol solutions over Pt/TiO_2 photocatalyst revealed a rapid oxidation of substrate to methoxy radical and showed that the rate of

the reaction between photogenerated holes and the substrate is much higher than the recombination rate of electron–hole pairs. This is a clear illustration for the possibility of fast formation of stable intermediates on the photocatalyst surface at high substrate concentration. As a consequence, the number of active sites and the rate of photocatalytic production of hydrogen decrease. Besides, organic compounds can compete with water in the interaction with photogenerated holes; this makes the generation of reactive oxidizing species (•OH radicals) less probable.[258]

IV.3.b. Photocatalytic production of hydrogen in aqueous suspensions of Na_2S and Na_2SO_3

The system $Na_2S-Na_2SO_3$ is often used as electron donor in photocatalytic production of hydrogen; therefore, the influence of various experimental parameters of this system on the process in question has been studied in quite detail.[76, 259] Nevertheless, a possible mechanism of photocatalytic production of hydrogen on sulfide photocatalysts and a relevant kinetic model were considered only by researchers from the Russian Federation.[127]

Dependence of the rate of photocatalytic hydrogen production on the concentration of suspended photocatalyst. The dependence of the rate of visible light-driven hydrogen production from aqueous solution of 0.1 M $Na_2S-0.02$ M Na_2SO_3 on the concentration of suspended photocatalyst $Cd_{0.3}Zn_{0.7}S$, which was varied from 0 to 1.54 g litre^{-1}, was studied.[76] As the photocatalyst concentration in the suspension increased from 0 to 0.38 g litre^{-1}, the rate of hydrogen production increased linearly and then reached a plateau as the photocatalyst concentration approached a value of 1.15 g litre^{-1}. This concentration dependence of the rate of hydrogen production can be explained as follows. At low photocatalyst concentrations, the absorption of light is proportional to the number of $Cd_{0.3}Zn_{0.7}S$ particles. As the photocatalyst concentration becomes higher than $\sim$1 g litre^{-1}, suspended particles aggregate, light absorption by the solution decreases and the rate of the photocatalytic reaction no longer increases.[260]

Dependence of the rate of photocatalytic hydrogen production on suspension pH. As in the case of photocatalytic hydrogen production from aqueous solutions of organic electron donors, the suspension acidity influences the rate of photocatalytic hydrogen production in complex manner. The influence of the suspension pH on the rate of photocatalytic hydrogen production in aqueous suspensions of $Na_2S-Na_2SO_3$ in the presence of platinized cadmium sulfide was studied.[261]

A change in suspension pH causes the top of the valence band and the bottom of the conduction band of cadmium sulfide to shift in accordance with Eqn (4). However, the electrode potential for reduction of water also linearly depends on suspension pH with the same slope of 0.059 (the term '0.059 pH'). As a result, the overpotential for the electrode reduction of water on the semiconductor surface remains unchanged upon variation of the medium pH. The medium acidity first of all influences the proportions of different forms of the electron donor, *viz*., sulfide (S^{2-} and HS^-). As pH value increases, so does the proportion of sulfide anions whose concentration affects the electrode potentials of the valence band and the conduction band of cadmium sulfide. As the proportion of S^{2-} ions increases, the potential of the bottom of the conduction band of CdS becomes more negative.[262] Correspondingly, the difference between the electrode potential of the bottom of the conduction band of CdS and that of the reduction of hydrogen by reaction (2) increases, which causes an increase in the electromotive force of the hydrogen production reaction. As the medium pH is shifted towards the strongly alkaline region, hydrogen production by reaction (2) is thermodynamically hampered. Thus, the influence of the medium pH on the rate of photocatalytic hydrogen production from aqueous solutions of $S^{2-}-SO_3^{2-}$ over CdS can be explained by the combined action of three main factors, that is, by the changes in position of the electrode potential of the conduction band of the photocatalyst (CdS), in the redox potential of H^+/H_2 and in the proportions of different ionized forms of hydrogen sulfide.[261]

The influence of the medium pH on the rate of visible light-driven production of hydrogen from aqueous solution of 0.1 M $Na_2S-0.02$ M Na_2SO_3 on $Cd_{0.3}Zn_{0.7}S$ catalyst was studied.[76] The initial pH value was varied from 5.5 to 13 by adding 1M H_2SO_4 and 0.1M NaOH. It was found that the addition of alkali causes the rate of photocatalytic hydrogen production to decrease. As the solution pH decreases from 12.7 to 6.5 upon adding sulfuric acid, the rate of photocatalytic hydrogen production monotonically increases. A further decrease in pH leads to an abrupt decrease in the rate due to a redox reaction between sulfide and sulfate anions resulting in S^0

$$8H^+ + 3S^{2-} + SO_4^{2-} \longrightarrow 4S^0 + 4H_2O \qquad (36)$$

An increase in the concentration of HO^- ions in accordance with Eqn (25) thermodynamically hampers the production of hydrogen, which seems to be a reason for the decrease in the rate of photocatalytic hydrogen production. Contrary to this, a decrease in pH, causes the rate of the process to increase.

A study[259] on the effect of alkali additives on the rate of visible light-driven photocatalytic hydrogen production in aqueous suspensions of $Na_2S-Na_2SO_3$ in the presence of cadmium sulfide revealed the following. The addition of less than 0.10 mol litre^{-1} of NaOH to the reaction suspension is followed by an increase in the initial rate of hydrogen production. However, if the initial concentration of NaOH increases to 0.15 mol litre^{-1}, the initial rate of hydrogen production remains unchanged. These data contradict the results reported in Refs 76 and 127 probably due to different surface properties of the photocatalysts based on cadmium sulfide.

As can be seen, variation of the medium acidity can lead to twofold or even greater variation of the rate of photocatalytic hydrogen production in aqueous solutions of $S^{2-}-SO_3^{2-}$.[76, 127] Therefore, the solution pH is a critically important parameter influencing the quantum efficiency of photocatalytic hydrogen production.

Dependence of the rate of photocatalytic hydrogen production on the concentration of S^{2-} and SO_3^{2-}. Photocatalytic hydrogen production is usually conducted using sulfide–sulfite mixtures containing 0.10 mol litre^{-1} of Na_2S and 0.02 mol litre^{-1} of Na_2SO_3 (Refs 130, 113, 263). In some cases, corresponding potassium salts are utilized.[132, 227] It was shown[127] that variation of the sulfide and sulfite concentrations causes the concentration dependence of the rate of hydrogen production to pass through a maximum at the same initial concentrations of the substrates: $c_0(Na_2S) = c_0(Na_2SO_3) = 0.10$ mol litre^{-1}.

Relying on the results of a study on the dependence of the reaction rate on the concentration of a 'sacrificial' substrate at a constant concentration of the other substrate, an equation was proposed,[127] which relates the initial reaction rate (W_0) to the initial concentrations of Na_2S and Na_2SO_3

$$W_0 = \frac{\alpha c_0(Na_2S) + \beta c_0(Na_2S)\, c_0(Na_2SO_3)}{[1 + K(Na_2S)c_0(Na_2S) + K(Na_2SO_3)c_0(Na_2SO_3)]^2} \quad (37)$$

where α and β are the effective rate constants, $c_0(Na_2S)$, $c_0(Na_2SO_3)$ are the initial reactant concentrations, and $K(Na_2S)$, $K(Na_2SO_3)$ are the adsorption constants of the reactants.

Approximation of experimental data by Eqn (37) gave the following results: $\alpha = 4.4 \pm 0.5$ μl min^{-1}, $\beta = 170 \pm 43$ μl mol^{-1} min^{-1}, $K(Na_2S) = 7.8 \pm 0.7$ mol^{-1} litre, $K(Na_2SO_3) = 14 \pm 2$ mol^{-1} litre.

For better description of the process, Eqn (37) was augmented with the term characterizing the acidity of the solution.[127] Experimental data are with high accuracy (confidence factor $R^2 = 0.99$) approximated by the equation

$$W_0 = \frac{G + Ic(H^+)}{[1 + Bc_0(Na_2S) + Dc_0(Na_2SO_3) + Jc(H^+)]^2} \quad (38)$$

where $G = 0.52 \pm 0.02$ μmol min^{-1}, $I = (8.4 \pm 0.5) \times 10^7$ μl min^{-1}, $J = (3.6 \pm 0.2) \times 10^7$ mol^{-1} litre. The parameter G can be treated as the reaction rate that is independent of proton concentration [*e.g.*, the rate of the reaction between sulfide and sulfite ions, which corresponds to the term $\beta c_0(Na_2S)c_0(Na_2SO_3)$ in Eqn (37)]; the parameter I is the product of the effective rate constant for the reaction between adsorbed protons and sulfide ions (γ) and the concentration of sulfide ions; J is the equilibrium constant for adsorption protons on the photocatalyst surface, and B and D are the adsorption constants of the sulfide and sulfite ions, respectively.

Combining Eqns (37) and (38) gives the dependence of the reaction rate on the concentrations of three reactants, namely, sodium sulfide, sodium sulfite and protons:

$$W_0 = [\alpha c_0(Na_2S) + \beta c_0(Na_2S)\, c_0(Na_2SO_3) + \gamma c(H^+)c_0(Na_2S)][1 + K(H^+)c_0(H^+) + K(Na_2S)c_0(Na_2S) + K(Na_2SO_3)c_0(Na_2SO_3)]^{-2} \quad (39)$$

The first term in Eqn (39) describes the dissociation rate of adsorbed hydrosulfide ion to sulfide ion and proton, the second term takes account of the contribution of the interaction between sulfide and sulfite anions to the overall rate of the process, while the third term is the production rate of HS^-. The contribution of the last-mentioned term becomes significant at low pH. This model approximates both experimental data[127] and other published data on the concentration dependences (Table 9) with a rather high accuracy.

Thus, the rate of photocatalytic hydrogen in aqueous suspensions of semiconductor photocatalysts depends on particular experimental conditions, such as the reaction medium pH and the substrate and photocatalyst concentrations. It should be noted that conventional kinetic methods developed for 'dark' catalytic transformations can hardly be used to establish the detailed nature and mechanism of photocatalytic transformations on particles in semiconductor suspensions because one should take account of specific features of light absorption and possible 'hidden' radical mechanism of elementary steps of the process in question.

IV.4. Effect of the substrate nature on the quantum efficiency of hydrogen production

The photocatalytic activity in the hydrogen production reactions is directly related to not only the nature of the photocatalyst, but also to the nature of the substrate acting as electron donor. In Sections II.2 and II.3 we have shown that the mechanisms of hydrogen production from aqueous solutions of organic and inorganic substrates are fundamentally different. Besides, differences in the nature and structure of organic substances used as 'sacrificial' agents manifest themselves in the specific features of their adsorption on active sites of the photocatalyst and, correspondingly, on its reactivity.[48]

Recall that the best studied electron donors for hydrogen production include the $Na_2S-Na_2SO_3$ system and a number of organic substrates, mainly alcohols (ethanol, methanol, glycerol). The rate of hydrogen production on sulfide photocatalysts is usually much

Table 9. Parameters calculated by approximating published data using Eqn (37).[127]

Photocatalyst	$K(Na_2S)$ /mol^{-1} litre	$K(Na_2SO_3)$ /mol^{-1} litre	α /μl min^{-1}	β /μl mol^{-1} min^{-1}	R^2	Ref.
CuS/ZnO	2.6 ± 0.2	4 ± 1	1.4 ± 0.2	15 ± 5	0.98	264
CdS	9.9 ± 0.4	6.6 ± 0.6	60 ± 12	2820 ± 434	0.98	259
CdS/Pt-TiO_2	0.6 ± 0.1	0.5 ± 0.1	1.25 ± 0.02	0.81 ± 0.01	0.99	265

Table 10. Photocatalytic activity of untreated and platinized $Zn(OH)_2$(amorph.)/$Cd_{0.3}Zn_{0.7}S$ catalysts in visible light-driven production of hydrogen from aqueous solutions of $Na_2S-Na_2SO_3$ and ethanol at $\lambda = 450$ nm.[210]

Photocatalyst	W /(μmol H_2) h^{-1} g^{-1}	Φ (%) (see [a])
Solution of 0.1 M Na_2S – 0.1 M Na_2SO_3		
10% $Zn(OH)_2/Cd_{0.3}Zn_{0.7}S$	2880	7.1
20% $Zn(OH)_2/Cd_{0.3}Zn_{0.7}S$	3130	7.7
1% Pt/20% $Zn(OH)_2/Cd_{0.3}Zn_{0.7}S$	7470	18.3
Ethanol (10 vol.%) solution		
1% Pt/20% $Zn(OH)_2/Cd_{0.3}Zn_{0.7}S$	132	0.4
10% $Zn(OH)_2/Cd_{0.3}Zn_{0.7}S$	72	0.2
1% Pt/10% $Zn(OH)_2/Cd_{0.3}Zn_{0.7}S$	432	1.1

[a] Calculated per H_2 molecule.

higher when using the sulfide–sulfite system (see Tables 1 and 2); the same holds for the composite photocatalysts containing CdS and $Cd_{1-x}Zn_xS$ (see Tables 5 and 6). This can be explained by the fact that sulfide anions in the liquid phase 'protect' the catalyst from photocorrosion, thus increasing the quantum efficiency of the target process.[174]

It should be noted that most experiments aimed at studying hydrogen production are performed using only one type of donor namely, $Na_2S-Na_2SO_3$ or organic compounds. However, there are a few publications where same photocatalysts were used with both types of electron donors (sulfide–sulfite system and organic substrates).[210, 220, 266]

Table 10 presents the results of a study[210] on visible light-driven photocatalytic hydrogen production from aqueous solutions of $Na_2S-Na_2SO_3$ and ethanol in the presence of pure and platinized composite photocatalysts $Zn(OH)_2$(amorph)/$Cd_{0.3}Zn_{0.7}S$. As can be seen, the Φ value achieved using the sulfide–sulfite system is tenfold higher than that obtained with ethanol; even for the noble metal non-promoted photocatalysts the rate of hydrogen production from $Na_2S-Na_2SO_3$ solutions is rather high.

Table 11. Photocatalytic activity of untreated and platinized $(TiO_2)_{1-x}(NiO)_x/Cd_{0.8}Zn_{0.2}S$ catalysts in visible light-driven production of hydrogen from aqueous solutions of $Na_2S-Na_2SO_3$ and a mixture of benzyl alcohol and acetic acid with a 400 W Xe lamp ($\lambda > 395$ nm) as light source.[220]

Photocatalyst	W /(μmol H_2) h^{-1} g^{-1}	Φ (%) (see [a])
Solution of 0.1 M Na_2S – 0.1 M Na_2SO_3		
$(TiO_2)_{0.17}(NiO)_{0.83}/Cd_{0.8}Zn_{0.2}S$	1600	1.5
$(TiO_2)_{0.05}(NiO)_{0.95}/Cd_{0.8}Zn_{0.2}S$	1400	1.3
Solution of 6 vol.% C_7H_8O + 6 vol.% CH_3COOH		
$(TiO_2)_{0.17}(NiO)_{0.83}/Cd_{0.8}Zn_{0.2}S$	6840	5.9
$(TiO_2)_{0.05}(NiO)_{0.95}/Cd_{0.8}Zn_{0.2}S$	8900	7.7

[a] Calculated per H_2 molecule.

Visible light-driven hydrogen production from aqueous solutions of $Na_2S-Na_2SO_3$ and a mixture of benzyl alcohol and acetic acid in the presence of $(TiO_2)_{1-x}(NiO)_x/Cd_{0.8}Zn_{0.2}S$ photocatalysts was also studied.[220]

The data presented in Table 11 show that rate of hydrogen production from aqueous solution of the mixture of benzyl alcohol with acetic acid is ~4.5–6 times higher than that achieved using inorganic electron donors. Unfortunately, this fact was not explained in the original publication.[220]

Yet another study[266] was devoted to photocatalytic hydrogen production in aqueous solutions of ethanol, $Na_2S-Na_2SO_3$ and in a mixture of these substrates on the 3% Au/CdS photocatalyst under illumination with light at $\lambda > 350$ nm. The rate of hydrogen production was 1400 (μmol H_2) h^{-1} g^{-1} for the solution containing 8 vol.% of ethanol, 6100 (μmol H_2) h^{-1} g^{-1} for the solution of 0.1 M Na_2S – 0.02 M Na_2SO_3 and 10 800 (μmol H_2) h^{-1} g^{-1} for a mixture of pure ethanol and a solution of 0.1 M Na_2S – 0.0 2M Na_2SO_3 (8/92 v/v); this corresponded to a quantum efficiency of ~4%.

It was assumed that the increased rate of hydrogen production in the mixture of ethanol and $Na_2S-Na_2SO_3$ is due to the mechanism schematically shown in Fig. 13. The primary processes are photogeneration of electron–hole pairs and dissociative adsorption of water on the surface of cadmium sulfide.

$$CdS + h\nu \longrightarrow e^- + h^+ + CdS \quad (40)$$

$$H_2O(liq) \longrightarrow OH^-(ads) + H^+(ads) \quad (41)$$

It is followed by the formation of disulfide ions from sulfide ions [see reaction (23)] in the interaction with photogenerated holes. The formation of $^{\bullet}OH$ radical and the radical oxidation of ethanol to acetaldehyde proceed as follows:

$$OH^-(ads) + h^+ \longrightarrow {}^{\bullet}OH(ads) \quad (42)$$

$$^{\bullet}OH(ads) + CH_3CH_2OH \longrightarrow CH_3{}^{\bullet}CHOH + H_2O \quad (43)$$

$$CH_3{}^{\bullet}CHOH + h^+ \longrightarrow CH_3{}^{\bullet}CHO + H^+(ads) \quad (44)$$

At pH 7, the standard electrode potential of the S^{2-}/S_2^{2-} transition in stage (23) is −0.14 V *vs.* NHE; the standard electrode potential of production of α-hydroethyl radical in step (43) is +1.38 V *vs.* NHE; the electrode potential of the top of the valence band of cadmium sulfide at the same pH value is +1.7 V *vs.* NHE. Probably, transfer of an electron from the sulfide ion to the valence band of CdS is thermodynamically more favourable than electron transfer from the ethanol molecule. This provides an explanation for the higher activity in the $Na_2S-Na_2SO_3$ system compared to the system containing aqueous ethanol solution. It is assumed that if ethanol and sulfide ions are used simultaneously, one deals with absorption of photogenerated holes [see reaction (44)], which increases the quantum efficiency of the target process

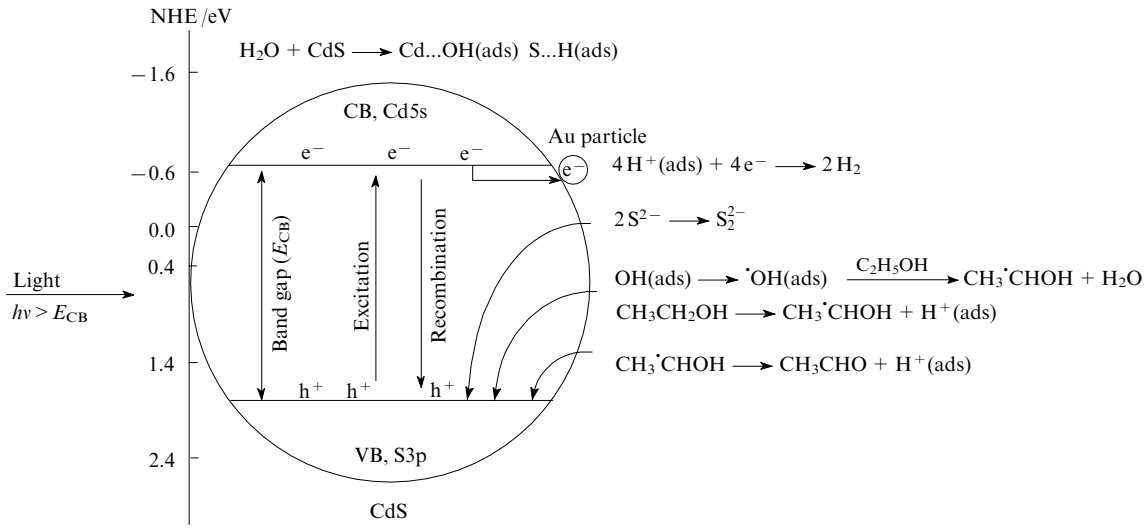


Figure 13. Tentative mechanism of hydrogen production from aqueous solutions of ethanol and $Na_2S-Na_2SO_3$ under illumination of Au/CdS photocatalyst at $\lambda > 350$ nm.[266]

using a mixture of ethanol and $Na_2S-Na_2SO_3$. Nevertheless, mention should be made of inadequate reasoning of the authors of Ref. 266, which, in particular, is due to the fact that the thermodynamics of photocatalytic hydrogen production requires an analysis of the running (concentration-dependent) rather than standard electrode potentials of the oxidizing agent–reducing agent pairs.

In contrast to comparison of the quantum efficiencies of photocatalytic hydrogen production from aqueous solutions of organic and inorganic electron donors, different-type organic electron donors are compared quite often. Examples are provided by the comparative studies on the activities in photocatalytic hydrogen production carried out using a large number of organic alcohols, aldehydes and acids as electron donors.[71, 267, 268]

Data presented in Fig. 14 illustrate changes in the rate of hydrogen production from the same-concentration aqueous solutions of organic substances of different nature in the presence of Pd/TiO_2 photocatalyst under the light of a 400 W Xe lamp. The highest rates of hydrogen production were achieved using polyols, that is, glycerol, butane-1,2,3-triol and butane-2,3-diol, whereas those observed using ketones, acetic acid or *tert*-butyl alcohol were close to zero. The hydrogen production rates obtained with sugars (D-glucose and saccharose) as electron donors are close to that obtained using ethanol, although lower than with glycerol.[71]

Following the authors of Ref. 267 and the mechanism of photocatalytic hydrogen production from aqueous alcohol solutions [see reactions (13)–(21)], efficient hydrogen production requires that the substrate molecule have at least one hydrogen atom at the carbon atom bound to oxygen; the larger the number of such hydrogen atoms the higher (on the average) the rate of hydrogen production. This provides an explanation for the high rate of photocatalytic hydrogen production from aqueous solutions of polyols and poor results

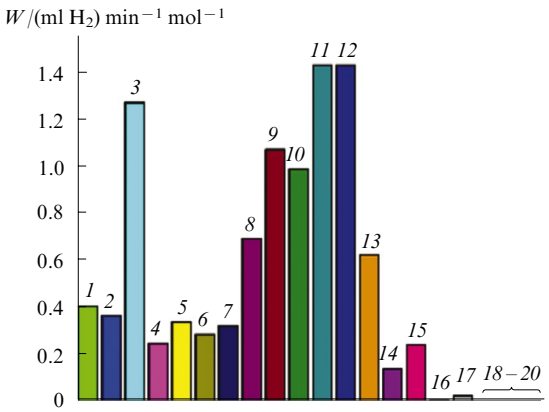


Figure 14. Rates of photocatalytic hydrogen production in aqueous solutions of different organic compounds on Pd/TiO_2 photocatalyst under illumination with a 400 W Xe lamp at a constant substrate concentration of 0.1 vol.%.[267]
Compounds: propan-2-ol (*1*), butan-2-ol (*2*), butane-2,3-diol (*3*), methanol (*4*), ethanol (*5*), n-propanol (*6*), n-butanol (*7*), propane-1,2-diol (*8*), propane-1,3-diol (*9*), butane-1,3-diol (*10*), butane-1,2,4-triol (*11*), glycerol (*12*), ethylene glycol (*13*), acetaldehyde (*14*), diethyl ether (*15*), acetone (*16*), acetic acid (*17*), 2-pentanone (*18*), benzyl alcohol (*19*), *tert*-butyl alcohol (*20*).

obtained with ketones and organic acids (except formic acid) as electron donors. It was also concluded that during photocatalytic hydrogen production, alkyl groups RCH_2 from alcohol molecules undergo transformation to corresponding alkanes in accordance with Eqn (17), while methyl groups are completely oxidized to carbon dioxide.[267]

Figure 15 presents the results of a study[105] on visible light-driven photocatalytic hydrogen production in aqueous solutions of various organic substances on the 0.2 mass % MoS_2/CdS catalyst. Among mono- and polyols, the highest photocatalytic activity was

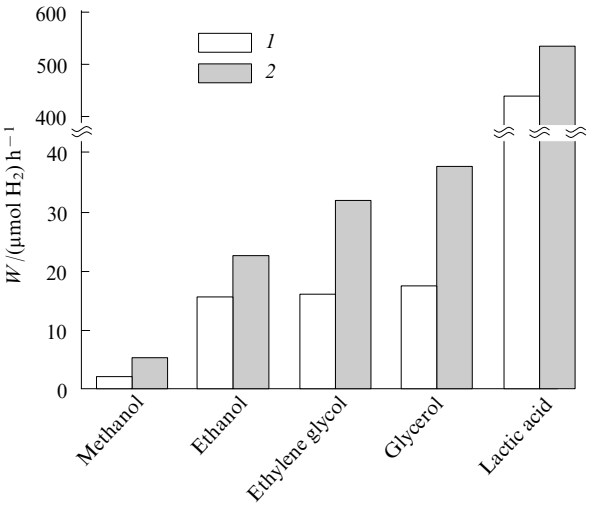


Figure 15. Rate of hydrogen production in aqueous solutions of different organic substrates on two photocatalysts, 0.2 mass % Pt/CdS (*1*) and 0.2 mass % MoS_2/CdS (2), under illumination with a 300 W Xe lamp at $\lambda > 420$ nm.[105]

achieved using glycerol; the activity obtained with lactic acid was tenfold higher than with glycerol provided the same concentration (10 vol.%).[105] Therefore, the presence of both carboxyl and hydroxyl groups in the organic electron donor molecule leads to significant enhancement of photocatalytic activity.

Thus, the nature of the 'sacrificial' electron donor significantly influences its photocatalytic activity in the hydrogen production. By varying the nature of the donor one can achieve more than a tenfold increase in the rate of the target process using the same photocatalyst.

The aforesaid suggests that attainment of high quantum efficiency in photocatalytic hydrogen production requires a proper choice of the nature of not only the photocatalyst, but also the substrate ('sacrificial agent'). Namely, it seems most appropriate to use sulfide photocatalysts with the $S^{2-}-SO_3^{2-}$ system, as well as to combine the noble metal promoted oxide and composite photocatalysts with organic substances containing COH groups (*e.g.*, water-soluble components of biomass or certain biomass-derived substances) as electron donors. Besides, the choice of reaction conditions, such as the suspension pH and the substrate and photocatalyst concentrations is critical when using organic and inorganic electron donors.

V. Activation and deactivation of semiconductor photocatalysts of hydrogen production reactions

As mentioned above, the best studied photocatalysts of visible light-driven hydrogen production are materials based on noble metal loaded CdS and $Cd_{1-x}Zn_xS$. However, systems based on water-insoluble sulfides are unstable under the hydrogen production conditions, especially when organic substrates are used as electron donors, because the optimum hydrogen production rates are achieved in alkaline media at pH $\approx$ 12 – 13.[206, 248, 269] Also, in most cases the concentration dependence of the rate of photocatalytic hydrogen production from aqueous solutions of organic compounds has an induction period during which the activity initially increases and then remains constant or even decreases.[206, 269 – 272] This suggests that the active component of the photocatalysts based on cadmium sulfide and zinc sulfide is formed in the course of hydrogen production. The authors of most studies leave this observation unattended; however, acquiring of detailed knowledge on the state of the active components of the working sulfide photocatalysts is necessary both for better insight into the mechanism process and for the design of novel photocatalysts. The surface and bulk transformations of sulfide photocatalysts in the course of photocatalytic hydrogen production have also been studied.[95, 118, 210, 273, 274]

Transformations of the 1% Pt/$Cd_{0.65}Zn_{0.35}S$/2D-β-$Zn(OH)_2$/ε-$Zn(OH)_2$/ZnO photocatalyst during visible light-driven hydrogen production from aqueous ethanol solutions irradiated at $\lambda = 450$ nm were investigated.[273] The rate of photocatalytic hydrogen production was measured in the course of twelve consecutive 5-h runs; after each catalytic cycle the reaction mixture was bubbled with argon. It was found that the initial rate of hydrogen production from aqueous ethanol solutions increases during the first three cycles (15 h) of irradiation, remains nearly constant throughout the next eight cycles and abruptly decreases in the course of the twelfth cycle (deactivation of the photocatalyst after 55 h of irradiation).

According to powder X-ray diffraction (PXRD) and X-ray fluorescence spectroscopy data, transformation of the photocatalyst during 60 h (or 12 cycles) involves the following three main steps (Fig. 16):

— transition of the surface 2D-β-$Zn(OH)_2$ to ε-$Zn(OH)_2$, thus making the surface of the photocatalytically active sulfide accessible (0 – 15 h) and activating the photocatalyst; a more than twofold increase in the initial rate of hydrogen production during the three cycles;

— partial dissolution of the $Cd_{0.65}Zn_{0.35}S$ phase leading to reduction of the photocatalyst activity between 15 and 50 h of irradiation.

— formation of cadmium carbonate $CdCO_3$ phase after 50 h of irradiation and subsequent deactivation of the photocatalyst; however, the rate of hydrogen production after 60 h of irradiation remains 1.5 times higher than in the first cycle.

Activation of the 1% Pt/$Zn(OH)_2$(amorph)/$Cd_{0.3}Zn_{0.7}S$ composite photocatalyst proceeds by a similar mechanism. Namely, in the course of visible light-driven hydrogen production amorphous zinc hydroxide undergoes transition to the active form ε-$Zn(OH)_2$.[210] The rate of hydrogen production using the 1% Pt/30% $Zn(OH)_2$/$Cd_{0.3}Zn_{0.7}S$ photocatalyst increased by a factor of 7 during four 90-min runs.

A tentative mechanism of formation of cadmium carbonate which deactivates the photocatalyst is as follows. The oxidation of cadmium sulfide by photogenerated holes is followed by the appearance of Cd^{2+} and SO_4^{2-} ions in the aqueous solution.[275] In accordance with Eqn (7), photocatalytic hydrogen production in aqueous ethanol solutions is accompanied by evolution of carbon dioxide which is transformed to carbonate ions in an alkaline medium with pH 13. As a

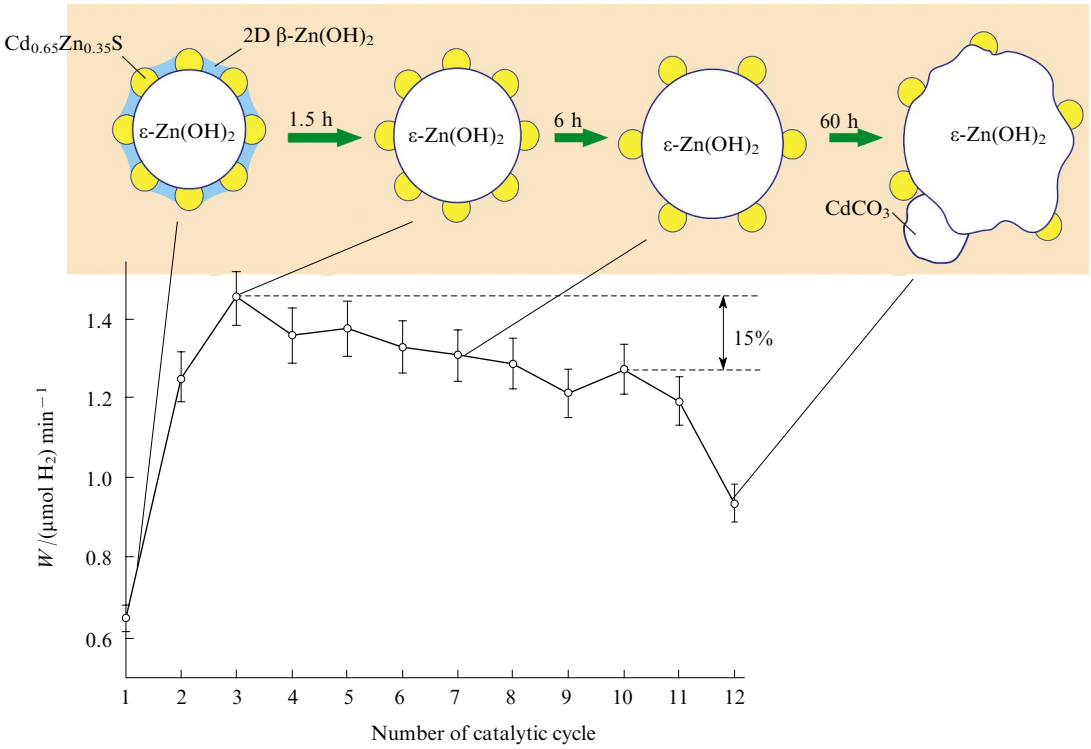


Figure 16. Tentative mechanism of transformation of the semiconductor photocatalyst 1% Pt/$Cd_{0.6}Zn_{0.4}S$/2D-β-$Zn(OH)_2$/ε-$Zn(OH)_2$/ZnO in the course of visible light-driven production of hydrogen.[273]

result, the interaction of carbonate anions and cadmium cations results in a water-insoluble salt, *viz.*, cadmium carbonate (solubility constant at 25 °C is 5.2×10^{-12} mol^{-1} litre).

Besides, photocatalytic hydrogen production is accompanied by fast dispersion and subsequent aggregation of platinum nanoparticles. According to X-ray fluorescence spectroscopy data, the surface mole fraction of platinum [Pt]/([Cd]+[Zn]) reaches a maximum value after irradiation of a period of ~5 h and the $Pt4f_{7/2}$ binding energy also reaches a maximum.[273] According to transmission electron microscopy data, the average size of metal particles increases from 1.3±0.2 to 1.7±0.5 nm after 60 h of irradiation. According to a mechanism proposed[269] for photocatalytic hydrogen production from aqueous glycerol solutions on the Pt/CdS and Pt/CdS/TiO_2 photocatalysts, the first step involves the formation of CO which deactivates the photocatalyst *via* irreversible adsorption on metallic platinum. Next, the interaction of water with photogenerated holes results in reactive species that oxidize CO to CO_2. Removal of CO from the photocatalyst surface *via* formation of CO_2 causes the rate to increase (this explains the appearance of an induction period in the photocatalytic hydrogen production). Moreover, the formation and subsequent oxidation of carbon monoxide, which is strongly adsorbed on the photocatalyst surface can significantly influence the dispersion (aggregation) of Pt nanoparticles.[273]

A number of studies are devoted to transformations of copper[118,274] and nickel[95] cocatalysts during photocatalytic production of hydrogen. In particular, a study[95] of transformations of the $Ni(OH)_2/Cd_{0.2}Zn_{0.8}S$ photocatalyst in the course of visible light-driven photocatalytic hydrogen production showed that nickel hydroxide is partially reduced to metallic nickel, thus activating the photocatalyst. Two photocatalysts, $Cu(OH)_2/Cd_{1-x}Zn_xS$ and $Cu/Cd_{1-x}Zn_xS$, undergo *in situ* transformation to $Cu_xS/Cd_{1-x}Zn_xS$ during photocatalytic hydrogen production in aqueous solutions of $Na_2S-Na_2SO_3$.[118] The photocatalytic process is accompanied by a decrease in the size of copper sulfide nanoparticles and, as a consequence, by a 1.5-fold increase in the rate of hydrogen production (Fig. 17).

This observation is consistent with a Boreskov rule, according to which 'solid catalysts change the chemical composition, surface structure and catalytic properties under the action of the reaction medium. Each composition of the reaction mixture and temperature corresponds to a particular steady state of the catalyst, which is independent of its initial state'.[276]

Deactivation of sulfide photocatalysts during hydrogen production from aqueous solutions of organic and inorganic electron donors is possible. It is believed[275] that deactivation of sulfide photocatalysts is mainly due to the oxidation of the lattice sulfide by photogenerated holes with the formation of elemental sulfur followed by escape of Cd^{2+} cations bearing uncompensated charge to the aqueous solution

$$CdS + 2h^+ \longrightarrow Cd^{2+} + S^0 \qquad (45)$$

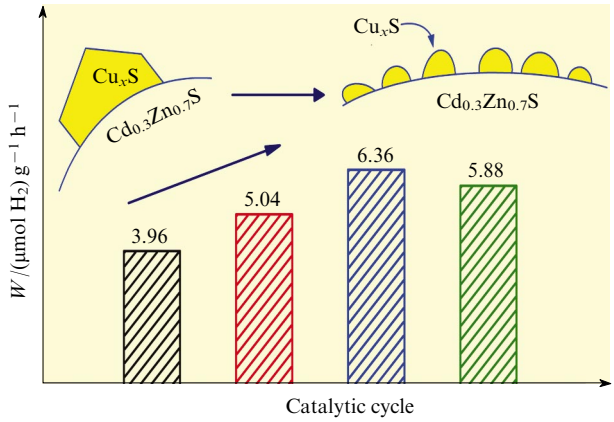


Figure 17. Tentative mechanism of transformation of the photocatalyst $Cu_xS/Cd_{1-x}Zn_xS$ and changes in the rate of hydrogen production in consecutive cycles of hydrogen production from aqueous $Na_2S-Na_2SO_3$ solutions under illumination at $\lambda = 450$ nm.

Deactivation of $Pt/Cd_{1-x}Zn_xS$ and $Cd_{1-x}Zn_xS$ photocatalysts in the course of hydrogen production from aqueous solutions of ethanol and $Na_2S-Na_2SO_3$ under irradiation with light at $\lambda = 450$ nm was investigated.[118,127,235,273] It was shown that the main reason for deactivation of the photocatalyst in the experiments with organic electron donors can be partial dissolution of cadmium sulfide followed by the formation of cadmium carbonate (Fig. 18 *a*); when using the $Na_2S-Na_2SO_3$ system, deactivation occurs *via* the growth of $Cd_{1-x}Zn_xS$ nanoparticles (Fig. 18 *b*).

The rate of hydrogen production after 6 h of irradiation decreases by a factor of 7 with ethanol as electron donor[273] and by only 20% after 12 h of irradiation using the sulfide–sulfite system.[235] The latter observation confirms the assumption that the $S^{2-}-SO_3^{2-}$ system protects photocatalysts based on $Cd_{1-x}Zn_xS$ from photocorrosion.[174]

Summing up, activation (deactivation) of working photocatalysts plays an important role in the photocatalytic production of hydrogen. Mechanisms of these processes are significantly different for organic and inorganic electron donors. Unfortunately, the processes in question remain poorly studied.

VI. Conclusion

Visible light-driven hydrogen production from aqueous solutions of organic and inorganic substrates over suspended semiconductor photocatalysts is considered as promising method for conversion of solar energy to the energy of chemical bonds. This is substantiated by the considerable literature published in the last decade. In this review we considered main classes of photocatalysts of hydrogen production from aqueous solutions of organic and inorganic electron donors. When analyzing relevant publications, particular attention was paid to methods for enhancement of activity of suspended semiconductor photocatalysts. We have shown that composite photocatalysts based on $Cd_{1-x}Zn_xS$ and wide-band-gap oxides (hydroxides) are most active in the visible light-driven hydrogen production from aqueous solutions of organic substrates. At the same time, hydrogen production from aqueous sulfide–sulfite solutions gives better results when using single-phase solid solutions of cadmium sulfide and zinc sulfide loaded with a metallic cocatalyst. It is important that transition metal compounds including MoS_2,[109] CuS,[118,127] and NiS[117] rather than noble metals have been used as cocatalysts with increasing frequency.[140–142]

Great potential for practical application of photocatalytic hydrogen production from aqueous suspensions of organic and inorganic electron donors is confirmed by the photocatalytic activity and quantum efficiency values of 33 mmol (~800 ml H_2) h^{-1} g^{-1}

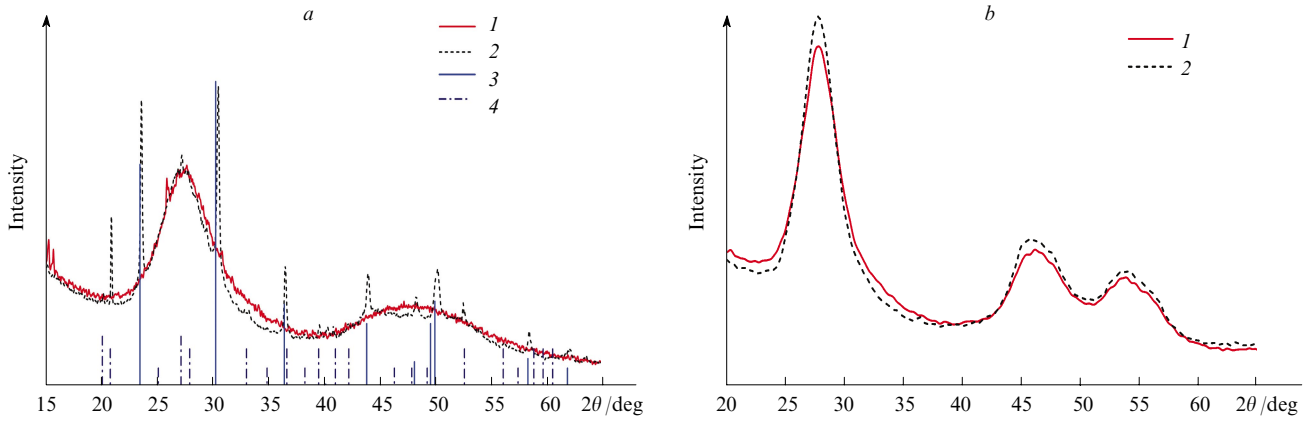


Figure 18. X-Ray diffraction patterns of photocatalysts for hydrogen production under illumination at $\lambda = 450$ nm: 1% $Pt/Cd_{0.6}Zn_{0.4}S$, aqueous solutions of ethanol (*a*)[237] and $Cd_{0.4}Zn_{0.6}S$, aqueous $Na_2S-Na_2SO_3$ solutions (*b*).[235]
Photocatalyst: (*a*) freshly prepared ($\langle D\rangle = 2$ nm; $\langle D\rangle$ is the averaged particle diameter calculated from powder X-ray diffraction patterns using the Scherrer equation; *1*); deactivated ($\langle D\rangle = 2.1$ nm; *2*); $CdCO_3$ ($D > 100$ nm; *3*); and ε-$Zn(OH)_2$ ($D > 100$ nm; *4*); (*b*) freshly prepared (*1*) and deactivated (*2*).

(see Ref. 221) and nearly 50%, respectively, achieved upon irradiation with light at 420 nm.[114, 115]

In addition to the development of optimum methods for the synthesis of active photocatalysts, considerable attention is paid to research into the mechanisms of photocatalytic hydrogen production in the presence of various electron donors. It was shown that the photocatalytic activity of the systems used for hydrogen production depends on the nature of not only the photocatalyst, but also the substrate being oxidized and on the operating parameters of the process, *viz.*, the substrate and photocatalyst concentrations and the pH of the aqueous phase of the suspension.

From a practical point of view, substrates for photocatalytic hydrogen production should be chosen taking account of not only the attainable rate of hydrogen production, but also the substrate cost and(or) availability. In particular, the observed rates of hydrogen production using the $Na_2S-Na_2SO_3$ system over sulfide photocatalysts are on the average higher than those achieved using organic electron donors. However, the use of organic substrates is practically more appropriate because most water pollutants are organic compounds, which makes it possible to purify water and produce hydrogen simultaneously.[25] Also, this is a possible method for transformation of biomass to valuable chemical products.[30]

Photocatalytic hydrogen production from aqueous solutions of organic and inorganic substrates over sulfide photocatalysts is usually carried out in alkaline media, which causes transformations of photocatalysts upon irradiation. In this review we for the first time considered tentative mechanisms of activation and deactivation of sulfide photocatalysts during hydrogen production *via* changes in their phase composition and surface properties.

At present, semiconductor suspensions are mainly used as photocatalysts. However, for practical applications, immobilized highly disperse semiconductor photocatalysts in porous matrices of different nature may appear to be more appropriate. Besides, optimization of the design of reactors for photocatalytic hydrogen production is required. Having solved these problems, one can make photocatalytic hydrogen production practically valuable, which will favour the development of new energy-saving and resource-saving technologies.[46]

The authors express their gratitude to the staff of the Group of Photocatalysis, Laboratory of Structural Methods of Investigation and Laboratory of Surface Studies at Boreskov Institute of Catalysis, Siberian Branch of the Russian Academy of Sciences for invaluable help in carrying out the research reported in this review.

The review has been written within the framework of the State Assignment to Boreskov Institute of Catalysis, Siberian Branch of the Russian Academy of Sciences (Project No. 0303-2016-0016) under partial financial support from the Russian Federation Presidential Grant for the Leading Scientific Schools (NSh-6902.2016.3).

References

1. N N Semenov *Nauka i Zhizn'* (10) 11 (1972)
2. K I Zamaraev, V N Parmon *Catal. Rev. Sci. Eng.* **22** 261 (1980)
3. M Gratzel *Energy Resources Through Photochemistry and Catalysis* (Orlando, FL: Academic Press, 1983)
4. *Chemistry for the Energy Future* (Eds V N Parmon, H Tributsch, A V Bridgwater, D O Hall) (Oxford: Blackwell, 1999)
5. E Shcherbakov *Ekspert-Sibir'* **40–41** 18 (2016)
6. X Li, J Yu, J Low, Y Fang, J Xiao, X Chen *J. Mater. Chem. A* **3** 2485 (2015)
7. E V Kukin *Logika Sluchaya* (Case Logic) (Moscow: Tsentrpoligraf, 2014)
8. O L Stroyuk, S Ya Kuchmiy, in *Photocatalysis: Fundamentals, Applications and Prospects* (Ed. M Howard) (New York: Nova Publishers, 2015) p. 31
9. J A Turner *Science* **305** 972 (2004)
10. A Fujishima, K Honda *Nature (London)* **37** 238 (1972)
11. K I Zamaraev, V N Parmon *Russ. Chem. Rev.* **49** 695 (1980)
12. K I Zamaraev, V N Parmon *Russ. Chem. Rev.* **52** 817 (1983)
13. K I Zamaraev, V N Parmon, in *Budushchee Nauki. Perspektivy. Gipotezy. Nereshennye Problemy. Ezhegodnik* (The Future of Science. Prospects. Hypotheses. Unresolved Problems. Annual) (Ed. K I Zamaraev, V N Parmon) (Moscow: Znanie, 1984) No. 17 p. 45
14. *Fotokataliticheskoe Preobrazovanie Solnechnoi Energii. Sbornik Statei* (Photocatalytic Conversion of Solar Energy. Collection of Articles) (Ed. V N Parmon) (Novosibirsk: Nauka, 1985)
15. I A Rodionov, I A Zvereva *Russ. Chem. Rev.* **85** 248 (2016)
16. E N Savinov, Candidate Thesis in Chemical Sciences, Institute of Catalysis, Siberian Branch of the RAS, Novosibirsk, 1982
17. E N Savinov, Doctoral Thesis in Chemical Sciences, Institute of Catalysis, Siberian Branch of the RAS, Novosibirsk, 1993
18. Yu A Gruzdkov, E N Savinov, V N Parmon *Khim. Vys. Energ.* **20** 445 (1986)
19. Yu A Gruzdkov, E N Savinov, V N Kolomeichuk, V N Parmon *Khim. Fiz.* **7** 1222 (1988)
20. Yu A Gruzdkov, E N Savinov, V N Parmon *Khim. Fiz.* **7** 44 (1988)
21. Y X Li, G X Lu, S B Li *Appl. Catal. A* **214** 179 (2001)
22. J Zhu, M Zich *Curr. Opin. Colloid Interface Sci.* **14** 260 (2009)
23. J Chen, Sh Lin, G Yan, L Yang, X Chen *Catal. Commun.* **9** 65 (2008)
24. H X Sang, X T Wang, C C Fan, F Wang *Int. J. Hydrogen Energy* **37** 1348 (2012)
25. E A Kozlova, A V Vorontsov *Int. J. Hydrogen Energy* **35** 7337 (2010)
26. Y X Li, Y Z Me, S Q Peng, G X Lu, S B Li *Chemosphere* **63** 1312 (2006)
27. Y X Li, G X Lu, S B Li *Chemosphere* **52** 843 (2003)
28. A Patsoura, D I Kondarides, X E Verykios *Appl. Catal., B* **64** 171 (2006)
29. M Stylidi, D I Kondarides, X E Verykios *Appl. Catal., B* **47** 189 (2004)
30. D I Kondarides, V M Daskalaki, A Patsoura, X E Verykios *Catal. Lett.* **122** 26 (2008)
31. G N Nomikos, P Panagiotopoulou, D I Kondarides, X E Verykios *Appl. Catal., B* **146** 249 (2014)

32. A Petala, E Ioannidou, A Georgaka, K Bourikas, D I Kondarides *Appl. Catal., B* **178** 201 (2015)
33. K C Christoforidis, P Fornasiero *ChemCatChem* (2017) doi: 10.1002/cctc.201601659
34. Q Gu, X Fu, X Wang, Sh Chen, D Y C Leung, X Xie *Appl. Catal., B* **106** 689 (2011)
35. S Protti, A Albini, N Serpone *Phys. Chem. Chem. Phys.* **16** 19790 (2014)
36. P Zeng, Q Zhang, X Zhang, T Peng *J. Alloys Compd.* **516** 85 (2012)
37. N Strataki, M Antoniadou, V Dracopoulos, P Lianos *Catal. Today* **151** 53 (2010)
38. K Takanabe, in *Solar Energy for Fuels* (Eds H Tüysüz, C K Chan) (New York: Springer, 2016) p. 73
39. A Kudo, K Omori, H Kato *J. Am. Chem. Soc.* **121** 11459 (1999)
40. G Hitoki, A Ishikawa, T Takata, J N Kondo, M Hara, K Domen *Chem. Lett.* **31** 736 (2002)
41. G Hitoki, T Takata, J N Kondo, M Hara, H Kobayashi, K Domen *Chem. Commun.* **38** 1698 (2002)
42. K Maeda, K Teramura, D Lu, T Takata, N Saito, Y Inoue, K Domen *Nature (London)* **440** 295 (2006)
43. W Shi, F Guo, H Wang, S Guo, H Li, Y Zhou, C Zhu, Y Liu, H Huang, B Mao, Y Liu, Z Kang *ACS Appl. Mater. Interfaces* **9** 20585 (2017
44. Z G Yi, J H Ye, N Kikugawa, T Kako, S X Ouyang, H Stuart-Williams, H Yang, J Y Cao, W J Luo, Z S Li, Y Liu, R L Withers *Nat. Mater.* **9** 559 (2010)
45. X Wang, K Maeda, A Thomas, K Takanabe, G Xin, J Carlsson, K Domen, M Antonietti *Nat. Mater.* **8** 76 (2009)
46. A Kudo, Y Miseki *Chem. Soc. Rev.* **38** 253 (2009)
47. D Jing, L Guo, L Zhao, X Zhang, H Liu, M Li, Sh Shen, G Liu, X Hu, X Zhang, K Zhang, L Ma, P Guo *Int. J. Hydrogen Energy* **35** 7087 (2010)
48. A Puga *Coord. Chem. Rev.* **315** 1 (2016)
49. A V Vorontsov, E A Kozlova, A S Besov, D V Kozlov, S A Kiselev, A S Safatov *Kinet. Catal.* **51** 801 (2010)]
50. S Chen, F Zhang *Chinese J. Catal.* **35** 1431 (2014)
51. V P Ananikov, L L Khemchyan, Y V Ivanova, V I Bukhtiyarov, A M Sorokin, I P Prosvirin, S Z Vatsadze, A V Medved'ko, V N Nuriev, A D Dilman, V V Levin, I V Koptyug, K V Kovtunov, V V Zhivonitko, V A Likholobov, A V Romanenko, P A Simonov, V G Nenajdenko, O I Shmatova, V M Muzalevskiy, M S Nechaev, A F Asachenko, O S Morozov, P B Dzhevakov, S N Osipov, D V Vorobyeva, M A Topchiy, M A Zotova, S A Ponomarenko, O V Borshchev, Y N Luponosov, A A Rempel, A A Valeeva, A Y Stakheev, O V Turova, I S Mashkovsky, S V Sysolyatin, V V Malykhin, G A Bukhtiyarova, A O Terent'ev, I B Krylov *Russ. Chem. Rev.* **83** 885 (2014)
52. I M Tsidil'kovskii *Elektrony i Dyrki v Poluprovodnikakh. Energeticheskii Spektr i Dinamika* (Electrons and Holes in Semiconductors. Energy Spectrum and Dynamics) (Moscow: Nauka, 1972)
53. Yu Ya Gurevich, Yu V Pleskov *Fotoelektrokhimiya Poluprovodnikov* (Photoelectrochemistry of Semiconductors) (Moscow: Nauka, 1983)
54. D V Kozlov, Candidate Thesis in Chemical Sciences, Institute of Catalysis, Siberian Branch of the RAS, Novosibirsk, 2002
55. B D Alexander, P J Kulesza, L Rutkowska, R Solarska, J Augustynski *J. Mater. Chem.* **18** 2298 (2008)
56. T Bak, J Nowotny, M Rekas, C C Sorrell *Int. J. Hydrogen Energy* **27** 991 (2002)
57. V N Parmon, E N Savinov, Yu A Gruzdkov *Khim. Fiz.* **7** 1070 (1988)
58. R Marschall, in *Solar Energy for Fuels* (Eds H Tüysüz, C K Chan) (New York: Springer, 2016) p. 143
59. Zh I Alferov *Fizika i Zhizn'* (Physics and Life) (St Petersburg: Nauka, 2000)
60. E A Kozlova, T P Korobkina, A V Vorontsov, V N Parmon *Appl. Catal. A* **367** 130 (2009)
61. J Zhang, Q Xu, Z Feng, M Li, C Li *Angew. Chem., Int. Ed.* **47** 1766 (2008)
62. X Wang, Q Xu, M Li, S Shen, X Wang, Y Wang, Z Feng, J Shi, H Han, C Li *Angew. Chem., Int. Ed.* **51** 13089 (2012)
63. Y Sui, J Liu, Y Zhang, X Tian, W Chen *Nanoscale* **5** 9150 (2013)
64. J Zhang, Y Wang, J Jin, J Zhang, Z Lin, F Huang, J Yu *ACS Appl. Mater. Interfaces* **5** 10317 (2013)
65. W Li, S Xie, M Li, X Ouyang, G Cui, X Lu, Y Tong *J. Mater. Chem. A* **1** 4190 (2013)
66. H G Kim, P H Borse, W Y Choi, J S Lee *Angew. Chem., Int. Ed.* **44** 4585 (2005)
67. E S Kim, N Nishimura, G Magesh, J Y Kim, J W Jang, H Jun, J Kubota, K Domen, J S Lee *J. Am. Chem. Soc.* **135** 5375 (2013)
68. S E Braslavsky, A M Braun, A E Cassano, A V Emeline, M I Litter, L Palmisano, V N Parmon, N Serpone *Pure Appl. Chem.* **83** 931 (2011)
69. K Domen, J N Kondo, M Hara, T Takata *Bull. Chem. Soc. Jpn.* **73** 1307 (2000)
70. S Ikeda, T Takata, M Komoda, M Hara, J N Kondo, K Domen, A Tanaka, H Hosono, H Kawazoe *Phys. Chem. Chem. Phys.* **1** 4485 (1999)
71. H Bahruji, M Bowker, P R Davies, L Saeed Al-Mazroai, A Dickinson, J Greaves, D James, L Millard, F Pedrono *J. Photochem. Photobiol., A* **216** 115 (2010)
72. V N Parmon *Zh. Obshch. Khim.* **62** 1703 (1992)
73. V Preethi, S Kanmani *Mater. Sci. Semicond. Proc.* **16** 561 (2013)
74. Yu Li, F He, Sh Peng, G Lu, Sh Li *Int. J. Hydrogen Energy* **36** 10565 (2011)
75. N Buehler, K Meier, J F Reber *J. Phys. Chem.* **88** 3261 (1984)
76. T P Lyubina, E A Kozlova *Kinet. Catal.* **53** 188 (2012)
77. X H Hao, L J Guo, X Mao, X M Zhang, X J Chen *Int. J. Hydrogen Energy* **28** 55 (2003)
78. K Maeda, K Domen *J. Phys. Chem. C* **111** 7851 (2007)
79. S Ye, R Wang, M-Z Wu, Y-P Yuan *Appl. Surf. Sci.* **358** 15 (2015)
80. X C Wang, K Maeda, A Thomas, K Takanabe, G J Xin, M Carlsson *Nat. Mater.* **280** 967 (2013)
81. Z G Zou, J H Ye, K Sayama, H Arakawa *Nature (London)* **414** 625 (2001)
82. Q Y Li, G X Lu *J. Mol. Catal. A* **266** 75 (2007)
83. A Makhmadmurodov, Yu A Gruzdkov, Yu A Savinov, V N Parmon *Kinet. Katal.* **27** 133 (1986)
84. *Kratkii Spravochnik Fiziko-Khimicheskikh Velichin* (Short Handbook of Physical and Chemical Quantities) (Ed. K P Mishchenko, A A Ravdel') (Leningrad; Khimiya, 1974)
85. Q Xiang, B Cheng, J Yu *Appl. Catal., B* **138** – **139** 299 (2013)
86. A Sathish, R P Viswanath *Catal. Today* **129** 421 (2007)
87. C M Janet, R P Viswanath *Nanotechnology* **17** 5271 (2006)
88. J S Jang, U A Joshi, J S Lee *J. Phys. Chem. C,* **111** 13280 (2007)
89. I Tsuji, H Kato, H Kobayashi, A Kudo *J. Am. Chem. Soc.* **126** 13406 (2004)

90. S I Sadovnikov, A I Gusev, A A Rempel *Russ. Chem. Rev.* **85** 731 (2016)
91. S H Shen, L Zhao, L J Guo *Int. J. Hydrogen Energy* **33** 4501 (2008)
92. S H Shen, L Zhao, L J Guo *J. Phys. Chem. Solids* **69** 2426 (2008)
93. S H Shen, L Zhao, L J Guo *Mater. Res. Bull.* **44** 100 (2009)
94. S H Shen, L Zhao, L J Guo *J. Phys. Chem. C* **112** 16148 (2008)
95. J Ran, J Zhang, J Yu, S Zh Qiao *ChemSusChem* **7** 3426 (2014)
96. S Sato, J M White *J. Catal.* **69** 128 (1981)
97. V N Parmon, Yu I Gruzdkov, E N Savinov *Int. J.Hydrogen Energy* **12** 393 (1987)
98. A V Vorontsov, E N Savinov, Z S Jin *J. Photochem. Photobiol., A* **125** 113 (1999)
99. E A Kozlova, Candidate Thesis in Chemical Sciences, Institute of Catalysis, Siberian Branch of the RAS, Novosibirsk, 2008
100. D V Markovskaya, T P Lyubina, E A Kozlova, S V Cherepanova, E Yu Gerasimov, A A Saraev, V V Kaichev *Kinet. Catal.* **55** 528 (2014)
101. M Nguyen, P D Tran, S S Pramana, R L Lee, S K Batabyal, N Mathews, L H Wong, M Graetzel *Nanoscale* **5** 1479 (2013)
102. S Yu Kochev, Yu N Bubnov, S S Abramchuk, O Yu Antonova, P M Valetsky, Yu A Kabachii *Mendeleev Commun.* **27** 1 (2017)
103. E N Savinov, L Gongxuan, V N Parmon *React. Kinet. Catal. Lett.* **48** 553 (1992)
104. N Li, B Zhou, P Guo, J Zhou, D Jing *Int. J. Hydrogen Energy* **38** 11268 (2013)
105. X Zong, G Wu, H Yan, G Ma, J Shi, F Wen, L Wang, C Li *J. Phys. Chem. C* **114** 1963 (2010)
106. X Zong, H Yan, G Wu, G Ma, F Wen, L Wang, C Li *J. Am. Chem. Soc.* **130** 7176 (2008)
107. Z Hu, J C Yu *J. Mater. Chem. A* **1** 12221 (2013)
108. D Recatalv, R Llusar, A L Gushchin, E A Kozlova, Yu A Laricheva, P A Abramov, M N Sokolov, R Gómez, T Lana-Villarreal *ChemSusChem* **8** 1299 (2015)
109. J Xu, X Cao *Chem. Eng. J.* **260** 642 (2015)
110. Yu A Gruzdkov, E N Savinov, V V Korolkov, V N Parmon *React. Kinet. Catal. Lett.* **36** 395 (1988)
111. V I Fedoseev, E N Savinov, V N Parmon *Kinet. Katal.* **28** 1111 (1987)
112. J Zhang, Q Xu, S Z Qiao, J Yu *ChemSusChem* **6** 2009 (2013)
113. W Zhang, R Xu *Int. J. Hydrogen Energy* **34** 8495 (2009)
114. H Yan, J Yang, G Ma, G Wu, X Zong, Z Lei, J Shi, C Li *J. Catal.* **266** 165 (2009)
115. J Yang, H Yan, X Wang, F Wen, Z Wang, D Fan, J Shi, C Li *J. Catal.* **290** 151 (2009)
116. J S Jang, D J Ham, N Lakshminarasimhan, W Y Choi, J S Lee *Appl. Catal. A* **346** 149 (2008)
117. J Wang, B Li, J Chen, N Li, J Zheng, J Zhao, Z Zhu *Appl. Surf. Sci.* **259** 118 (2012)
118. E A Kozlova, D V Markovskaya, O A Stonkus, A A Saraev, P A Kolinko, S V Cherepanova, V N Parmon, in *The IVth Scientific Conference Dedicated to the 110th Anniversary of Academician Georgii K Boreskov: Abstracts, Novosibirsk, 2017* p. 41
119. J Xu, L W Zhang, R Shi, Y F Zhu *J. Mater. Chem.* **1** 14766 (2013)
120. Y J Zhang, L Zhang *J. Inorg. Mater.* **23** 66 (2008)
121. S Y Ryu, W Balcerski, T K Lee, M R Hoffmann *J. Phys. Chem. C* **111** 18195 (2007)
122. G Q Guan, T Kida, K Kusakabe, K Kimura, X M Fang, T L Ma *Chem. Phys. Lett.* **385** 319 (2004)
123. S H Shen, L J Guo *Mater. Res. Bull.* **43** 437 (2008)
124. Yu Chen, Sh Zhao, X Wang, Q Peng, R Lin, Y Wang, R Shen, X Cao, L Zhang, G Zhou, J Li, A Xia, Y Li *J. Am. Chem. Soc.* **138** 4286 (2016)
125. A P Gaikwad, D Tyagi, C A Betty, R Sasikala *Appl. Catal., A* **517** 91 (2016)
126. Y Zhou, Y Wang, T Wen, S Zhang, B Chang, Y Guo, B Yang *J. Colloid Interface Sci.* **467** 97 (2016)
127. D V Markovskaya, S V Cherepanova, A A Saraev, E Yu Gerasimov, E A Kozlova *Chem. Eng. J.* **262** 146 (2015)
128. E Hong, D Kim, J H Kim *J. Ind. Eng. Chem.* **20** 3869 (2014)
129. L-X Hao, G Chen, Y-G Yu, Y-S Zhou, Z-H Han, Y Liu *Int. J. Hydrogen Energy* **39** 14479 (2014)
130. L Wang, W Wang, M Shang, W Yin, S Sun, L Zhang *Int. J. Hydrogen Energy* **35** 19 (2010)
131. X Zhang, Y Du, Zh Zhou, L Guo *Int. J. Hydrogen Energy* **35** 3313 (2010)
132. L Ren, F Yang, Y Deng, N Yan, S Huang, D Lei, Q Sun, Y Yu *Int. J. Hydrogen Energy* **35** 3297 (2010)
133. C Wu, H Cho, W Chang, T Lee *Chem. Eng. Sci.* **65** 141 (2010)
134. F F del Valle, A Ishikawa, K Domen, J A Villoria de la Mano, M C Sanchez-Sanchez, I D Gonzalez, S Herreras, N Mota, M E Rivas, M C Alvarez Galvan, J L G Fierro, R M Navarro *Catal. Today* **143** 51 (2009)
135. D Jing, L Guo *J. Phys. Chem. B* **110** 11139 (2006)
136. I Tsuji, H Kato, H Kobayashi, A Kudo *J. Phys. Chem. B,* **109** 7323 (2005)
137. S Peng, M Ding, T Yi, Z Zhan, Y Li *Environ. Prog. Sustain. Energy* **35** 141 (2016)
138. Y Li, J Wang, S Peng, G Lu, S Li *Int. J. Hydrogen Energy* **35** 7116 (2010)
139. S-Q Peng, Y-J Peng, Y-X Li, G-X Lu, S-B Li *Res. Chem. Intermed.* **35** 739 (2009)
140. Z Jin, Q Li, L Feng, Z Chen, X Zheng, C Xi *J. Mol. Catal., A* **50** 315 (1989)
141. Z Jin, Q Li, X Zheng, C Xi, C Wang, H Zhang, L Feng, H Wang, Z Chen, Z Jiang *J. Photochem. Photobiol., A* **71** 85 (1993)
142. M Matsumura, M Hiramoto, T Iehara, H Tsubomura *J. Phys. Chem.* **88** 248 (1984)
143. I Postnova, E Kozlova, S Cherepanova, S Tsybulya, A Rempel, Yu Shchipunov *RSC Adv.,* **5** 8544 (2015)
144. N S Kolobov, D A Svintsitskiy, E A Kozlova, D S Selishchev, D V Kozlov *Chem. Eng. J.* **314** 600 (2017)
145. D S Selishchev, N S Kolobov, A A Pershin, D V Kozlov *Appl. Catal. B* **200** 503 (2017)
146. Y V Kolen'ko, K A Kovnir, A I Gavrilov, A V Garshev, P E Meskin, B R Churagulov, M Bouchard, C Colbeau-Justin, O I Lebedev, G Van Tendeloo, M Yoshimura *J. Phys. Chem. B* **109** 20303 (2005)
147. A I Gavrilov, S V Balakhonov, B R Churagulov *Inorg. Mater.* **52** 1240
148. J Highfield *Molecules* **20** 6739 (2015)
149. D Y C Leung, X Fu, C Wang, M Ni, M K H Leung, X Wang, X Fu *ChemSusChem* **3** 681 (2010)
150. T Sun, J Fan, E Liu, L Liu, Y Wang, H Dai, Y Yang, W Hou, X Hu, Z Jiang *Powder Technol.* **228** 210 (2012)
151. T Sun, E Liu, X Liang, X Hu, J Fan *Appl. Surf. Sci.* **347** 696 (2015)

152. S Taylor, M Mehta, A Samokhvalov *ChemPhysChem* **15** 942 (2014)
153. R Asahi, T Morikawa, T Ohwaki, K Aoki, Y Taga *Science* **293** 269 (2001)
154. H Irie, Y Watanabe, K Hashimoto *J. Phys. Chem. B* **107** 5483 (2003)
155. J C Yu, J G Yu, W K Ho, Z T Jiang, L Z Zhang *Chem. Mater.* **14** 3808 (2002)
156. H Kim, W Choi *Appl. Catal., B* **69** 127 (2007)
157. T Ohno, M Akiyoshi, T Umebayashi, K Asai, T Mitsui, M Matsumura *Appl. Catal., A* **265** 115 (2004)
158. K Demeestere, J Dewulf, T Ohno, P H Salgado, H Van Langenhove *Appl. Catal., B* **61** 140 (2005)
159. T Sreethawong, S Laehsalee, S Chavadej *Catal. Commun.* **10** 538 (2009)
160. T Sreethawong, S Laehsalee, S Chavadej *Int. J. Hydrogen Energy* **33** 5947 (2008)
161. Y Li, C Xie, S Peng, G Lu, S Li *J. Mol. Catal. A* **282** 117 (2008)
162. X Chen, L Liu, F Huang *Chem. Soc. Rev.* **44** 1861 (2015)
163. X Chen, L Liu, P Y Yu, S S Mao *Science* **331** 746 (2011)
164. A Gallo, T Montini, M Marelli, A Minguzzi, V Gombac, R Psaro, P Fornasiero, V Dal Santo *ChemSusChem,* **5** 1800 (2012)
165. A Gallo, M Marelli, R Psaro, V Gombac, T Montini, P Fornasiero, R Pievo, V Dal Santo *Green Chem.* **14** 330 (2012)
166. X Yang, L Wu, L Du, X Li *Catal. Lett.* **145** 1771 (2015)
167. F Zuo, L Wang, T Wu, Z Zhang, D Borchardt, P Feng *J. Am. Chem. Soc.* **132** 11856 (2010)
168. F Chang, Y C Xie, C L Li, J Chen, J R Luo, X F Hu, J W Shen *Appl. Surf. Sci.* **5** 6717 (2012)
169. Y Wang, X C Wang, M Antonietti *Angew. Chem., Int. Ed.* **51** 68 (2012)
170. Y G Gong, M M Li, Y Wang *ChemSusChem* **8** 931 (2015)
171. S W Cao, J X Low, J G Yu, M Jaroniec *Adv. Mater.* **1** 2150 (2015)
172. D J Martin, P J T Reardon, S J A Moniz, J Tang *J. Am. Chem. Soc.* **136** 12568 (2014)
173. P Niu, L Zhang, G Liu, H M Cheng *Adv. Funct. Mater.* **22** 4763 (2012)
174. E N Savinov, Yu A Gruzdkov, V N Parmon *Int. J. Hydrogen Energy* **14** 1 (1989)
175. L Liu, Y H Qi, J S Hu, Y H Liang, W Q Cui *Appl. Surf. Sci.* **351** 1146 (2015)
176. Q J Xiang, J G Yu, M Jaroniec *J. Phys. Chem. C* **115** 7355 (2011)
177. S W Cao, Y P Yuan, J Fang, M M Shahjamali, F Y C Boey, J Barber, S C J Loo, C Xue *Int. J. Hydrogen Energy* **38** 1258 (2013)
178. B Chai, T Y Peng, J Mao, K Li, L Za *Phys. Chem. Chem. Phys.* **14** 16745 (2012)
179. J S Zhang, M W Zhang, R Q Sun, X C Wang *Angew. Chem., Int. Ed.* **51** 10145 (2012)
180. F Dong, Z W Zhao, T Xiong, Z L Ni, W D Zhang, Y J Sun, W K Ho *ACS Appl. Mater. Interfaces* **5** 11392 (2013)
181. J G Yu, S Wang, B Cheng, Z Lin, F Huang *Catal. Sci. Technol.* **3** 1782 (2013)
182. Y Y Kang, Y Q Yang, L C Yin, X D Kang, G Liu, H M Cheng *Adv. Mater.* **27** 4572 (2015)
183. X She, L Liu, H Ji, Z Mo, Y Li, L Huang, D Du, H Xu, H Li *Appl. Catal., B* **187** 144 (2016)
184. J-P Zou, L-C Wang, J Luo, Y-C Nie, Q-J Xing, X-B Luo, H-M Du, S-L Luo, S L Sui *Appl. Catal., B* **193** 103 (2016)
185. J Yan, H Wu, H Chen, L Pang, Y Zhang, R Jiang, L Li, S Liu *Appl. Catal., B* **194** 74 (2016)
186. H Yu, P Xiao, P Wang, J Yu *Appl. Catal., B* **193** 217 (2016)
187. Z Li, Y Wu, G Lu *Appl. Catal., B* **188** 56 (2016)
188. L Ge, C Han, J Liu, Y Li *Appl. Catal., A* **409** 215 (2011)
189. Y Hou, A B Laursen, J Zhang, G Zhang, Y Zhu, X C Wang, S Dahl, I Chorkendorff *Angew. Chem., Int. Ed.* **52** 3621 (2013)
190. J Hong, Y Wang, W Zhang, R Xu *ChemSusChem* **6** 2263 (2013)
191. H Ahmad, S K Kamarudin, L J Minggu, M Kassim *Renew. Sustain. Energy Rev.* **43** 599 (2015)
192. S Nakamura *Solid State Commun.* **102** 237 (1997)
193. J Sato, N Saito, Y Yamada, K Maeda, T Takata, J N Kondo, M Hara, H Kobayashi, K Domen, Y Inoue *J. Am. Chem. Soc.* **127** 4150 (2005)
194. K Maeda, T Takata, M Hara, N Saito, Y Inoue, H Kobayashi, K Domen *J. Am. Chem. Soc.* **127** 8286 (2005)
195. K Maeda, K Teramura, K Domen *J. Catal.* **254** 198 (2008)
196. Sh Higashimoto, N Kitao, N Yoshida, T Sakura, M Azuma, H Ohue, Y J Sakata. *J. Catal.* **266** 279 (2009)
197. V Keller, P Bernhardt, F Garin *J. Catal.* **215** 129 (2003)
198. Zh Yu, S S C Chuang *J. Catal.* **246** 118 (2007)
199. C Salazar, M A Nanny *J. Catal.* **269** 404 (2010)
200. L Wu, J C Yu, X Fu *J. Mol. Catal., A* **244** 25 (2006)
201. A A Rempel, E A Kozlova, T I Gorbunova, S V Cherepanova, E Yu Gerasimov, N S Kozhevnikova, A A Valeeva, E Yu Korovin, V V Kaichev, Yu A Shchipunov *Catal. Commun.* **68** 61 (2015)
202. E A Kozlova, N S Kozhevnikova, S V Cherepanova, T P Lyubina, E Yu Gerasimov, V V Kaichev, A V Vorontsov, S V Tsybulya, A A Rempel, V N Parmon *J. Photochem. Photobiol.* **250** 103 (2012)
203. S Chen, M Paulose, C Ruan, G K Mor, O K Varghese, D Kouzoudis, C A Grimes *J. Photochem. Photobiol., A* **177** 177 (2006)
204. C Li, J Yuan, B Han, L Jiang, W Shangguan *Int. J. Hydrogen Energy* **35** 7073 (2010)
205. R Vogel, P Hoyer, H Weller *J. Phys. Chem.* **98** 3183 (1994)
206. T P Lyubina, D V Markovskaya, E A Kozlova, V N Parmon *Int. J. Hydrogen Energy* **38** 14172 (2013)
207. E A Kozlova, D V Markovskaya, S V Cherepanova, A A Saraev, E Yu Gerasimov, T V Perevalov, V V Kaichev, V N Parmon *Int. J. Hydrogen Energy* **39** 18758 (2014)
208. J Yuan, J Wen, Y Zhong, X Li, Y Fang, S Zhang, W Liu *J. Mater. Chem., A* **3** 18244 (2015)
209. X Wang, W-C Peng, X-Y Li *Int. J. Hydrogen Energy* **39** 13454 (2014)
210. D V Markovskaya, E A Kozlova, S V Cherepanova, A A Saraev, E Yu Gerasimov, V N Parmon *Top. Catal.* **59** 1297 (2016)
211. P A L Lopes, A J S Mascarenhas, L A Silva *J. Alloys Compd.* **649** 332 (2015)
212. X Jia, M Tahir, L Pan, Z-F Huang, X Zhang, L Wang, J-J Zou *Appl. Catal., B* **198** 154 (2016)
213. W Zhao, L Xie, M Zhang, Z Ai, H Xi, Y Li, Q Shi, J Chen *Int. J. Hydrogen Energy* **41** 6277 (2016)
214. R Cheng, L Zhang, X Fan, M Wang, M Li, J Shi *Carbon* **101** 62 (2016)
215. L Chen, X Zhou, B Jin, J Luo, X Xu, L Zhang, Y Hong *Int. J. Hydrogen Energy* **41** 7292 (2016)

216. K Song, F Xiao, L Zhang, F Yue, X Liang, J Wang, X Su *J. Mol. Catal., A* **418** – **419** 95 (2016)
217. A Roy, S R Lingampalli, S Saha, C N R Rao *Chem. Phys. Lett.* **637** 137 (2015)
218. H Liu, Z Xu, Z Zhang, D Ao *Appl. Catal., B* **192** 234 (2016)
219. F Cheng, H Yin, Q Xiang *Appl. Surf. Sci.* **391** 432 (2016)
220. A Roy, S R Lingampalli, I M Nassar, C N R Rao *Solid State Commun.* **243** 1 (2016)
221. L Yao, D Wei, Y Ni, D Yan, C Hu *Nano Energy* **26** 248 (2016)
222. H Liu, Z Xu, Z Zhang, D Ao *Appl. Catal., A* **518** 150 (2016)
223. Y-J Yuan, J-R Tu, Z-J Ye, D-Q Chen, B Hu, Y-W Huang, T-T Chen, D-P Cao, Z-T Yu, Z-G Zou *Appl. Catal., B* **188** 13 (2016)
224. Y V Kolen'ko, B R Churagulov, M Kunst, L Mazerolles, C Colbeau-Justin *Appl. Catal., B* **54** 51 (2004)
225. A I Gavrilov, I A Rodionov, D Yu Gavrilova, I A Zvereva, B R Churagulov, Yu D Tret'yakov *Dokl. Chem.* **444** 133 (2012)
226. V K Ivanov, V D Maksimov, A S Shaporev, A E Baranchikov, B P Churagulov, I A Zvereva, Yu D Tret'yakov *Russ. J. Inorg. Chem.* **55** 150 (2010)
227. A Bhirud, N Chaudhari, L Nikam, R Sonawane, K Patil, J-O Baeg, B Kale *Int. J. Hydrogen Energy* **36** 11628 (2011)
228. F E Osterloh, in *Solar Energy for Fuels* (Eds H Tüysüz, C K Chan) (New York: Springer, 2016) p. 105
229. A A Rempel *Russ. Chem. Rev.* **76** 435 (2007)
230. M A Nasalevich, E A Kozlova, T P Lyubina, A V Vorontsov *J. Catal.* **287** 138 (2012)
231. T K Townsend, N D Browning, F E Osterloh *ACS Nano* **6** 7420 (2012)
232. L Liao, Q Zhang, Z Su, Z Zhao, Y Wang, Y Li, X Lu, D Wei, G Feng, Q Yu, X Cai, J Zhao, Z Ren, H Fang, F Robles-Hernandez, S Baldelli, J Bao *Nat. Nanotechnol.* **9** 69 (2014)
233. K O Hamaloglu, B Çelebi, E Sag, A Tuncel *Micropor. Mesopor. Mater.* **207** 17 (2015)
234. H Weiss, A Fernandez, H Kisch *Angew. Chem., Int. Ed.* **40** 3825 (2001)
235. E A Kozlova, A Yu Kurenkova, V S Semeykina, E V Parkhomchuk, S V Cherepanova, E Yu Gerasimov, A A Saraev, V V Kaichev, V N Parmon *ChemCatChem.* **7** 4108 (2015)
236. S A Machas-Sánchez, R Nava, V Hernández-Morales, Y J Acosta-Silva, B Pawelec, S M Al-Zahrani, R M Navarro, J L G Fierro *Int. J. Hydrogen Energy* **37** 9948 (2012)
237. R Mitchell, R Brydson, R E Douthwaite *Phys. Chem. Chem. Phys.* **17** 493 (2015)
238. X Cui, Y Wang, G Jiang, Z Zhao, C Xu, Y Wei, A Duan, J Liu, J Gao *RSC Adv.* **4** 15689 (2014)
239. P Zhang, T Tachikawa, M Fujitsuka, T Majima *Chem. Commun.* **51** 7187 (2015)
240. P Pichat, J M Herrmann, J Disdier, H Courbon, M N Mozzanega *New. J. Chem.* **5** 627 (1981)
241. T Sreethawong, T Puangpetch, S Chavadej, S Yoshikawa *J. Power Sources* **165** 861 (2007)
242. A Speltini, M Sturini, D Dondi, E Annovazzi, F Maraschi, V Caratto, A Profumo, A Buttafava *Photochem. Photobiol. Sci.* **13** 1410 (2014)
243. A Speltini, M Sturini, F Maraschi, D Dondi, A Serra, A Profumo, A Buttafava, A Albini *Int. J. Hydrogen Energy* **39** 11433 (2014)
244. D Bao, P Gao, X Zhu, S Sun, Y Wang, X Li, Y Chen, H Zhou, Y Wang, P Yang *Chem. – Eur. J.* **21** 12728 (2015)
245. S A L Bastos, P A L Lopes, F N Santos, L Almeida Silva *Int. J. Hydrogen Energy* **39** 14588 (2014)
246. J C Liu, C P Huang *Langmuir* **8** 1851 (1992)
247. M Kosmulski *Adv. Colloid. Interface Sci.* **152** 14 (2009)
248. Y Li, D Gao, Sh Peng, G Lu, Sh Li *Int. J. Hydrogen Energy* **36** 4291 (2011)
249. C Ma, Y Li, H Zhang, Y Chen, C Lu, J Wang *Chem. Eng. J* **273** 277 (2015)
250. A Dickinson, D James, N Perkins, T Cassidy, M Bowker *J. Mol. Catal., A* **146** 211 (1999)
251. S Nishimoto, B Ohtani, T Kagiya *J. Chem. Soc., Faraday Trans.* **1** 2467 (1985)
252. X-J Zheng, L-F Wei, Z-H Zhang, Q-J Jiang, Y-J Wei, B Xie, M-B Wei *Int. J. Hydrogen Energy* **34** 9033 (2009)
253. X Fu, J Long, X Wang, D Y C Leung, Z Ding, L Wu, Z Zhang, Z Li, X Fu *Int. J. Hydrogen Energy* **33** 6484 (2008)
254. Y-X Li, Y-Z Xie, S-Q Peng, G-X Lu, S-B Li *Chem. J. Chin. Univ.* **28** 156 (2007)
255. B Ohtani *Phys. Chem. Chem. Phys.* **16** 1788 (2014)
256. B Ohtani *Chem. Lett.* **37** 217 (2008)
257. T Chen, Z Feng, G Wu, J Shi, G Ma, P Ying, C Li *J. Phys. Chem. C* **111** 8005 (2007)
258. N Strataki, V Bekiari, D I Kondarides, P Lianos *Appl. Catal., B* **77** 184 (2007)
259. J Sabate, S Cervera-March, R Simarro, J Gimenez *Chem. Eng. Sci.* **45** 3089 (1990)
260. O Carp, C L Huisman, A Reller *Prog. Solid State Chem.* **32** 33 (2004)
261. N Z Bao, L M Shen, T Takata, K Domen *Chem. Mater.* **20** 110 (2008)
262. J F Reber, K Meier *J. Phys. Chem.* **88** 5903 (1984)
263. C J Xing, Y J Zhang, W Yan, L J Guo *Int. J. Hydrogen Energy* **31** 2018 (2006)
264. P Gomathinskar, K Hachisuka, H Katsumata, T Suzuki, K Funasaka, S Kaneco *Int. J. Hydrogen Energy* **38** 8625 (2013)
265. H Park, Y K Kim, W Choi *J. Phys. Chem. C* **115** 6141 (2011)
266. I Majeed, M Amtiaz Nadeem, M Al-Oufi, M Arif Nadeem, G I N Waterhouse, A Badshah, J B Metson, H Idriss *Appl. Catal., B* **182** 266 (2016)
267. H Bahruji, M Bowker, P R Davies, F Pedrono *Appl. Catal., B* **107** 205 (2011)
268. M Bowker *Catal. Lett.* **142** 923 (2012)
269. M de Oliveira Melo, L Almeida Silva *J. Photochem. Photobiol., A* **226** 36 (2011)
270. C Dinh, M Pham, Y Seo, F Kleitz, T Do *Nanoscale* **6** 4819 (2014)
271. V Gombac, L Sordelli, T Montini, J J Delgado, A Adamski, G Adami, M Cargnello, S Bernal, P Fornasiero *J. Phys. Chem. A* **114** 3916 (2010)
272. V M Daskalaki, D I Kondarides *Catal. Today* **144** 75 (2009)
273. E A Kozlova, S V Cherepanova, D V Markovskaya, A A Saraev, E Y Gerasimov, V N Parmon *Appl. Catal., B* **183** 197 (2016)
274. M Jung, J N Hart, J Scott, Y H Ng, Y Jiang, R Amal *Appl. Catal., A* **521** 190 (2016)
275. D Meissner, R Memming, L Shuben, S Yesodharan, M Graetzel *Ber. Bunsenges. Phys. Chem.* **89** 121 (1985)
276. G K Boreskov *Geterogennyi Kataliz* (Heterogeneous Catalysis) (Moscow: Nauka, 1986)